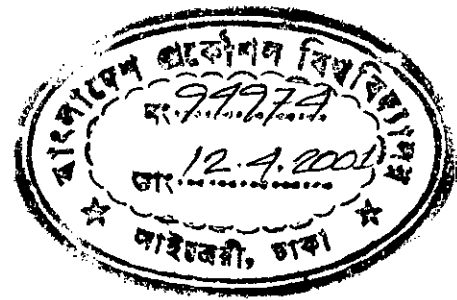
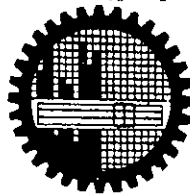


ELASTIC-PLASTIC BEHAVIOR OF A CIRCULAR ROD UNDER COMBINED TENSION AND TORQUE

BY
PRODIP KUMAR DAS
B.SC. ENGG. (MECH.)



A THESIS
SUBMITTED TO THE DEPARTMENT OF MECHANICAL
ENGINEERING IN PARTIAL FULFILLMENT OF THE REQUIREMENTS
FOR
THE DEGREE OF MASTER OF SCIENCE IN MECHANICAL
ENGINEERING




DEPARTMENT OF MECHANICAL ENGINEERING
BANGLADESH UNIVERSITY OF ENGINEERING & TECHNOLOGY
(BUET)
DHAKA, BANGLADESH

FEBRUARY 2001


CERTIFICATE OF APPROVAL

The board of examiners hereby recommends to the Department of Mechanical Engineering, BUET, Dhaka, the acceptance of this thesis, "ELASTIC-PLASTIC BEHAVIOR OF A CIRCULAR ROD UNDER COMBINED TENSION AND TORQUE", submitted by Prodip Kumar Das, in partial fulfillment of the requirements for the degree of Master of Science in Mechanical Engineering.


Chairman (Supervisor) :


Dr. Abu Rayhan Md. Ali 8/2/01
Associate Professor
Department of Mechanical Engineering
BUET, Dhaka, Bangladesh.


Member (Ex-officio) :


Dr. Md. Abdur Rashid Sarkar
Professor & Head
Department of Mechanical Engineering
BUET, Dhaka, Bangladesh.

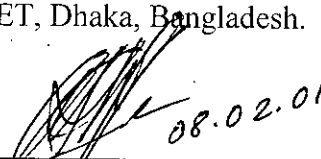
Member :


Dr. Dipak Kanti Das
Professor
Department of Mechanical Engineering
BUET, Dhaka, Bangladesh.

Member :



Dr. Sheikh Reaz Ahmed
Assistant Professor
Department of Mechanical Engineering
BUET, Dhaka, Bangladesh.


Member (external) :


Dr. A. S. M. A. Haseeb 08.02.01
Professor
Department of Materials & Metallurgical Engg.
BUET, Dhaka, Bangladesh.

CERTIFICATE OF RESEARCH

This is to certify that the work presented in this dissertation is the outcome of the investigation carried out by the author under the supervision of Dr. Abu Rayhan Md. Ali, Associate Professor, Department of Mechanical Engineering, Bangladesh University of Engineering & Technology (BUET), Dhaka, Bangladesh and it has not been submitted anywhere for the award of any degree or diploma.


Supervisor: 8/2/2001
Dr. Abu Rayhan Md. Ali


Author:
Prodip Kumar Das

ACKNOWLEDGEMENT

The author would like to take this opportunity of expressing his heartfelt gratitude and indebtedness to his thesis supervisor Dr. Abu Rayhan Md. Ali, Associate Professor, Department of Mechanical Engineering, BUET, Dhaka, for his valuable and continuous guidance, suggestions in the course of the present work.

The author feels grateful to Dr. Abdur Rashid Sarkar, Professor & Head, Department of Mechanical Engineering, BUET, for his valuable suggestions from time to time.

The author is also grateful to all of the teachers of Mechanical Engineering Department who cooperated by giving permission to use the computers of teachers' computer room.

Finally the author also thanks his colleagues, family and relatives, another's who shared the troubles with him.

ABSTRACT

In the present research work the elastic-plastic behavior of a circular rod under combined tension and torque within the elastic-plastic region has been investigated theoretically. Here a theoretical model has been developed in order to examine the elastic-plastic behavior of the rod under the two types of loading. This model is based on the Prandtl-Reuss incremental stress-strain laws and the von Mises yield criterion. Finally, a computational program has been developed to obtain the theoretical results based on the model. To this end two bi-axial loading paths were considered. In the first type of loading, a circular rod was initially subjected to various levels of torque, that is, $T_0/T_Y=1.0, 0.75, 0.5$ and 0.25 , and then keeping the initial angle of twist constant, subsequently it was subjected to gradual increasing (quasistatic strain rate) axial tension and hence axial strain. In the second type of loading, a circular rod was initially subjected to various levels of axial load, that is, $F_0/F_Y=1.0, 0.75, 0.5$ and 0.25 , and then keeping the initial extension constant, subsequently it was subjected to gradual increasing torque and hence shear strain. Variation of different parameters such as axial and shear stresses, axial tension and torque were determined. Moreover, results obtained from the present investigation were compared with the available experimental results for similar types of bi-axial loading.

CONTENTS

TITLES		Page No.
Certificate of Approval		III
Certificate of Research		IV
Acknowledgement		V
Abstract		VI
Contents		VII
List of Figures		IX
Nomenclature		XII
Chapter-1	Introduction	
1.1	General	01
1.2	Justification	02
1.3	Objectives	04
1.4	Layout of The Thesis	04
Chapter-2	Literature Survey	
2.1	General	05
2.2	Previous Work	05
2.3	Yield Criterion	06
	2.3.1 Maximum Shear Stress Theory	06
	2.3.2 Distortion Energy Theory	07
2.4	Plastic Stress-Strain Relations	09
2.5	Prandtl-Reuss Stress-Strain Equation	10
Chapter-3	Mathematical Model	
3.1	General	15
3.2	Cylindrical Bars under Different Types of Loading	15
	3.2.1 Simple Tension Test	15
	3.2.2 Pure Torsion Test	16
	3.2.3 Combined Torsion and Tension	18
3.3	Effective Stress and Strain	22

Chapter-4	Numerical Solution	
4.1	General	23
4.2	Numerical Procedure	23
4.2.1	Torsion Followed by Tension for Constant Angle of Twist	23
4.2.2	Tension Followed by Torsion for Constant Axial Displacement	26
4.3	Strain Hardening Model	28
4.4	Computer Program	28
Chapter-5	Results and Discussion	
5.1	General	29
5.2	Theoretical Investigation	29
5.2.1	Variation of Axial and Shear Stresses	29
5.2.2	Variation of the Axial Load and Torque	32
5.3	Comparison of Theoretical Results with Experimental Results	34
Chapter-6	Conclusion and Recommendation	
6.1	General	37
6.2	Conclusion	37
6.3	Recommendation for Future Work	39
References		75
Appendix – A	Computer Program	77
Appendix – B	Mechanical Properties of Steel and Copper	89

LIST OF FIGURES



Figure 5.1	Schematic diagram of the model when the circular bar is subjected to initial torque first (CASE-I)	
Figure 5.2	Schematic diagram of the model when the circular bar is subjected to axial load first (CASE-II)	41
Figure 5.3	Non-dimensional axial and shear stresses distributions along the half of the cross-section of a circular rod for CASE-I, i.e., $P (= \gamma_0/\gamma_y)=1.0$ & $\varepsilon/\varepsilon_y=1.0$ when the circular bar is subjected to initial torque first	42
Figure 5.4	Non-dimensional axial and shear stresses distributions along the half of the cross-section of a circular rod for CASE-II, i.e., $Q (= \varepsilon_0/\varepsilon_y)=1.0$ & $\gamma/\gamma_y =1.0$, when the circular bar is subjected to initial axial load first	43
Figure 5.5	Non-dimensional axial and shear stresses distributions along the half of the cross-section of a circular rod for the conditions $P (= \gamma_0/\gamma_y)=1.0$ & $\varepsilon/\varepsilon_y=1.0$ for Case-I and $\gamma/\gamma_y=1.0$ & $Q (= \varepsilon_0/\varepsilon_y)=1.0$ for CASE-II	44
Figure 5.6	Variation of non-dimensional axial and shear stresses at the outer surface of the circular rod for CASE-I, i.e., $\gamma_0/\gamma_y=1.0$ & $\xi(=r/a)=1.0$	45
Figure 5.7	Variation of non-dimensional axial and shear stresses at the outer surface of the circular rod for CASE-II, i.e., $\varepsilon_0/\varepsilon_y=1.0$ & $\xi(=r/a)=1.0$	46
Figure 5.8	Non-dimensional axial stress distribution along the half of the cross-section of a circular rod for the conditions $\varepsilon/\varepsilon_y=1.0$ & different levels of initially applied torque, i.e., $P (= \gamma_0/\gamma_y)$	47
Figure 5.9	Non-dimensional shear stress distribution along the half of the cross-section of a circular rod for the conditions $\varepsilon/\varepsilon_y=1.0$ & different levels of initially applied torque, i.e., $P (= \gamma_0/\gamma_y)$	48
Figure 5.10	Non-dimensional axial stress distribution along the half of the cross-section of a circular rod for the condition $\gamma/\gamma_y=1.0$ & different levels of initially applied axial load, i.e., $Q (= \varepsilon_0/\varepsilon_y)$	49
Figure 5.11	Non-dimensional shear stress distribution along the half	50

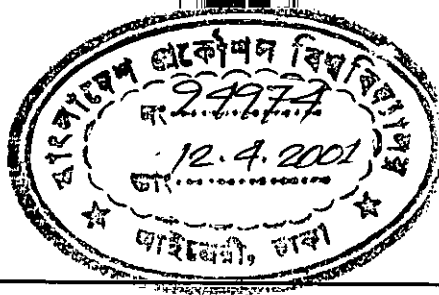
of the cross-section of a circular rod for the condition $\gamma/\gamma_y = 1.0$ & different levels of initially applied axial load, i.e., $Q (= \epsilon_0/\epsilon_y)$

- Figure 5.12** Variation of non-dimensional axial stress with subsequently applied axial strain for different levels of initial torque, when the circular bar is twisted first 51
- Figure 5.13** Variation of non-dimensional shear stress with subsequently applied axial strain for different values of initial torque, when the circular bar is twisted first 52
- Figure 5.14** Variation of non-dimensional shear stress with subsequently applied shear strain for different levels of initially applied axial load, when the circular bar is axially loaded first 53
- Figure 5.15** Variation of non-dimensional axial stress with subsequently applied axial strain for different levels of initially applied axial load, when the circular bar is axially loaded first 54
- Figure 5.16** Non-dimensional axial stress distribution along the half of the cross-section of a circular rod for different levels of subsequently applied axial strain for the condition P ($=\gamma_0/\gamma_y=1.0$) 55
- Figure 5.17** Non-dimensional shear stress distribution along the half of the cross-section of a circular rod for different levels of subsequently applied axial strain for the condition P ($=\gamma_0/\gamma_y=1.0$) 56
- Figure 5.18** Non-dimensional axial stress distribution along the half of the cross-section of a circular rod for different levels of subsequently applied shear strain for the condition Q ($=\epsilon_0/\epsilon_y=1.0$) 57
- Figure 5.19** Non-dimensional shear stress distribution along the half of the cross-section of a circular rod for different levels of subsequently applied shear strain for the condition Q ($=\epsilon_0/\epsilon_y=1.0$) 58
- Figure 5.20** Variation of normalized axial load and torque with subsequently applied normalized axial strain in a circular rod for CASE-I, i.e., $T_0/T_Y=1.0$ 59
- Figure 5.21** Variation of normalized axial load and torque with subsequently applied normalized shear strain in a circular rod for CASE-II, i.e., $F_0/F_Y=1.0$ 60

Figure 5.22	Variation of normalized torque with subsequently applied axial strain for different values of initial torque, when the circular bar is twisted first	61
Figure 5.23	Variation of normalized axial load with subsequently applied axial strain for different values of initial torque, when the circular bar is twisted first	62
Figure 5.24	Variation of normalized axial load with subsequently applied shear strain for different values of initially applied axial load, when the circular bar is extended first	63
Figure 5.25	Variation of normalized torque with subsequently applied shear strain for different values of initially applied axial load, when the circular bar is extended first	64
Figure 5.26	Comparison of the theoretical and experimental results of steel for CASE-I, when yield at 0.02% offset	65
Figure 5.27	Comparison of the theoretical and experimental results of steel for CASE-I, when yield at proportional limit	66
Figure 5.28	Comparison of the theoretical and experimental results of copper for CASE-I, when yield at 0.02% offset	67
Figure 5.29	Comparison of the theoretical and experimental results of copper for CASE-I, when yield at proportional limit	68
Figure 5.30	Comparison of the theoretical and experimental results of steel for CASE-II	69
Figure 5.31	Comparison of the theoretical and experimental results of copper for CASE-II	70
Figure 5.32	Comparison of the theoretical results obtained considering post yield flow stresses with the available experimental results of steel for CASE-I	71
Figure 5.33	Comparison of the theoretical results obtained considering post yield flow stresses with the available experimental results of steel for CASE-II	72
Figure 5.34	Comparison of the theoretical results obtained considering post yield flow stresses with the available experimental results of copper for CASE-I	73
Figure 5.35	Comparison of the theoretical results obtained considering post yield flow stresses with the available experimental results of copper for CASE-II	74

NOMENCLATURE

<p>a radius of the rod</p> <p>c elastic core radius</p> <p>E Young's modulus</p> <p>F axial load</p> <p>G shear modulus</p> <p>J polar moment of inertia</p> <p>J_2 second invariant</p> <p>l length</p> <p>P non-dimensional shear strain ($=\gamma_0/\gamma_Y$)</p> <p>Q non-dimensional axial strain ($=\varepsilon_0/\varepsilon_Y$)</p> <p>r radius</p> <p>T torque</p> <p>Y yield strength</p> <p style="text-align: center;">Greek</p> <p>ε axial strain</p> <p>$\bar{\varepsilon}$ effective strain</p>	<p>γ shear strain</p> <p>ξ non-dimensional radius ($=r/a$)</p> <p>η non-dimensional elastic core radius ($=c/a$)</p> <p>φ the total angle of twist</p> <p>σ axial stress</p> <p>$\bar{\sigma}$ effective stress</p> <p>τ shear stress</p> <p>θ angle of twist</p> <p style="text-align: center;">Subscript</p> <p>0 initial value</p> <p>e in elastic region</p> <p>p in plastic region</p> <p>oct octahedral</p> <p>Y, y yield value</p> <p>u ultimate load</p>
---	--



CHAPTER - ONE INTRODUCTION

1.1 GENERAL

The history of plasticity as a science began in 1864 when Tresca [1] published his results on punching and extrusion experiments and formulated his famous yield criterion. A few years later, using Tresca's results, Saint-Venant [2] and Levy [3] laid some of the foundations of the modern theory of plasticity. For the next 75 years progress was slow and spotty, although important contributions were made by von Mises [4], Hencky [5], Prandtl [6], and others. It is only since approximately 1945 that a unified theory began to emerge. Since that time, concentrated efforts by many researchers have produced a voluminous literature, which is growing at a rapid rate. Brief but excellent historical sketches are furnished by Hill [7] and Westergaard [8].

The theories of plasticity fall into two categories: physical theories and mathematical theories. The physical theories seek to explain why metals flow plastically. Looking at materials from a microscopic viewpoint, an attempt is made to determine what happens to the atoms, crystals, and grains of a material when plastic flow occurs. The mathematical theories, on the other hand, are phenomenological in nature and attempt to formalize. The eventual hope, of course, is for a merger of these two approaches into one unified theory of plasticity, which will both explain the material behavior and provide the engineer and scientist with the necessary tools for practical application. The present treatise is concerned with the second of these categories, i.e., the mathematical theories of plasticity and their application, as distinct from the physical theories.

In short, plasticity is the behavior of solid bodies in which they deform permanently under the action of external loads, whereas elasticity is the behavior of solid bodies in which they return to their original shape when the external force are removed. Actually, however, the elastic body is an idealization, because all bodies exhibit more or less plastic behavior even at the smallest loads. For the so-called

elastic body, however, this permanent deformation sufficiently small. Plasticity theory thus concerns itself with situations in which the loads are sufficiently large so that a measurable amount of permanent deformation occurs. It should further be noted that plastic deformation is independent of the time under load.

The theory of plasticity can conveniently be divided into two ranges. At one end are metal-forming processes such as forging, extrusion, drawing, rolling, etc., which involve very large plastic strains and deformations. For these types of problems the elastic strains can usually be neglected and the material can be assumed to be perfectly plastic. At the other end of the scale are a host of problems involving small plastic strains on the order of the elastic strains. These types of problems are of prime importance to the structural and machine designer. With the great premium currently placed on the saving of weight in aircraft, missile, and space applications, the designer can no longer use large factors of safety and beef up his design. He must design for maximum load to weight ratio, and this inevitably means designing into the plastic range. Even in more prosaic industrial applications the competitive market is forcing the application of more efficient design.

When a material is subjected to external forces its behavior depends not only upon the magnitudes of the forces and the inherent strength of the material itself, but also upon the way the forces are applied and combined. The particular combination of forces may cause the material to deform elastically, when on release of the forces it returns to its original dimensions; or the material may deform plastically, when a permanent change of shape occurs; or it may break. The amount of deformation, elastic or plastic, depends on the intensity of the forces at all points throughout the material.

1.2 JUSTIFICATION

The demands for assurance of quality and reliability in engineering structures or components have steadily increased over the past two decades. In mechanically fasten assemblies, reliability has frequently been assured by the simple expedient of overdesign. This results in additional cost, either in component costs or in running costs. However, pressure on costs has also been increasing, and there is a need to

eliminate overdesign while, at the same time, maintaining reliability. This can often be done by detailed analysis of working loads, component stress distribution, and materials capabilities. The design and assembling of bolted joints must assure that the joint remains tightly clamped when it is loaded. The fastener must be capable of withstanding the static and dynamic loads also.

When a bolt is tighten, it is subjected to both axial as well as torsional loading. From the simple torsion theory we know that maximum shear stress is developed at the outer surface of a circular rod. So when a bolt is tightened, yielding will start first at the outer periphery of the bolt. Furthermore, if the bolt is tightened upto or beyond the combined yields point of the material, how the material will behave with the application of further tightening or axial loading needs further investigation. As in the case of a bolted joint, there exists a complex relationship among tightening torque, pre-load and lubricant used, in the present investigation a simple circular rod has been used which has been subjected to similar type of loading. A lot of research has been done in tightening the bolts and their performance under combined load.

In assessing the ultimate load carrying capacity of some structures, it is frequently necessary to consider the elastic-plastic behavior of those parts. The stress distribution in most structural members loaded into the elastic-plastic range is difficult to determine, because the shape of the elastic-plastic interface itself is related to the stress distribution and is therefore unknown until the complete solution is found. However, for a solid rod subjected to combined torque and tension, this restriction is removed since the shape of the interface must be annular to preserve axial symmetry. If a circular rod is subjected to combined axial load and torsion, yielding will take place first at the outer surface of the rod. Upon reaching the yield locus, if further axial load or torque is gradually increased beyond the combined yield stress within the plastic region, holding the angle of twist or axial displacement constant, for an initial torque or axial load within the elastic range, the manner in which the subsequently applied parameter affects the magnitude of the initially applied parameter requires careful study. The findings of this work have direct bearing on the relaxation of tightening torque or axial loads as experienced by critical

engineering components, such as couplings, bolted joints and rotating shafts, which are subjected to similar type of bi-axial loading.

1.3 OBJECTIVES

The present work is done to examine the effects of the subsequently applied tensile load or torque on the variations of the initially applied torque or axial load of a circular rod respectively. This study has the following main objectives:

- a) To develop a theoretical model for the case when a circular rod will be subjected to combined torque-tension loading within the plastic region.
- b) To develop a computational scheme for obtaining the axial stress, shear stress, axial load and torque during the application of combined loading.
- c) To study the effect of subsequently applied tensile load on the variations of the initially applied torque.
- d) To study the effect of subsequently applied torque on the variations of the initially applied tensile load.
- e) To compare the present results with the available experimental results.

1.4 LAYOUT OF THE THESIS

For the convenience of presentation, the total contents of this thesis are divided into several chapters. In this chapter a brief introduction has been presented with aim, objectives and application. Chapter-2 consists of brief discussion on the available literatures related to the present investigation along with their limitations and scope of further work. In Chapter-3 and Chapter-4, a mathematical model has been presented along with numerical techniques and solutions. Chapter-5 consists of results and discussions on the numerical computation of the present investigation.

Finally, conclusions drawn from the present investigation are given in Chapter-6. This chapter also contains suggestions for further works in this field.

CHAPTER - TWO

LITERATURE SURVEY

2.1 GENERAL

Analysis of stress strain relation in combined loading in the plastic region has not been investigated to a great extent because of complexity of loading history and variety of influential parameters. Some of the problems, associated with it, are discussed in the previous chapter. Researchers put emphasis on a particular condition and mainly restricted themselves within the elastic region.

2.2 PREVIOUS WORK

It is well known that, under a uni-axial state of stress or a state of stress due to pure torsion, most materials exhibit the Bauschinger effect, i.e., possess a lower yield stress upon the reversal of the load. While under more general circumstances (such as a bi-axial state of stress), no experimental evidence seems to be available with regard to the shape of subsequent yield surfaces (or loading functions) beyond the initial yield, sufficient information is available to conclude that successive yield (or loading) surfaces are not merely blown-up versions of the original.

The incremental-strain theories of plasticity in general, and their stress-strain relations in particular, are dominated by the concept of a loading function which, corresponding to a given state of increments of stress, predicts the absence (during unloading and neutral loading) or presence (during loading) of additional increments of plastic strains. As plastic deformation is physically an anisotropic phenomenon in character, the loading function for a work-hardening material depends on the history of loading and exhibits Bauschinger effect as well as strain-hardening anisotropy, even if the material, in the unstrained state, is isotropic. In fact, as has been pointed out by Drucker [9] that an isotropic work-hardening theory of plasticity cannot properly predict a Bauschinger effect during plastic deformation. It is relevant to mention here that loading functions which account for various degrees of initial and strain-hardening anisotropy as well as a Bauschinger effect have been considered by

Drucker [10] and Edelman and Drucker[11], and that the difficulties of fitting mathematical theories of plasticity to experimental results are discussed by Stockton and Drucker [12]

Monaghan and Duff [13], Newnham *et al.*[14], Chapman *et al.*[15], Hagiwara *et al.*[16] and Hariri [17] have carried out experimental investigations on the behavior of the bolted joints in the elastic-plastic region. However, they all tested fasteners. Recently, Ali *et al.* [18-19] have carried out experimental investigations on the behavior of both copper and steel rods, which were subjected to similar type of bi-axial loading as has been considered in the present investigation. Analytical solutions for a solid rod of non-straining material under combined torque and tension loading, based upon the assumption of incompressibility, within the plastic region have been presented by Prager and Hodge [20] and Sved and Brooks [21]. However, in the present study a theoretical model has been developed to examine the elastic-plastic behavior of a circular rod under combined torque-tension loading within the plastic region for different levels of initial loading. Here particular attention has been given to observe the effects of subsequently applied axial load or torque on different levels of initial torque or axial loads of an elastic-perfectly plastic material.

2.3 YIELD CRITERION

2.3.1 Maximum Shear Theory or Tresca Criterion

This theory (sometimes called the Coulomb theory) assumes that yielding will occur when the maximum shear stress reaches the value of the maximum shear stress occurring under simple tension. The maximum shear stress is equal to half the difference between the maximum and minimum principal stresses. For simple tension, therefore, since $\sigma_2 = \sigma_3 = 0$, the maximum shear stress at yield is $1/2\sigma_Y$. The Tresca criterion then asserts that yielding will occur when any one of the following six conditions is reached:

$$\begin{aligned}\sigma_1 - \sigma_2 &= \pm\sigma_Y \\ \sigma_2 - \sigma_3 &= \pm\sigma_Y \\ \sigma_3 - \sigma_1 &= \pm\sigma_Y\end{aligned}\tag{2.1}$$

For the bi-axial case with $\sigma_3 = 0$, we have

$$\begin{aligned}
 \sigma_1 - \sigma_2 &= \sigma_Y && \text{if } \sigma_1 > 0, \sigma_2 < 0 \\
 \sigma_1 - \sigma_2 &= -\sigma_Y && \text{if } \sigma_1 > 0, \sigma_2 > 0 \\
 \sigma_2 &= \sigma_Y && \text{if } \sigma_2 > \sigma_1 > 0 \\
 \sigma_1 &= \sigma_Y && \text{if } \sigma_1 > \sigma_2 > 0 \\
 \sigma_1 &= -\sigma_Y && \text{if } \sigma_1 < \sigma_2 < 0 \\
 \sigma_2 &= -\sigma_Y && \text{if } \sigma_2 < \sigma_1 < 0
 \end{aligned} \tag{2.2}$$

It is to be noted that one limitation of this theory is the requirement that the yield stresses in tension and compression be equal. The Tresca criterion is in fair agreement with experiment and is used to a considerable extent by designers. It suffers, however, from one major difficulty-it is necessary to know in advance which are the maximum and minimum principal stresses. For the case of pure shear,

$$\sigma_1 = -\sigma_2 = k \quad \sigma_3 = 0 \tag{2.3}$$

the Tresca criterion predicts yielding to occur when

$$\sigma_1 - \sigma_2 = 2k = \sigma_Y$$

$$\text{or} \quad k = \frac{1}{2} \sigma_Y \tag{2.4}$$

This is, the yield stress in pure shear is $\frac{1}{2}$ the yield stress in simple tension.

2.3.2 Distortion Energy Theory, or von Mises Yield Criterion

The distortion energy theory (also associated with Hencky) assumes that yielding begins when the distortion energy equals the distortion energy at yield in simple tension. Thus,

$$U_d = \frac{1}{2G} J_a = \frac{3}{4G_{\text{oct}}} \tau_{\text{oct}}^2 \tag{2.5}$$

At the yield point in simple tension, from

$$J_2 = \frac{1}{3} \sigma_Y^2 \tag{2.6}$$

Therefore the yield condition becomes

$$\frac{1}{2} \left[(\sigma_1 - \sigma_2)^2 + (\sigma_2 - \sigma_3)^2 + (\sigma_3 - \sigma_1)^2 \right] = \sigma_Y^2 \tag{2.7}$$

and, for the biaxial case,

$$\sigma_1^2 - \sigma_1\sigma_2 + \sigma_2^2 = \sigma_0^2 \quad (2.8)$$

This plots as an ellipse, called the von Mises ellipse, in the σ_1 σ_2 plane. For the case of pure shear

$$\begin{aligned} \sigma_1 &= -\sigma_2 = k \quad \sigma_3 = 0 \\ J_2 &= \frac{1}{\sigma} \left[(\sigma_1 - \sigma_2)^2 + (\sigma_2 - \sigma_3)^2 + (\sigma_3 - \sigma_1)^2 \right] \\ &= \sigma_1^2 = k^2 \end{aligned} \quad (2.9)$$

and the von Mises criterion would predict yielding to occur when

$$k^2 = \frac{1}{3} \sigma_Y^2$$

$$\text{or} \quad k = \frac{\sigma_Y}{\sqrt{3}} \quad (2.10)$$

That is, the yield stress in pure shear is $1/\sqrt{3}$ times the yield stress in simple tension. Thus the von Mises criterion predicts a pure shear yield stress which is about 15 percent higher than predicted by the Tresca criterion. The von Mises yield criterion usually fits (but not always) the experimental data better than the other theories, and it is usually easier to apply than the Tresca criterion because no knowledge is needed regarding the relative magnitudes of the principal stresses. For these reasons, this criterion is widely used at the present time. If, however, the relative magnitudes of the principal stresses are known, as, for example, in the case of the thick-walled tube, the Tresca criterion is easier to apply.

Von Mises originally proposed his criterion because of mathematical convenience. Hencky later showed that it was equivalent to assuming that yielding will take place when the distortion or shear strain energy reaches a critical value, as shown above. Also, since the octahedral shear stress is equal to

$$\tau_{oct} = \frac{1}{3} \sqrt{(\sigma_1 - \sigma_2)^2 + (\sigma_2 - \sigma_3)^2 + (\sigma_3 - \sigma_1)^2} \quad (2.11)$$

which for simple tension at yield becomes

$$\tau_{oct,0} = \frac{\sqrt{2}}{3} \sigma_Y \quad (2.12)$$

That is, yielding will occur when the octahedral shear stress reaches the octahedral shear stress at yield in simple tension.

Alternatively, the criterion can be looked upon as stating that yielding will occur when the second invariant J_2 of the stress deviator tensor reaches a critical value, i.e., the value of J_2 at yield in simple tension. The assumption that the yield criterion should depend on the invariants of the stress deviator tensor is generally accepted, as will be discussed in the next section.

2.4 PLASTIC STRESS-STRAIN RELATIONS

The strains are linearly related to the stresses by Hooke’s law in the elastic range, the relation will generally be nonlinear in the plastic range, as is evident from the uniaxial stress-strain curve. A more complicated distinction between elastic and plastic stress-strain relations arises from the fact they whereas in the elastic range the strains are uniquely determined by the stresses, i.e., for a given set of stresses we can compute the strains directly using Hooke’s law without any regard as to how this stress state was attained, in the plastic range the strains are in general not uniquely determined by the stresses but depend on the whole history of loading or how the stress state was reached.

Consider the initial yield curve to be as shown in figure 2.1. Let the specimen be strained in uniaxial tension beyond the initial yield to some point C, where CDE defines the subsequent yield curve. The plastic strains will then be

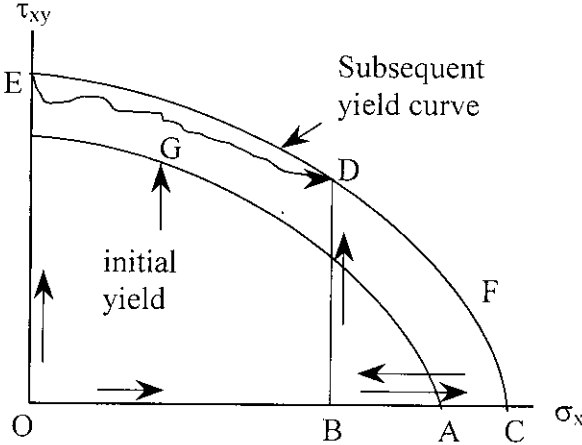


Fig.2.1 Effect of loading path on plastic strains

$$\begin{aligned}
\varepsilon_x^p &= \varepsilon_p \\
\varepsilon_y^p &= \varepsilon_z^p = -\frac{1}{2} \varepsilon_p \\
\varepsilon_{xy}^p &= \varepsilon_{yz}^p = \varepsilon_{zy}^p = 0
\end{aligned} \tag{2.13}$$

Let the specimen now be unloaded to the point B and let us apply a shear stress increasing from B to D on the new yield locus. The plastic strains will still be as given above. Any other path could have been used in arriving at D from C such as OCFD, such as EGD, were stressed to the point D. the plastic strains would be

$$\begin{aligned}
\varepsilon_{xy}^p &= \gamma_p \\
\varepsilon_x^p &= \varepsilon_y^p = \varepsilon_z^p = \varepsilon_{yz}^p = 0
\end{aligned} \tag{2.14}$$

which is obviously completely unrelated to the previous strain state. Thus even though the same stress states at D exist for both loading paths, and therefore the elastic strain states are the same, the plastic strain states are different.

Because of the above dependence of the plastic strains on the loading path, it becomes necessary, in general, to compute the differentials or increments of plastic strain throughout the loading history and then obtain the total strains by integration or summation.

2.5 PRANDTL-REUSS STRESS-STRAIN EQUATIONS

The first approach to plastic stress-strain relations was suggested by Saint-Venant in 1870[2], who proposed that the principal axes of strain increment coincided with the principal stress axes. The general three-dimensional equations relating the increments of total strain to the stress deviations were given by Levy in 1871[3] and independently by von Mises in 1931[4]. These are known as the Levy-Mises equations. These equations are

$$\frac{d\varepsilon_x}{S_x} = \frac{d\varepsilon_y}{S_y} = \frac{d\varepsilon_z}{S_z} = \frac{d\varepsilon_{yz}}{S_{yz}} = \frac{d\varepsilon_{zx}}{S_{zx}} = \frac{d\varepsilon_{xy}}{S_{xy}} = d\lambda \tag{2.15}$$

or $d\varepsilon_{ij} = S_{ij} d\lambda$

where S_{ij} is the stress deviator tensor and $d\lambda$ is a nonnegative constant, which may vary throughout the loading history. In these equations the total strain increments are assumed to be equal to the plastic strain increments, the elastic strains being ignored. Thus these equations can only be applied to problems of large plastic flow and cannot be used in the elasto-plastic range. The generalization of equation (2.15) to include both elastic and plastic components of strain is due to Prandtl [6] and Reuss [22] and is known as the Prandtl-Reuss equation.

Reuss assumed that the plastic strain increment is, at any instant of loading, proportional to the instantaneous stress deviation, i.e.,

$$\frac{d\varepsilon_x}{S_x} = \frac{d\varepsilon_y^p}{S_y} = \frac{d\varepsilon_z^p}{S_z} = \frac{d\varepsilon_{xz}^p}{\tau_{xy}} = \frac{d\varepsilon_{yz}^p}{\tau_{yz}} = \frac{d\varepsilon_{zx}^p}{\tau_{zx}} = d\lambda \quad (2.16)$$

$$\text{or} \quad d\varepsilon_{ij}^p = S_{ij} d\lambda$$

Equation (2.15) can then be considered as a special case of (2.16) where the elastic strain components are neglected.

Equations (2.16) state that the increments of plastic strain depend on the current values of the deviatoric stress state, not on the stress increment required to reach this state. They also imply that the principal axes of stress and of plastic strain increment tensors coincide. The equations themselves merely give a relationship between the ratios of plastic strain increments in different directions. If the principal directions are considered, equation (2.16) can be written

$$\frac{d\varepsilon_1^p}{S_1} = \frac{d\varepsilon_2^p}{S_2} = \frac{d\varepsilon_3^p}{S_3} = d\lambda$$

$$\text{or} \quad d\varepsilon_1^p = S_1 d\lambda \quad d\varepsilon_2^p = S_2 d\lambda \quad d\varepsilon_3^p = S_3 d\lambda \quad (2.17)$$

$$\text{or} \quad \frac{d\varepsilon_1^p - d\varepsilon_2^p}{S_1 - S_2} = \frac{d\varepsilon_2^p - d\varepsilon_3^p}{S_2 - S_3} = \frac{d\varepsilon_3^p - d\varepsilon_1^p}{S_3 - S_1} = d\lambda \quad (2.18)$$

The numerators of the first three term's in equation (2.18) are the diameters of the three Mohr's circles for the plastic strain increments and the denominators are the diameters of Mohr's stress circles. Equations (2.18) therefore imply that the Mohr's circles of stress and plastic strain increment are similar. Also from the

relations for the principal shears, equations (2.18) can be considered as stating that the ratios of the three principal plastic shear strain increments to the principal shear stresses are constant at any instant.

Equation (2.16) can be written in terms of the actual stresses as

$$\begin{aligned}
 d\varepsilon_x^p &= \frac{2}{3} d\lambda \left[\sigma_x - \frac{1}{2}(\sigma_y + \sigma_z) \right] \\
 d\varepsilon_y^p &= \frac{2}{3} d\lambda \left[\sigma_y - \frac{1}{2}(\sigma_z + \sigma_x) \right] \\
 d\varepsilon_z^p &= \frac{2}{3} d\lambda \left[\sigma_z - \frac{1}{2}(\sigma_x + \sigma_y) \right] \\
 d\varepsilon_{xy}^p &= d\lambda \tau_{xy} \\
 d\varepsilon_{yz}^p &= d\lambda \tau_{yz} \\
 d\varepsilon_{zx}^p &= d\lambda \tau_{zx}
 \end{aligned} \tag{2.19}$$

Therefore, if $d\lambda$ were known, we would have the desired stress-strain relations. To determine $d\lambda$ use is made of the yield criterion as follows. By means of equations (2.16).

$$\begin{aligned}
 & \left(d\varepsilon_x^p - d\varepsilon_y^p \right)^2 + \left(d\varepsilon_y^p - d\varepsilon_z^p \right)^2 + \left(d\varepsilon_z^p - d\varepsilon_x^p \right)^2 + 6 \left(d\varepsilon_{xy}^p \right)^2 + 6 \left(d\varepsilon_{yz}^p \right)^2 + 6 \left(d\varepsilon_{zx}^p \right)^2 \\
 &= (d\lambda)^2 \left[(\sigma_x - \sigma_y)^2 + (\sigma_y - \sigma_z)^2 + (\sigma_z - \sigma_x)^2 + 6\tau_{xy}^2 + 6\tau_{yz}^2 + 6\tau_{zx}^2 \right]
 \end{aligned} \tag{2.20}$$

The bracketed quantity on the right side of equation (2.20) is seen to be proportional to the square of the octahedral shear stress and the left side is proportional to the square of the increment of octahedral plastic shear strain defined by

$$\left(d\gamma_0^p \right)^2 = \frac{1}{9} \left[\left(d\varepsilon_x^p - d\varepsilon_y^p \right)^2 + \left(d\varepsilon_y^p - d\varepsilon_z^p \right)^2 + \left(d\varepsilon_z^p - d\varepsilon_x^p \right)^2 + 6 \left(d\varepsilon_{xy}^p \right)^2 + 6 \left(d\varepsilon_{yz}^p \right)^2 + 6 \left(d\varepsilon_{zx}^p \right)^2 \right] \tag{2.21}$$

The constant $d\lambda$ now becomes

$$d\lambda = \frac{d\gamma_0^p}{\tau_{\text{oct}}} = \sqrt{\frac{3}{2}} \frac{d\gamma_0^p}{\sqrt{J_2}} \tag{2.22}$$

where J_2 is the second invariant of the stress deviator tensor.

It is convenient to define an equivalent or effective stress and an equivalent or effective plastic strain increment as

$$\begin{aligned}
\sigma_e &\equiv \frac{1}{\sqrt{2}} \left[(\sigma_x - \sigma_y)^2 + (\sigma_y - \sigma_z)^2 + (\sigma_z - \sigma_x)^2 + 6(\tau_{xy}^2 + \tau_{yz}^2 + \tau_{zx}^2) \right]^{1/2} \\
&= \frac{3}{\sqrt{2}} \tau_{oct} \\
&= \sqrt{3} J_2
\end{aligned} \tag{2.23}$$

and

$$\begin{aligned}
d\varepsilon_p &\equiv \frac{\sqrt{2}}{3} \left[(d\varepsilon_x^p - d\varepsilon_y^p)^2 + (d\varepsilon_y^p - d\varepsilon_z^p)^2 + (d\varepsilon_z^p - d\varepsilon_x^p)^2 + 6(d\varepsilon_{xy}^p)^2 \right]^{1/2} \\
&\quad + 6(d\varepsilon_{yz}^p)^2 + 6(d\varepsilon_{zx}^p)^2 \\
&= \sqrt{2} d\gamma_0^p
\end{aligned} \tag{2.24}$$

For an uni-axial tensile test in the x direction the equivalent stress and equivalent plastic strain increment reduce to

$$\begin{aligned}
\sigma_e &= \sigma_x \\
d\varepsilon_p &= d\varepsilon_x^p
\end{aligned} \tag{2.25}$$

The convenience of the above definitions now becomes apparent. The equivalent or effective stress, σ_e and the equivalent or effective plastic strain increment, $d\varepsilon_p$, will henceforth be used in this text rather than the octahedral shear stress and octahedral plastic shear strain increment.

The constant $d\lambda$ can therefore be written

$$d\lambda = \frac{3}{2} \frac{d\varepsilon_p}{d\varepsilon_x^p} \tag{2.26}$$

and the stress-strain relations[2.19] become

$$\begin{aligned}
d\varepsilon_x^p &= \frac{d\varepsilon_p}{\sigma_e} \left[\sigma_x - \frac{1}{2}(\sigma_y + \sigma_z) \right] \\
d\varepsilon_y^p &= \frac{d\varepsilon_p}{\sigma_e} \left[\sigma_y - \frac{1}{2}(\sigma_z + \sigma_x) \right] \\
d\varepsilon_z^p &= \frac{d\varepsilon_p}{\sigma_e} \left[\sigma_z - \frac{1}{2}(\sigma_x + \sigma_y) \right] = -(d\varepsilon_x^p + d\varepsilon_y^p)
\end{aligned} \tag{2.27}$$

$$\begin{aligned}
 d\varepsilon_{xy}^p &= \frac{3}{2} \frac{d\varepsilon_p}{\sigma_e} \tau_{xy} \\
 d\varepsilon_{yz}^p &= \frac{3}{2} \frac{d\varepsilon_p}{\sigma_e} \tau_{yz} \\
 d\varepsilon_{zx}^p &= \frac{3}{2} \frac{d\varepsilon_p}{\sigma_e} \tau_{zx}
 \end{aligned}
 \tag{2.28}$$

$$\text{or} \quad d\varepsilon_{ij}^p = \frac{3}{2} \frac{d\varepsilon_p}{\sigma_e} S_{ij}
 \tag{2.29}$$

if one compares equation (2.23) for the equivalent stress σ_e with equation (2.7), which gives the von Mises yield criterion, it is seen that just as yielding begins when

$$\sigma_e = \sigma_Y
 \tag{2.30}$$

where σ_Y is the yield stress in simple tension. The equivalent stress is thus the same as the von Mises yield function, and since equations (2.26) make use this function, the original Prandtl-Reuss assumptions imply the von Mises yield criterion.

CHAPTER - THREE

MATHEMATICAL MODEL

3.1 GENERAL

In this chapter mathematical models for pure tension, torsion and combined tension-torsion are described. The behavior of a material under any combination of loading can be easily analyzed by using simple tension or pure torsion test. In case of pure torsion test it is complicated to calculate the shear stress and strain graph from the torque-angle of twist graph, and vice versa, in the plastic region. So special relation is used in the plastic region. But in most practical cases, some complexity is always introduced due to combined loading specially in the plastic region because of various types of loading and the loading history. In the present investigation two cases of combined loading are considered, one is torsion followed by tension and the other is tension followed by torsion, where in the first case the angle of twist is held constant and in the second case the axial displacement is held constant.

3.2 CYLINDRICAL BARS UNDER DIFFERENT TYPES OF LOADINGS

3.2.1 Simple Tension Test

To know the mechanical properties of a material the simplest and the most important experiment is the standard tensile test. Initially the relation between stress and strain is essentially linear. This linear part of the curve is called the proportional limit. It is in this range that the linear theory of elasticity, using Hook's law, is valid. Upon further increase of the load, the strain no longer increases linearly with stress, but the material still remains elastic; i.e., upon removal of the load the specimen returns to its original length. This condition will prevail until some point, called the elastic limit, or yield point. In most materials there is very little difference between the proportional limit and the elastic limit. For some materials the yield point is defined by using a fixed value of permanent strain. Beyond the elastic limit, permanent deformation, called plastic deformation, takes place. As the load is

increased beyond the elastic limit, the strain increases at a greater rate. However, the specimen will not deform further unless the load is increased. This called work hardening, or strain hardening. The stress required for further plastic flow is called flow stress. Finally a point is reached, where the load is a maximum. Beyond this point, called the point of maximum load, or point of instability, the specimen necks down. The stress at the maximum load point is called the tensile strength, or ultimate stress.

If at any point between the elastic limit and the maximum load point the load is removed, unloading will take place along a line parallel to the elastic. Part of the strain is thus recovered and part remains permanently. The total strain can therefore be considered as being made up of two parts, ε^e , the elastic component, and ε^p , the plastic component:

$$\varepsilon = \varepsilon^e + \varepsilon^p \quad (3.1)$$

3.2.2 Pure Torsion Test

When a solid cylindrical bar of radius a , subjected to a twisting moment T . As long as the bar is elastic, the shear stress acting over any cross section is proportional to the radial distance r from the central axis. The applied torque T is the resultant moment of the stress distribution about this axis. If the angle of twist per unit length of the bar is denoted by θ , the elastic shear stress may be written as

$$\tau = Gr\theta = \frac{2Tr}{\pi a^4} \quad (3.2)$$

Since the shear stress has its greatest value at $r = a$, the bar begins to yield at this radius when the torque is increased to T_e , the corresponding twist being θ_e . Setting $\tau = k$ at $r = a$, we get

$$T_e = \frac{1}{2} \pi k a^3 \quad \theta_e = \frac{k}{Ga} \quad (3.3)$$

If the torque is increased further, a plastic annulus forms near the boundary, leaving a central zone of elastic material within a radius c (figure 3.1). The stress distribution in the elastic region is linear, with the shear stress reaching the value k at

$r = c$. For a non-hardening material, the shear stress has the constant value k throughout the plastic region, and the stress distribution becomes

$$\begin{aligned} \tau &= k \frac{r}{c} & 0 \leq r \leq c \\ \tau &= k & c \leq r \leq a \end{aligned} \quad (3.4)$$

Since the shear stress within the elastic zone is also equal to $Gr\theta$, we have $\theta = \frac{k}{Gc}$.

The twisting moment is

$$T = 2\pi \int_0^a \tau r^2 dr = \frac{2}{3} \pi k \left(a^3 - \frac{1}{4} c^3 \right) = \frac{1}{3} T_e \left\{ 4 - \left(\frac{\theta_e}{\theta} \right)^3 \right\} \quad (3.5)$$

As the elastic/plastic torsion continues, the torque rapidly approaches the fully plastic value $\frac{2}{3} \pi k a^3$. Since θ tends to infinity as c tends to zero, an elastic core of material must exist for all finite values of the angle of twist.

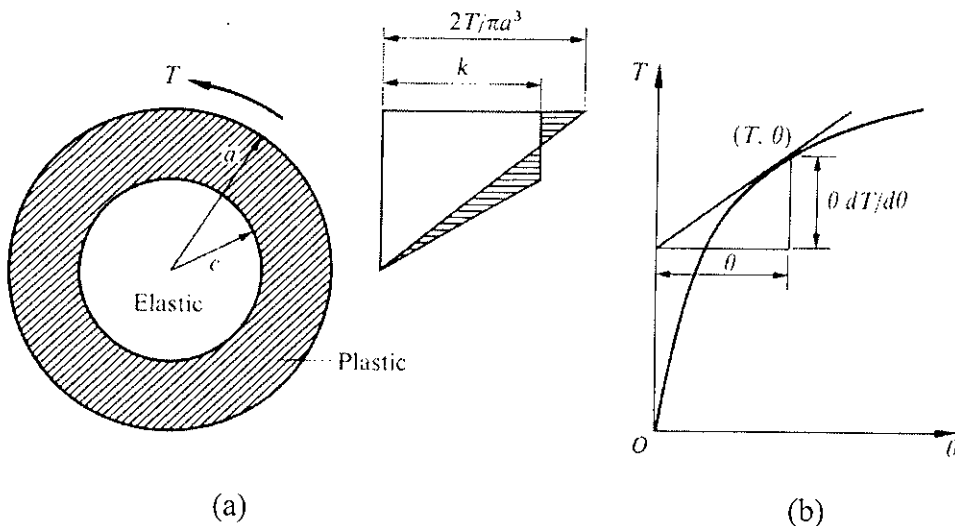


Figure 3.1: Torsion of a solid cylindrical bar. (a) Plastic annulus and stress distribution for $H=0$; (b) Torque-angle of twist relationship

In the case of an annealed material, there is no well-defined yield point, and the elastic/plastic boundary is therefore absent. Since the engineering shear strain at any radius r is $\gamma = r\theta$, the torque may be expressed as

$$T = 2\pi \int_0^a \tau r^2 dr = \frac{2\pi}{\theta^3} \int_0^a \tau \gamma^2 d\gamma \quad (3.6)$$

When the shear stress-strain curve of the material is given, the torque can be calculated from above, using the known (τ, γ) relationship. Conversely, if the torque-twist relationship for a solid bar has been experimentally determined, the shear stress-strain curve can be easily derived from it. The differentiation of the above equation with respect to θ gives

$$\frac{d}{d\theta} (T\theta^3) = 2\pi a^3 \theta^2 \tau_o \quad (3.7)$$

where τ_o is the value of τ at $r = a$ where the shear strain is $\gamma_o = a\theta$. The relationship between τ_o and γ_o is therefore given by

$$\tau_o = \frac{1}{2\pi a^3} \left(\theta \frac{dT}{d\theta} + 3T \right) \quad \gamma_o = a\theta \quad (3.8)$$

The geometrical significance of the first term in the bracket is indicated in Figure 3.1b. Since $dT/d\theta$ must be obtained numerically or graphically from the measured (T, θ) curve, the computation based on equation (3.8) is not very accurate for the initial part of the curve. The accuracy may, however, be improved by rewriting the shear stress as

$$\tau_o = \frac{1}{2\pi a^3} \left\{ \theta^2 \frac{dT}{d\theta} \left(\frac{T}{\theta} \right) + 4T \right\} \quad (3.9)$$

The ratio T/θ is constant in the elastic range, and decreases slowly over the initial part of the plastic range. The contribution of the first term in the bracket is therefore small over this part.

3.2.3 Combined Torsion and Tension

A solid cylindrical bar of radius a and length l is subjected to any combination of twist and axial extension. While the deformation is elastic, the longitudinal stress σ is constant over the cross section, and the shear stress τ is directly proportional to the radial distance r from the axis. It follows the yielding first occurs at $r = a$ when the stresses satisfy the von Mises yield criterion

$$\sigma^2 + 3\tau^2 = Y^2 \quad (3.10)$$

When the loading is continued into the plastic range, so that the radius to the elastic-plastic boundary is c , the stresses in the elastic region for an incompressible material are

$$\sigma = 3G\varepsilon \quad \tau = \frac{Gr\phi}{l} \quad 0 \leq r \leq c \quad (3.11)$$

where ε is the total longitudinal strain and ϕ the total angle of twist. In the plastic region ($c \leq r \leq a$), the Prandtl-Reuss stress-strain equations give

$$\begin{aligned} d\varepsilon &= \frac{dl}{l} = \frac{d\sigma}{3G} + \frac{2}{3}\sigma d\lambda \\ d\gamma &= \frac{rd\phi}{2l} = \frac{d\tau}{2G} + \tau d\lambda \end{aligned} \quad (3.12)$$

Case-I: Torsion followed by tension

Suppose that a cylindrical bar of radius a is first twisted elastically and then extended into the elastic/plastic range by an increasing axial load. The angle of twist of the bar is maintained at a constant value θ_0 per unit length during the extension. Yielding begins at the outer radius when the longitudinal strain is ε_0 , the corresponding axial stress being $3G\varepsilon_0$ for an incompressible material. Since the shear stress is $Ga\theta_0$ at $r = a$, the relationship between θ_0 and ε_0 is

$$a^2\theta_0^2 + 3\varepsilon_0^2 = \frac{Y^2}{3G^2} \quad (3.13)$$

in view of the von Mises yield criterion. Subsequently, when the bar is plastic to a radius c , the stresses in the elastic zone corresponding to an axial strain ε are

$$\sigma = 3G\varepsilon \quad \tau = Gr\theta_0 \quad 0 \leq r \leq c \quad (3.14)$$

Since the element at $r = c$ must be at the point of yielding, the radius to the elastic/plastic boundary is given by

$$c^2\theta_0^2 + 3\varepsilon^2 = \frac{Y^2}{3G^2} \quad (3.15)$$

In the plastic region, the stresses must satisfy the von Mises yield criterion (3.10) and the Prandtl-Reuss stress-strain equations (3.12), where $d\gamma = 0$. When $d\gamma = 0$ then

from equation (3.12), we get $d\lambda = -d\tau/2G\tau$ and for von Mises criterion $d\tau = -\sigma.d\sigma/3\tau$. Eliminating $d\lambda$, and substituting the value of $d\tau/\tau$, we obtain

$$3G d\varepsilon = \frac{Y^2 d\sigma}{Y^2 \sigma^2} \quad (3.16)$$

which is readily integrated to

$$\frac{3G}{Y} \varepsilon = \tanh^{-1} \left(\frac{\sigma}{Y} \right) + \text{const} \quad c \leq r \leq a \quad (3.17)$$

The constant of integration must be determined from the condition that

$$\sigma = 3G\varepsilon = \sqrt{Y^2 - 3G^2 r^2 \theta_0^2} \quad (3.18)$$

when an element at radius r first becomes plastic. Hence the tensile stress in the plastic region ($c \leq r \leq a$) is given by

$$\frac{\sigma}{Y} = \tanh \left(\frac{3G}{Y} \varepsilon - \sqrt{1 - \frac{3G^2}{Y^2} r^2 \theta_0^2} + \tanh^{-1} \sqrt{1 - \frac{3G^2}{Y^2} r^2 \theta_0^2} \right) \quad (3.19)$$

The shear stress in the plastic region follows from (3.19) and the von Mises yield criterion (3.10). The variations of load and torque with extension can be calculated numerically if required.

If the bar is initially twisted to an extent that makes it just plastic at $r = a$, then $Ga\theta_0 = Y\sqrt{3}$ and $\varepsilon_0 = 0$. Substituting in equation (3.19), the stress distribution in the plastic region is obtained as

$$\frac{\sigma}{Y} = \tanh \left(\frac{3G}{Y} \varepsilon - \sqrt{1 - \frac{r^2}{a^2}} + \tanh^{-1} \sqrt{1 - \frac{r^2}{a^2}} \right) \quad (3.20)$$

The bar becomes completely plastic ($c=0$) when $\varepsilon = Y/3G$, giving $\sigma/Y = \tanh 1 \sim 0.762$ at $r = a$. If the extension is continued in the fully plastic range, equation (3.20) holds over the entire cross section of the bar. The stresses σ and τ at the boundary $r = a$ approach their asymptotic values Y and zero respectively as the strain is increased. The approach is so rapid that σ is within 0.5 percent of Y when ε is only equal to Y/G .

Case-II: Tension followed by torsion

Consider now the situation where the bar is first extended to produce an axial strain ϵ_0 elastically, and then twisted by a gradually increasing torque while the extension is held constant. The bar begins to yield at the outer radius again when the angle of twist per unit length is θ_0 , given by (3.13). When the specific angle of twist θ is large enough to render the bar plastic to a radius c , the stresses in the elastic region are

$$\sigma = 3G\epsilon_0 \quad \tau = Gr\theta \quad 0 \leq r \leq c \quad (3.21)$$

Since the material at $r = c$ is at the point yielding,

$$c^2\theta^2 + 3\epsilon_0^2 = \frac{Y^2}{3G^2} \quad (3.22)$$

Setting $d\epsilon = 0$ and $d\phi = l d\theta$ in the Prandtl-Reuss stress-strain equations (3.12), we get $d\lambda = -d\sigma/2\gamma\sigma$ and for von Mises criterion $d\sigma = -3\tau.d\tau/\sigma$. Eliminating $d\lambda$ and substituting the value of $d\tau/\tau$, we obtain the differential equation

$$Gr d\theta = \frac{Y^2 d\tau}{Y^2 - 3\tau^2} \quad (3.23)$$

in view of (3.10). The integration of the above equation gives

$$\frac{\sqrt{3}G}{Y} r\theta = \tanh^{-1}\left(\frac{\sqrt{3}\tau}{Y}\right) + const \quad c \leq r \leq a \quad (3.24)$$

When an element first becomes plastic, its tensile stress is $\sigma_0 = G\epsilon_0$, the corresponding shear stress being given by

$$\sqrt{3}\tau = \sqrt{Y^2 - \sigma_0^2} = \sqrt{3}Gr\theta \quad (3.25)$$

The constant of integration follows from this initial condition, and the shear stress in the plastic region ($c \leq r \leq a$) finally becomes

$$\frac{\sqrt{3}\tau}{Y} = \tanh\left(\frac{\sqrt{3}G}{Y} r\theta - \sqrt{1 - \frac{\sigma_0^2}{Y^2}} + \tanh^{-1}\sqrt{1 - \frac{\sigma_0^2}{Y^2}}\right) \quad (3.26)$$

The tensile stress in the plastic region then follows from the yield criterion. If the bar is initially extended just to the yield point before the torque is applied, $\sigma_0 = Y$ and $\theta_0 = 0$, giving

$$\frac{\sqrt{3}\tau}{Y} = \tanh\left(\frac{\sqrt{3}G}{Y}r\theta\right) \quad \frac{\sigma}{Y} = \operatorname{sech}\left(\frac{\sqrt{3}G}{Y}r\theta\right) \quad (3.27)$$

These expressions hold throughout the cross section of the bar, which is now completely plastic. When $a\theta$ is equal to $\sqrt{3} Y/G$, the value of $\sqrt{3} \tau$ at $r = a$ is already within 0.5 percent of Y .

3.3 EFFECTIVE STRESS AND STRAIN

A convenient mathematical formulation for strain hardening is obtained by assuming further that the yield surface uniformly expands without change in shape. Since the yield locus merely increases in size, any given state of hardening may be defined by the current yield stress in uniaxial tension. It is, therefore, necessary to relate the current yield yielding. To this end, we replace Y in the yield criterion by σ , which is known as the equivalent stress, effective stress, or generalized stress. Referring to the von Mises

$$\bar{\sigma} = \sqrt{\frac{1}{2} \left\{ (\sigma_x - \sigma_y)^2 + (\sigma_y - \sigma_z)^2 + (\sigma_z - \sigma_x)^2 + 6\tau_{xy}^2 + 6\tau_{yz}^2 + 6\tau_{zx}^2 \right\}} \quad (3.28)$$

For bi-axial tension and torsion, $\sigma_x = \sigma$, $\sigma_y = \sigma_z = 0$, $\tau_{xy} = \tau$ and $\tau_{yz} = \tau_{zx} = 0$, putting these values in equation 3.30 we get

$$\bar{\sigma} = \sqrt{\sigma^2 + 3\tau^2} \quad (3.29)$$

The simplest measure of generalized strain, suggested by Dorn (1945), is the “effective strain” $\bar{\epsilon}$ defined as

$$\bar{\epsilon} = \frac{\sqrt{2}}{3} \sqrt{(\epsilon_1 - \epsilon_2)^2 + (\epsilon_2 - \epsilon_3)^2 + (\epsilon_3 - \epsilon_1)^2} \quad (3.30)$$

This is proportional to the “octahedral shear strain”. According to the effective-strain measure of generalized strain, a body under multi-axial stress has the same amount of strain hardening as a tensile specimen when the effective strain $\bar{\epsilon}$ equals the plastic tensile strain in the tensile specimen ϵ_0 .

CHAPTER - FOUR

NUMERICAL SOLUTION

4.1 GENERAL

In a deformable body subjected to external loads of gradually increasing magnitude, plastic flow begins at a stage when the yield criterion is first satisfied in the most critically stressed element. Further increase in loads causes spreading of the plastic zone, which is separated from the elastic material by an elastic-plastic boundary. The position of the boundary is an unknown of the problem, and is generally so complicated in shape that the solution of the boundary-value problem often involves numerical methods. The solution must be carried out in a succession of small increments of strain even when the deformation is restricted to elastic stresses and displacements in the elastic and plastic regions satisfy the conditions of continuity across the elastic-plastic boundary. In this chapter mainly numerical procedure of the solution of two cases of combined torsion and tension loading in the elastic-plastic region (Case-I: Torsion followed by tension and Case-II: Tension followed by torsion) are described.

4.2 NUMERICAL PROCEDURE

4.2.1 Torsion Followed by Tension for Constant Angle of Twist

To obtain the numerical values of torque with the change of axial strain, for different levels of initial torque equation (3.19) can be modified as

$$\frac{\sigma}{Y} = \tanh \left(\frac{\epsilon}{\epsilon_y} \sqrt{1 - P^2 \xi^2} + \tanh^{-1} \sqrt{1 - P^2 \xi^2} \right) \quad (4.1)$$

where ϵ_y is the yield strain in tension, $P = \gamma_0 / \gamma_y$, $\xi = r/a$, γ_0 is the corresponding shear strain of the initially applied torque which is to be calculated at the outer surface of the cylinder and γ_y is the yield shear strain. Thus different values of P for different levels of initial torque, i.e., different levels of initial shear strains within the elastic and up to the yield point regime, can be set into the above equation. Then to calculate

the numerical values of F/F_y for a specific value of ε ($=\varepsilon/\varepsilon_y$), equation (4.1) is to be integrated over the entire cross-section of the bar. Considering a axial load, F is applied to a solid rod with cross-sectional area, A then stress developed is calculated from

$$\sigma = \frac{F}{A} \quad (4.2)$$

if the radius of the solid is r then we can write the above equation in the following form

$$F = \sigma \cdot \pi r^2 \quad \text{or} \quad dF = \sigma \cdot 2\pi r \cdot dr \quad (4.3)$$

But $r = a\xi$ where a is the outer radius of a rod so, $dr = a \cdot d\xi$, putting the value of dr in the equation (4.3), we get $dF = \sigma \cdot 2\pi a^2 \xi d\xi$, hence by using equation (4.1) we get

$$\frac{dF}{\sigma_y \cdot 2\pi a^2 \cdot \xi d\xi} = \tanh \left[\frac{\varepsilon}{\varepsilon_y} - \sqrt{1 - P^2 \xi^2} + \tanh^{-1} \sqrt{1 - P^2 \xi^2} \right] \quad (4.4)$$

and finally we found the differential form of equation

$$\frac{dF}{F_y} = 2\xi \cdot \tanh \left[\frac{\varepsilon}{\varepsilon_y} - \sqrt{1 - P^2 \xi^2} + \tanh^{-1} \sqrt{1 - P^2 \xi^2} \right] d\xi \quad (4.5)$$

where $F_y = \sigma_y \cdot 2\pi a^2$

Integrating equation (4.5) form $\xi=0.0$ to $\xi=1.0$ we get

$$\frac{F}{F_y} = 2 \int_0^1 \xi \cdot \tanh \left[\frac{\varepsilon}{\varepsilon_y} - \sqrt{1 - P^2 \xi^2} + \tanh^{-1} \sqrt{1 - P^2 \xi^2} \right] d\xi \quad (4.6)$$

The values of shear stress can be calculated from the following equation by knowing the different values of σ/Y from equation (4.1).

$$\frac{\tau}{\tau_y} = \frac{\sqrt{3}\tau}{Y} = \sqrt{1 - \left(\frac{\sigma}{Y} \right)^2} \quad (4.7)$$

For calculating the values of T/T_y , considering a torque T is applied to a solid rod then stresses developed due to the torque is

$$\tau = \frac{Tr}{J} \quad (4.8)$$

where τ = shear stress, r = radius & J = polar moment of inertia = $\pi r^4/2$

Considering an element dr in a distance r , if a force F is applied in the element to developed a torque dT then $dT = \tau 2\pi r^2 dr$, but $\tau_y = T_y a/J = 2T_y/\pi a^3$ hence $T_y = \tau_y \cdot \pi a^3/2$. Now,

$$\frac{dT}{T_y} = 4 \left(\frac{r^2}{a^3} \right) \frac{\tau}{\tau_y} dr \quad (4.9)$$

Since $dr = a d\xi$

$$\text{So, } \frac{dT}{T_y} = 4\xi^2 \frac{\tau}{\tau_y} d\xi \quad (4.10)$$

However, during the present investigation as variations of torque with the axial strains are to be plotted, the numerical values of torque can be calculated by direct integration of equation (4.10) between $\xi=0.0$ to $\xi=1.0$, which is

$$\frac{T}{T_y} = 4 \int_0^1 \xi^2 \frac{\tau}{\tau_y} d\xi \quad (4.11)$$

Finally by using the equation (4.7), we get

$$\frac{T}{T_y} = 4 \int_0^1 \xi^2 \sqrt{1 - \left(\frac{\sigma}{Y} \right)^2} d\xi \quad (4.12)$$

The above equation was numerically calculated using Simpson's rule for the increment of $\Delta\xi=0.1$. However if the bar becomes plastic only up to η , where $\eta=c/a$, then the integration is to be performed over $\xi = \eta$ to 1.0 and, torque in the elastic core (i.e., for the range $\xi = 0$ to η) can be found from the elastic theory. Then the total torque becomes

$$\frac{T}{T_y} = \left(\frac{\tau_e}{\tau_y} \right) \eta^3 + 4 \int_{\xi=\eta}^1 \xi^2 \sqrt{1 - \left(\frac{\sigma}{Y} \right)^2} d\xi \quad (4.13)$$

where τ_e is the maximum elastic shear stress at the layer $\xi = \eta$, which is a constant, and τ_p is the shear stress within the plastic region which varies along ξ . During the determination of the numerical values of torque, it was assumed, that once the yielding starts at the outer fiber of the bar due to combined loading, the elastic-plastic boundary η moves inwards in such a way that $\Delta\epsilon = \Delta\eta$. However, for any values of

initial shear stresses for which yielding begins can be found from the yield criteria, which can be written as

$$\left(\frac{\gamma}{\gamma_y}\right)^2 + \left(\frac{\varepsilon}{\varepsilon_y}\right)^2 = 1 \quad (4.14)$$

When $\varepsilon/\varepsilon_y = 1.0$, equation (4.12) is valid over the entire cross-section of the bar. But for elastic-plastic case equation (4.13) is used to plots T/T_y for different initial values of P , such as P equal to 1.0, 0.75, 0.50 and 0.25.

4.2.2 Tension Followed by Torsion for Constant Axial Displacement

To calculate the numerical values of axial load with shear strain, for different levels of initial load equation (3.26) can be modified as

$$\frac{\tau}{\tau_y} = \tanh\left(\frac{\gamma}{\gamma_y} \xi - \sqrt{1-Q^2} + \tanh^{-1} \sqrt{1-Q^2}\right) \quad (4.15)$$

where γ_y is the yield shear strain and $Q = \varepsilon_0/\varepsilon_y$. Thus different levels of initial load, and hence its corresponding different levels of initial axial strains, within elastic and up to the yield point can be set into the above equation by changing the values of Q . During the present investigation as variations of torque with the shear strains are to be plotted, the numerical values of torque are calculated by direct integration of equation (4.15) between $\xi=0.0$ to $\xi=1.0$, which is (from equation (4.10))

$$\frac{T}{T_y} = 4 \int_0^1 \xi^2 \frac{\tau}{\tau_y} d\xi \quad (4.16)$$

By using equation (4.15) we get

$$\frac{T}{T_y} = 4 \int_0^1 \xi^2 \tanh\left(\frac{\gamma}{\gamma_y} \xi - \sqrt{1-Q^2} + \tanh^{-1} \sqrt{1-Q^2}\right) d\xi \quad (4.17)$$

The values of axial stress can be calculated from the following equation by knowing the different values of τ/τ_y from equation (4.15).

$$\frac{\sigma}{\sigma_y} = \frac{\sigma}{Y} = \sqrt{1 - \left(\frac{\tau}{\tau_y}\right)^2} \quad (4.18)$$

However, during the present investigation as the variations of the axial load with the shear strain is required to plot, the numerical values of axial load can be obtained by Integrating dF/F_Y form $\xi=0.0$ to $\xi=1.0$ we get

$$\frac{F}{F_Y} = 2 \int_0^1 \xi \cdot \frac{\sigma}{\sigma_y} d\xi \quad (4.19)$$

using equation (4.18), we get

$$\frac{F}{F_Y} = 2 \int_0^1 \xi \sqrt{1 - \left(\frac{\tau}{\tau_y}\right)^2} d\xi \quad (4.20)$$

Integration of the above equation was numerically done using Simpson's rule for the increment of $\Delta\xi=0.1$. However, when the bar becomes plastic only up to η , then to obtain the axial load with in the plastic region the integration is to be performed over $\xi = \eta$ to 1.0. Axial load within the elastic core (i.e., for $\xi = 0$ to η) can be obtained from the elastic theory. Then the total load can be calculated as

$$\frac{F}{F_Y} = \left(\frac{\sigma_e}{Y_y}\right) \eta^3 + 2 \int_{\xi=\eta}^1 \xi \sqrt{1 - \left(\frac{\sigma_p}{Y}\right)^2} d\xi \quad (4.21)$$

where σ_e is the maximum elastic axial stress for the cross-section whose radius is η , which is a constant, and σ_p is the axial stress within the plastic region which varies along ξ . However, to calculate numerical values of load it was assumed that once the yielding starts at the outer fiber of the bar due to combined loading, the elastic-plastic boundary η moves inwards in such a way that $\Delta\gamma = -\Delta\eta$. For different levels of values of initial load, the values of the corresponding shear strains when yielding starts can be obtain from equation (4.14). When $\gamma/\gamma_y = 1.0$, equation (4.20) is valid over the entire cross-section of the bar. But for elastic-plastic case equation (4.21) is used to plots F/F_Y for different initial values of Q , such as Q equal to 1.0, 0.75, 0.50 and 0.25.

4.3 STRAIN HARDENING MODEL

For strain hardening material relationship of effective stress-strain is used to determine the yield loci. In the equation (3.30), effective stress $\bar{\sigma}$ is replaced by σ_u for determination of yield loci based on post-yield flow stress. Hence we get

$$\sigma_u^2 = \sigma^2 + 3\tau^2 \quad (4.22)$$

For $\sigma = \sigma_y$, τ is calculated from the above equation and plotted as σ vs. τ for theoretical model. Again for $\tau = \tau_y$, σ is calculate from equation (4.22) and plotted as τ vs. σ . Finally these model are compared with experimental results.

4.4 COMPUTER PROGRAM

A FORTRAN program has been developed to evaluate the variation of the axial and shear stresses throughout the x-section as well as at the outer periphery of the circular rod for the two types the bi-axial torque-tension loading which have been considered in the present investigation. Furthermore, technique has been developed in the same program to evaluate the corresponding force and torque. The integral is defined as a function and different subroutines are used for integration methods say $f(x)=x*(\exp(-x))$, upper limit=1.0, lower limit=0.0. Detail of the program is given in Appendix – A with different subroutines.

CHAPTER - FIVE

RESULTS AND DISCUSSION

5.1 GENERAL

In the previous chapter, a computational technique along with the details of a theoretical model is presented. In this chapter, results obtained numerically for elastic-plastic behavior of a circular rod under combined torque and tensile loading within the plastic region are being presented and discussed. In the present investigation the following two cases are considered.

CASE-I: In the first type of loading, the rod is initially subjected to different levels of torque within and upto the yield point of the material, and then keeping the angle of twist constant, axial tension and hence axial strain are increased gradually.

CASE-II: In the second type of loading, the rod is initially subjected to different levels of axial tension within and upto the yield point of the material, and then keeping the axial extension constant, torque and hence shear strain are increased gradually.

5.2 THEORETICAL INVESTIGATION

In case of an uni-axial tension test within the elastic range, the axial stress distribution along the cross-section of the rod is uniform and in simple torsion test maximum shear stress is developed at the outer periphery of the rod and zero at the center of the rod. But in case of combined loading different a pattern of stress distribution is developed depending upon the type and combination of loading.

5.2.1 Variation of Axial and Shear Stresses

Along X-Section of the Rod

Figure 5.1 shows the non-dimensional axial and shear stresses distribution along the cross section of a circular rod for CASE-I, when the bar is twisted up to yield point first, i.e., $\gamma_0/\gamma_y=1.0$ and then axial load hence axial strain is gradually increased to $\varepsilon/\varepsilon_y=1.0$, keeping the initial angle of twist constant. Figure 5.2 shows the

non-dimensional axial and shear stresses distribution along the cross section of a circular rod for CASE-II, when the bar is axially loaded up to yield point first, i.e., $\varepsilon_0/\varepsilon_Y=1.0$ and then torque, hence shear strain is increased to $\gamma/\gamma_Y=1.0$, holding the initial axial extension constant. It is seen from figure 5.1, at the center of the rod, the shear stress is zero & the axial stress is maximum i.e., $\sigma/\sigma_Y=1.0$ at $\xi=0$. At the outer periphery i.e., when $\xi=1.0$, τ/τ_Y increases to 0.65 and σ/σ_Y decreases to 0.762. Thus for CASE-I, the axial stress decreases by 23.8% at the outer periphery. For CASE-II (figure 5.2), at the center of the rod, the shear stress is zero and the axial stress is maximum i.e., $\sigma/\sigma_Y=1.0$ at $\xi=0$. At the outer periphery i.e., when $\xi=1.0$, τ/τ_Y increases to 0.762 and σ/σ_Y decreases to 0.65. Thus for CASE-II, the axial stress decreases by 35% at the outer periphery. The distributions of σ/σ_Y and τ/τ_Y for the above mentioned two cases compared and shown in figure 5.3. The first strain path is represented by solid curves and the second strain path by dotted curves. Although the final states of deformation in the two cases are same, the stress distribution differs as a consequence of its path dependence.

At Outer Periphery of the Rod

Figure 5.4 represents the variation of non-dimensional axial and shear stresses at the outer surface of the circular rod with dimensionless axial strain for CASE-I, i.e., at first the rod was subjected to various levels of initial torques, within and upto the yield points of the materials, and then keeping the angle of twist constant, axial load and hence axial strain was gradually increased. Similarly figure 5.5 shows the variation of non-dimensional axial and shear stresses at the outer surface of the circular rod with dimensionless shear strain for CASE-II, i.e., at first the rod was subjected to various levels of initial axial loads, within and upto the yield points of the materials, and then keeping the axial extension constant, torque and hence shear strain was gradually increased. To this end, it is worth mentioning here that for an elastic-perfectly plastic material under uni-axial tension, the value of σ/σ_Y is one at $\varepsilon/\varepsilon_Y=1.0$. Figure 5.4 shows that when $\varepsilon/\varepsilon_Y=1.0$, the value of σ/σ_Y increases only upto 0.76 and τ/τ_Y decreases by 35% for CASE-I. However, when $\varepsilon/\varepsilon_Y$ is increased to 3.0, the value of σ/σ_Y reaches nearly equal to 1.0 and τ/τ_Y decreases by 90%. Figure 5.5 shows that when $\gamma/\gamma_Y=1.0$, the value of τ/τ_Y increases only upto 0.76

and σ/σ_Y decreases by 35% for CASE-II. However, when γ/γ_Y is increased to 3.0, the value of τ/τ_Y reaches to 0.995 and σ/σ_Y decreases by 90%.

Effect of Different Levels of Initial Load

Figures 5.6 and 5.7 show the non-dimensional axial and shear stresses distribution along the X-section of a solid rod for CASE-I for different levels of initial torque i.e., $T_0/T_Y=1.0, 0.75, 0.5$ & 0.25 respectively. Figures 5.8 and 5.9 show the non-dimensional axial and shear stresses distribution along the X-section of a solid rod for CASE-II for different levels of initially applied axial i.e., $F_0/F_Y=1.0, 0.75, 0.5$ and 0.25 respectively. It is seen from figures 5.6 and 5.7 that, at the center of the rod, the shear stress is zero & the axial stress is maximum i.e., $\sigma/\sigma_Y=1.0$ at $\xi=0$. At the outer periphery i.e., when $\xi=1.0$, τ/τ_Y increases to 0.65 and σ/σ_Y decreases to 0.76, for the case when $T_0/T_Y=1.0$. However, when the initially applied torque were equal to 0.75 and 0.50, the corresponding decrease of σ/σ_Y at $\xi=1.0$ are 18% & 10% respectively. When the initially applied torque is 0.25 times of the yield torque, the value of σ/σ_Y is very close to 0.97 at $\xi=1.0$ which implies that if initially applied torque is very close to zero, then axial stress distribution will be nearly uniform, which is observed in case of an uni-axial tension test. For CASE-II (figures 5.8 and 5.9), at the center of the rod, the shear stress is zero and the axial stress is maximum i.e., $\sigma/\sigma_Y=1.0$ at $\xi=0$, when the bar is axially loaded upto yield point first. At the outer periphery i.e., when $\xi=1.0$, τ/τ_Y increases to 0.762 and σ/σ_Y decreases to 0.65 for the case when $F_0/F_Y=1.0$. Thus for this case, the axial stress decreases by 35% at the outer periphery. But when the initial applied axial load was lower than the yield value, the axial stress distribution is uniform upto a specific value (depends on yield criterion) and after that shear stress distribution is linear.

Figures 5.10 and 5.11 represent the variation of non-dimensional axial and shear stresses at the outer surface of the circular rod with dimensionless axial strain for CASE-I for different levels of initial torque. Similarly figures 5.12 and 5.13 show the variation of non-dimensional shear and axial stresses at the outer surface of the circular rod with dimensionless shear strain for CASE-II, for different levels of axial load. It is observed from figure 5.10 that with the increase in the value of initially applied torque, the modulus of elasticity of the material decreases considerably.

Similarly figure 5.12 shows that with the increase in the initially applied axial load, the shear modulus of rigidity of the materials decreases rapidly.

Effect of Different Levels of Subsequently Applied Load

Figure 5.14 shows the non-dimensional axial stress and Figure 5.15 shows the non-dimensional shear stress distributions along the cross section of a solid rod for the initial torque $T_0/T_Y=1.0$, for different levels of subsequently applied axial load. Here four different levels of subsequently applied axial load and hence axial strain, were considered, that is, $\epsilon/\epsilon_Y = 1.0, 1.5, 2.0$ and 2.5 . It is observed from figure 5.14 that at a higher value of subsequently applied axial strain, axial stress distribution throughout the x-section is closely near to uniform. This happens because at the higher value of subsequently applied axial strain, axial stress dominates over the shear stress. Figure 5.15 shows that the lower the value of ϵ/ϵ_Y , the higher the magnitude of the shear strain, that the material can sustain. Figures 5.16 and 5.17 show the non-dimensional axial and shear stresses distributions along the cross section of a solid rod for the initial axial load $F_0/F_Y=1.0$ respectively, for different levels of subsequently applied torque and hence shear strain. Here four different levels of subsequently applied shear strains were considered, that is, $\gamma/\gamma_Y = 1.0, 1.5, 2.0$ and 2.5 . It is observed from figure 5.16 that at a higher value of subsequently applied shear strain, axial stress decreases rapidly compare to that of at lower values of γ/γ_Y . When $\gamma/\gamma_Y=1.0$, axial stress reduced by 35% at the outer periphery of the circular rod but when $\gamma/\gamma_Y=2.5$, axial stress reduced by 84%. Figure 5.17 shows that shear stress reaches nearly equal to one at the outer surface of the rod when subsequently applied shear strain $\gamma/\gamma_Y=2.5$.

5.2.2 Variation of the Axial Load and Torque

Figure 5.18 represents the variation of the axial load and torque with axial strain for CASE-I, when the initially applied torque was equal to yield torque, i.e. $\gamma_0/\gamma_Y=1.0$, which was kept constant during the subsequently applied axial load and hence axial strain. Figure 5.19 represents the variation of axial load and torque with shear strain for CASE-II, when the initially applied axial load was equal to yield load, i.e., $\epsilon_0/\epsilon_Y=1.0$, which is kept constant during the subsequently applied torque

and hence shear strain. It is observed from figure 5.18 that when the value of the axial strain is increased to the yield strain, the axial load reaches 0.84 times of its yield load. Furthermore, at this point the initially applied torque reduces to 0.75 i.e., reduced by 25%. This happens because when the axial load increases, the outer layer of the material begin to yield and the torque begins to decreases in a specific manner which is govern by the yield criterion & the stress-strain relationship in the plastic region. Similarly from figure 5.19, it is observed that when the value of shear strain is increased to the yield strain, the torque reaches 0.42 times of its yield value. Furthermore, at this point the initially applied axial load reduces to 0.80 i.e., reduced by 20%.

Effect of Different Levels of Initial Loading

Figure 5.20 depicts the variation of the initial torque with subsequently applied axial load and hence axial strain for CASE-I. Here four different levels of initial torque were considered, that is $T_0/T_Y = 1.0, 0.75, 0.5$ and 0.25 . It is observed from the figure that as long as the combined stresses do not reach a specific value, the initially applied torque does not start to decrease with the subsequently applied axial strain. However, when the combined stress becomes equal to a specific value, which is govern by the yield criterion, the initially applied torque starts decreasing with the axial strain. As seen for the case when $T_0/T_Y = 1.0$, the initially applied torque starts decreasing immediately with the increase in the axial strain, but for the case $T/T_0=0.75$, the initially applied torque does not decrease until the subsequently applied axial strain nearly increases to 0.66. Similar conclusion can be drawn for the cases when $T_0/T_Y = 0.5$ and 0.25 . It is worth mentioning here that when the subsequently applied axial strain, i.e., $\varepsilon/\varepsilon_Y$ becomes equal to 2.0, the corresponding decrease in the initial torques for $T_0/T_Y = 1.0, 0.75, 0.50$ and 0.25 are 74%, 68%, 64% and 68% respectively. From figure 5.21, it is observed that with the increase of the initially applied torque, material yielded at a much lower value of F/F_Y which is obviously due to the effect of combined loading.

Figure 5.22 shows the variation of the initially applied load with subsequently applied shear strain for CASE-II. Here four different levels of initial axial loads were considered, that is $F_0/F_Y = 1.0, 0.75, 0.5$ and 0.25 . It is observed from the figure that as

long as the combined stresses do not reach a specific value the initially applied axial load does not start to decrease with the subsequently applied shear strain. However, when the combined stress becomes equal to a specific value, which is governed by the yield criterion, the initially applied axial load starts decreasing with shear strain. As seen for the case when $F_0/F_Y=1.0$, the initially applied axial load starts decreasing immediately with the increase in the shear strain but, for the case $F_0/F_Y=0.75$, the initially applied axial load does not decrease until the subsequently applied shear strain nearly increases to 0.66. Similar conclusion can be drawn for the case $F_0/F_Y=0.5$ and 0.25. It is worth mentioning here that when the subsequently applied shear strain, i.e., γ/γ_y becomes equal to 2.0, the corresponding decrease in the initially applied axial load for $F_0/F_Y=1.0, 0.75, 0.50$ and 0.25 are approximately 48%, 39%, 30% and 20% respectively. From figure 5.23, it is observed that with the increase in the initially applied axial load, the material yielded at a much lower value of T/T_Y which is obviously due to the effect of combined loading.

5.3 COMPARISON OF THEORETICAL RESULTS WITH EXPERIMENTAL RESULT

Comparison of the theoretical results obtained from the present investigation with available experimental results [18-19] are presented in figures 5.24 and 5.25 for steel and figures 5.26 and 5.27 for copper, for the first type of loading, where four different levels of initial torque, i.e., $T_0/T_Y=1.0, 0.75, 0.5$ and 0.25 were considered. In figure 5.24, when the initial torque was equal to 100% of the yield torque (which is obtained by 0.02% offset method), theoretical results show good agreement with the experimental results in the plastic region nearly up to the $\varepsilon/\varepsilon_Y=1.35$. However, when the initial $T_0/T_Y= 0.75$ and 0.5, the experimental results match up to the $\varepsilon/\varepsilon_Y=1.0$. When the initial torque was 25% of the yield torque then the experimental results do not show any variation in the initial torque unlike theoretical models. Figure 5.25 shows similar results when the yield point is defined at the proportional limit. Here the deviations between the experimental and theoretical results are more. However, for the copper rod (figures 5.26 and 5.27) when yield point is defined at the proportional limit, relatively better agreement is observed between the

experimental and theoretical results than that when the yield point is defined at 0.02% offset. Figure 5.27 shows that, when the initial $T_0/T_Y=1.0$ and 0.75, the experimental results match well with the theoretical results nearly up to $\varepsilon/\varepsilon_Y=1.2$ and 1.4 respectively. The deviations between the experimental and theoretical results are obviously due to the strain hardening and compressibility effect of the material tested experimentally. It is worth mentioning here that in the theoretical model, the material tested experimentally was considered as elastic-perfectly plastic.

Comparison of the theoretical and experimental results are presented in figure 5.28 for steel and figure 5.29 for copper, for the second type of loading, where four different levels of initial axial load, i.e., $F_0/F_Y=1.0, 0.75, 0.5$ and 0.25 were considered. In Figure 5.28, when the initial axial load was equal to 100% of the yield load, theoretical results match with the experimental results in the plastic region nearly up to the $\gamma/\gamma_Y=0.9$. However, when the initial $F_0/F_Y=0.75$ and 0.5, the experimental results match up to the $\gamma/\gamma_Y=0.8$. When the initial axial load was 25% of the yield load then the experimental results do not show any variation in the initial axial load unlike theoretical models. However, for the copper rod (figure 5.29), when the initial $F_0/F_Y=1.0, 0.75$ and 0.5, the experimental results match well with the theoretical results nearly up to $\gamma/\gamma_Y=1.0, 0.95$ and 1.5 respectively. When the initial axial load was 25% of the yield load then the experimental results do not show any variation in the initial axial load unlike theoretical models. However, it is observed that in case of copper, there is comparatively better agreement between the theoretical and experimental results than in the case of steel for both CASE-I and CASE-II. This is because of the fact that the stress-strain curve of the copper rod (given in appendix B) behaves more closely like an elastic-perfectly plastic material than that of the steel rod.

For the two types of bi-axial loading, CASE-I and CASE-II, it was possible to determine the magnitudes of the combined stresses when the material yielded due to combined loading. The experimental results of the first case in terms of the axial and shear stresses for the steel and copper are plotted in figures 5.30 and 5.32 respectively. Similarly the experimental results of the second case for the steel and

copper, shown in the figures 5.31 and 5.33 respectively. The solid lines, shown in the figure, depict the Mises yield loci based on the post-yield flow stress of the material investigated. These figures reveal that most of the experimental points of the combined loading fall within the domains contained by these yield loci (i.e., based on post-yield flow stress). However, few points remain outside these domains which may be due to the fact that von Mises yield criteria alone is not the governing factor of the material response within the plastic region, as it is well known that the behavior of the material strongly dependent on the strain path in the plastic region. Furthermore, it is seen from both figures that most of the experimental point's overshoot the yield loci based on the initial yield stress (i.e., proof stress) and this might have happened because of the strain hardening of the materials.

CHAPTER - SIX

CONCLUSION AND RECOMMENDATION

6.1 GENERAL

Elastic-plastic behavior of a circular rod under combined torque-tension loading within the plastic region has been studied in the present investigation. This chapter summarizes the accuracy and reliability of the present prediction, embodied in the numerical results by comparing with the available experimental data and suggests the scope of further works on the present study.

6.2 CONCLUSION

The conclusions that have been arrived at from the present study are presented below:

- 1) It has been observed from the present investigation that even for the same loading condition, that is, $\varepsilon/\varepsilon_Y=1.0$ and $\gamma/\gamma_Y=1.0$, the stress distribution across the cross-section of the rod is different and this depends entirely on the loading history.
- 2) Axial stress decreases rapidly for the case when tension is followed by torsion as compared to torsion followed by tension.
- 3) Shear stress increases slowly for the case when torsion is followed by tension as compared to tension followed by torsion.
- 4) The higher the value of the initially applied torque, the greater the variations in the subsequently applied axial stress along the cross-section of the rod.
- 5) The higher the value of the initially applied axial load and torque, the lower the value of the modulus of elasticity and shear modulus of rigidity respectively.

- 6) In the first type of loading (CASE-I), where the rod was initially subjected to a torque and then, keeping the angle of twist constant, to a gradually increasing axial load, an increase in the axial load resulted in a decrease in the initially applied torque according to the yield criterion. The initially applied torque started to decrease with the axial load only when the combined stress of the material reached approximately the uni-axial yield stress of the material. The higher the magnitude of the initially applied torque, the greater is the rate of decrease of the torque with the increasing axial load.
- 7) In the second type of loading (CASE-II), where the axial load was applied first, an increase in the torque resulted in a decrease in the initially applied axial load according the yield criterion. The initially applied axial load started to decrease with the torque only when the combined stress of the material reached approximately the uni-axial yield stress of the material. The higher the magnitude of the initially applied load, the greater is the rate of decrease of the axial load with the increasing torque.
- 8) For the CASE-I, the theoretical results agree well with the experimental torque variation, a behavior that is closely like an elastic-perfectly plastic material. In the present case, the theory has a better agreement with the test results of the copper rod than those of steel.
- 9) For the CASE-II, the theoretical results show relatively poor agreement with the experimental load variation curves of the material behaving closely like an elastic- perfectly plastic material.
- 10) From the comparison of the theoretical results, based on post-yield flow stress, with the experimental results, it can be concluded that von Mises yield criteria alone is not the governing factor of the material response within the plastic region. As it is well known that the behavior of the material is strongly dependent on the strain path in the plastic region.

6.3 RECOMMENDATION FOR FUTURE WORK

6.3.1 Introduction

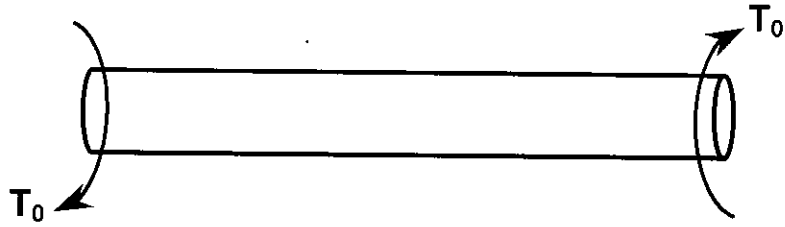
In the present investigation elastic-plastic behavior of a circular rod under combined torque-tension loading within the plastic region has been studied theoretically using a computational program. Here the material is considered as incompressible, which behaves like an elastic-perfectly plastic material i.e., non strain hardening. Present model was developed on the basis of von Mises yield criterion and Prandtl-Reuss stress-strain equation. And finally integration was performed by using Simpson's 1/3 rule.

6.3.2 Recommendation

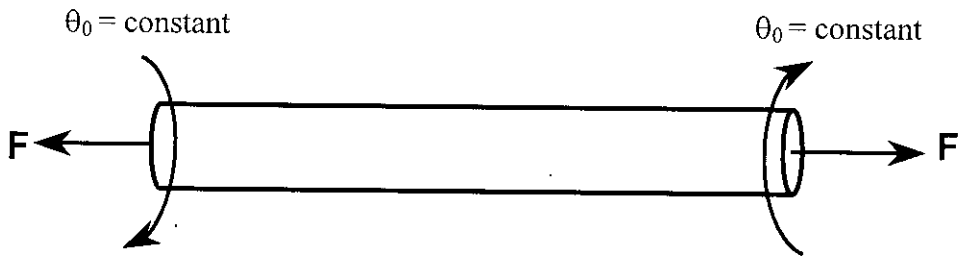
Present work can be extended further

- a) To develop a model for strain hardening material considering the compressibility effect.
- b) To study the effect of simultaneous elongation and twisting.
- c) To study other types of combined loading.
- d) To study the effect of combined loading having more than two loads.
- e) To study the effect of combined loading in the elastic-plastic region for other geometry.

The above works are specially recommended because they can be solved by using the present numerical model. One needs first to modify this model for different strain-hardening models.

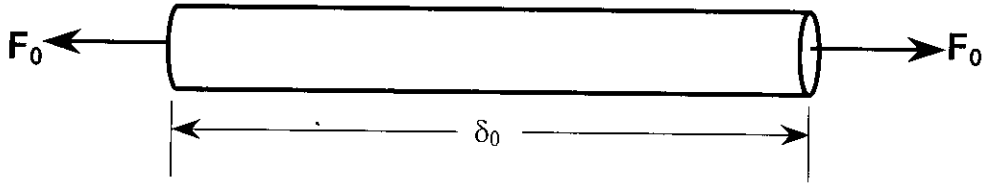


a) Torque applied first and then corresponding angle of twist (θ_0) was kept constant

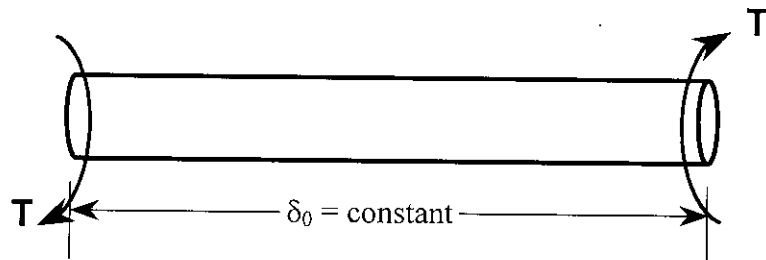


b) Subsequently applied axial load was gradually increased

Figure 5.1: Schematic diagram of the model when the circular bar is subjected to initial torque first (CASE-I).



a) Axial load applied first and then corresponding axial extension (δ_0) was kept constant



b) Subsequently applied torque was gradually increased

Figure 5.2: Schematic diagram of the model when the circular bar is subjected to axial load first (CASE-II).

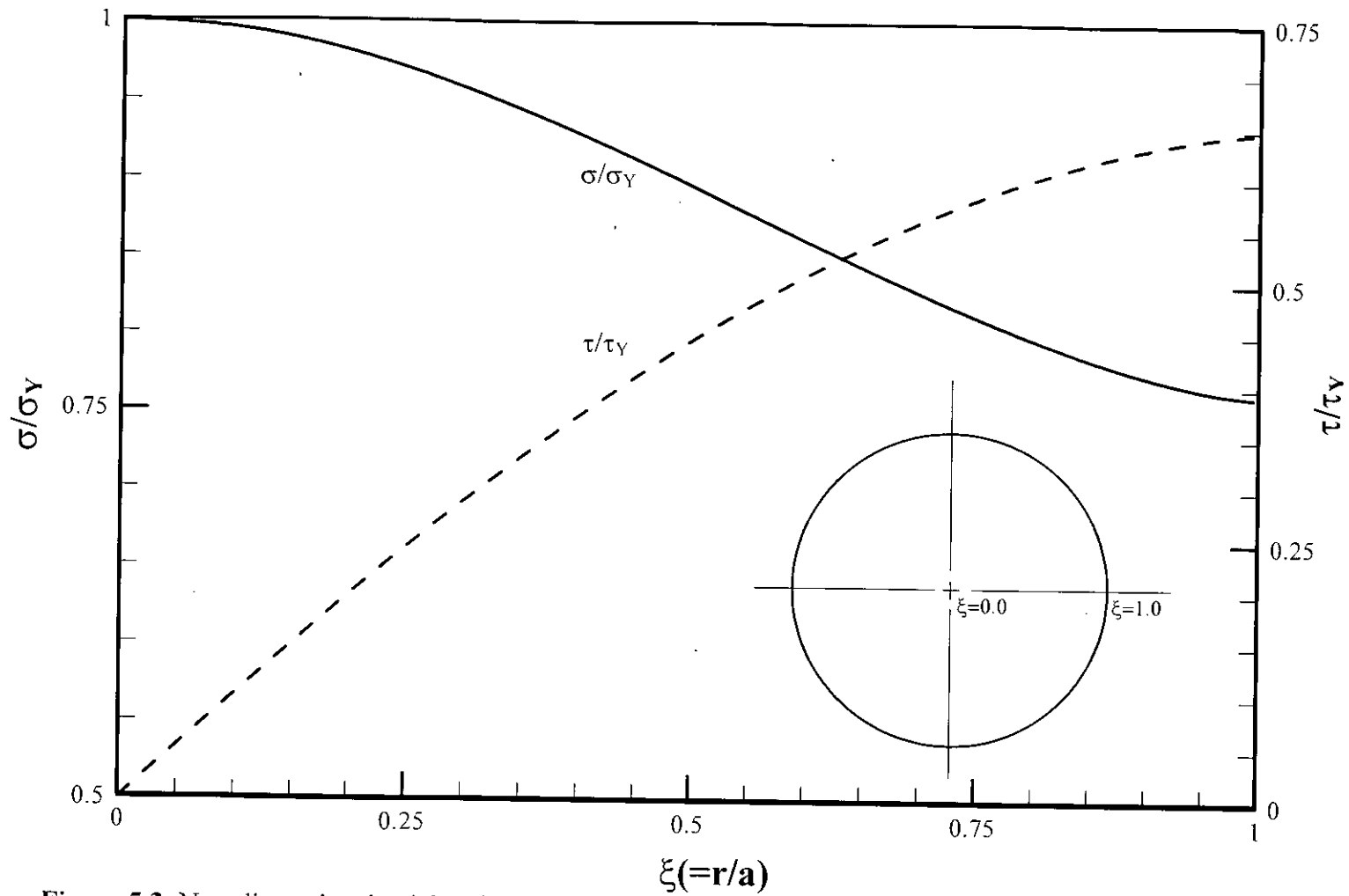


Figure 5.3: Non-dimensional axial and shear stresses distributions along the half of the cross-section of a circular rod for CASE-I, i.e., $P (= \gamma_0/\gamma_y) = 1.0$ & $\epsilon/\epsilon_y = 1.0$ when the circular bar is subjected to initial torque first

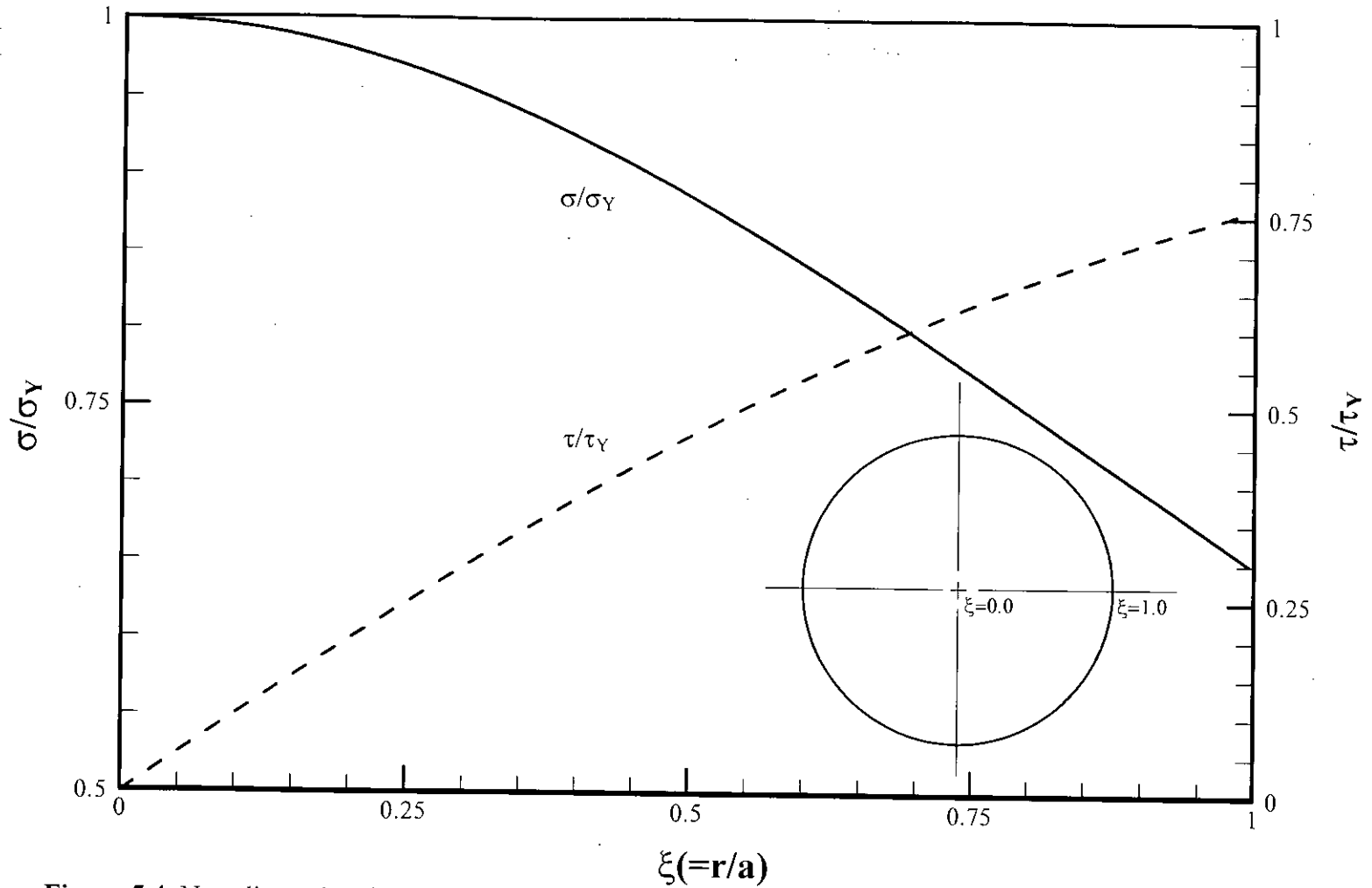


Figure 5.4: Non-dimensional axial and shear stresses distributions along the half of the cross-section of a circular rod for CASE-II, i.e., $Q (= \epsilon_0/\epsilon_\gamma) = 1.0$ & $\gamma/\gamma_\gamma = 1.0$, when the circular bar is subjected to initial axial load first

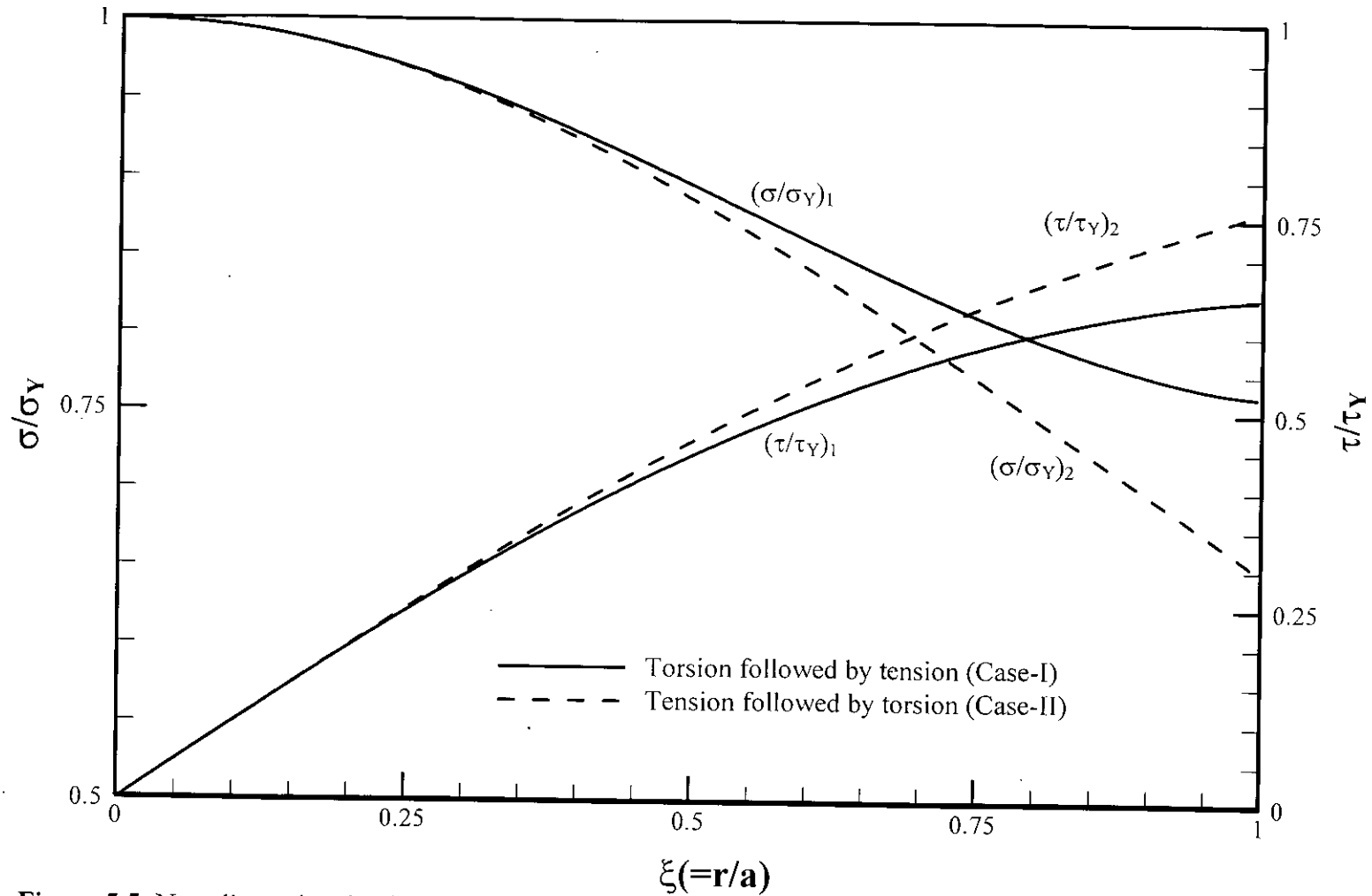


Figure 5.5: Non-dimensional axial and shear stresses along the half of the cross-section of a circular rod for the conditions P ($\gamma_0/\gamma_y=1.0$ & $\varepsilon/\varepsilon_y=1.0$) for Case-I and $\gamma/\gamma_y=1.0$ & Q ($\varepsilon_0/\varepsilon_y=1.0$) for CASE-II

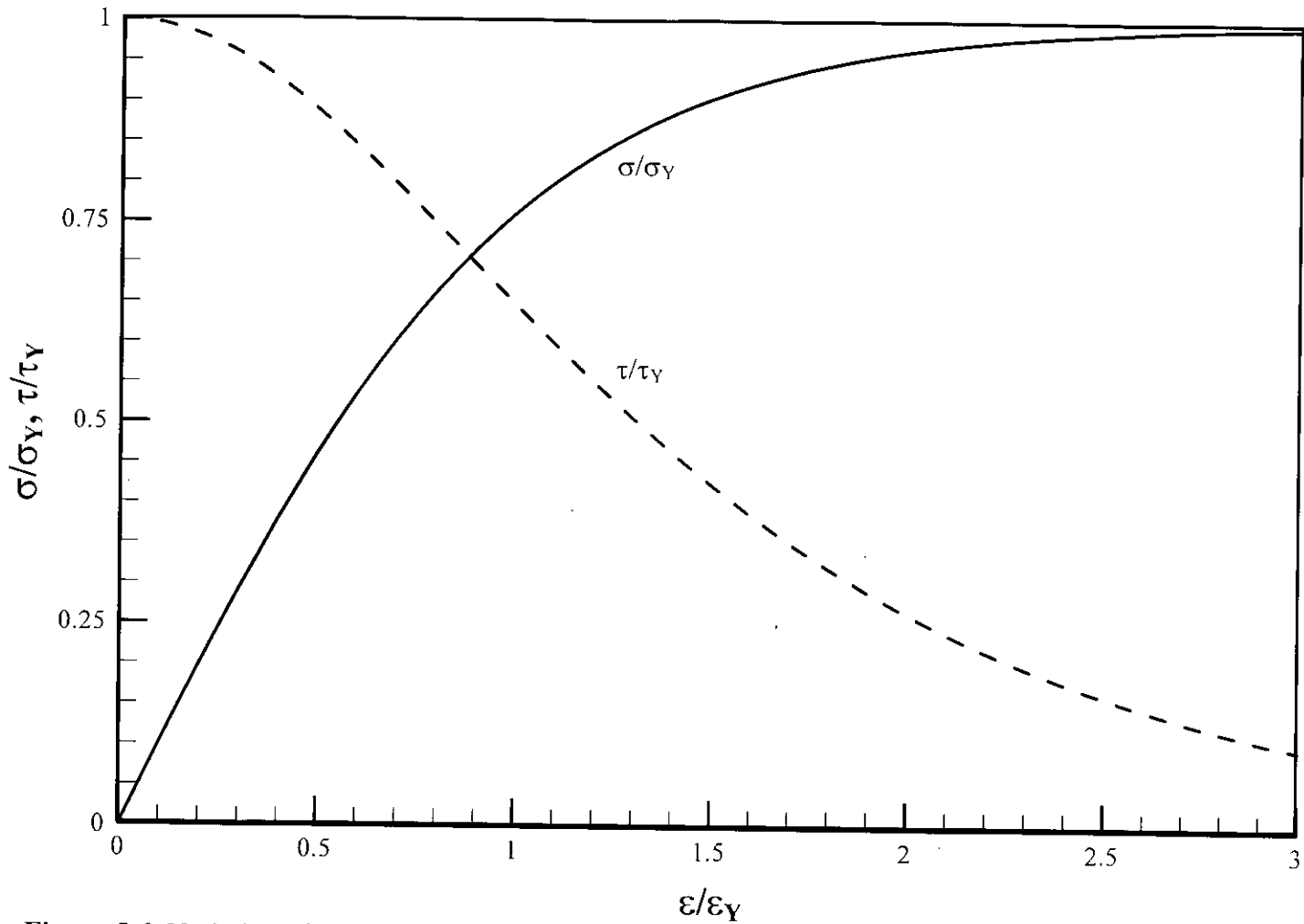


Figure 5.6: Variation of non-dimensional axial and shear stresses at the outer surface of the circular rod for CASE-I
i.e., $\gamma_0/\gamma_Y=1.0$ & $\xi(=r/a)=1.0$

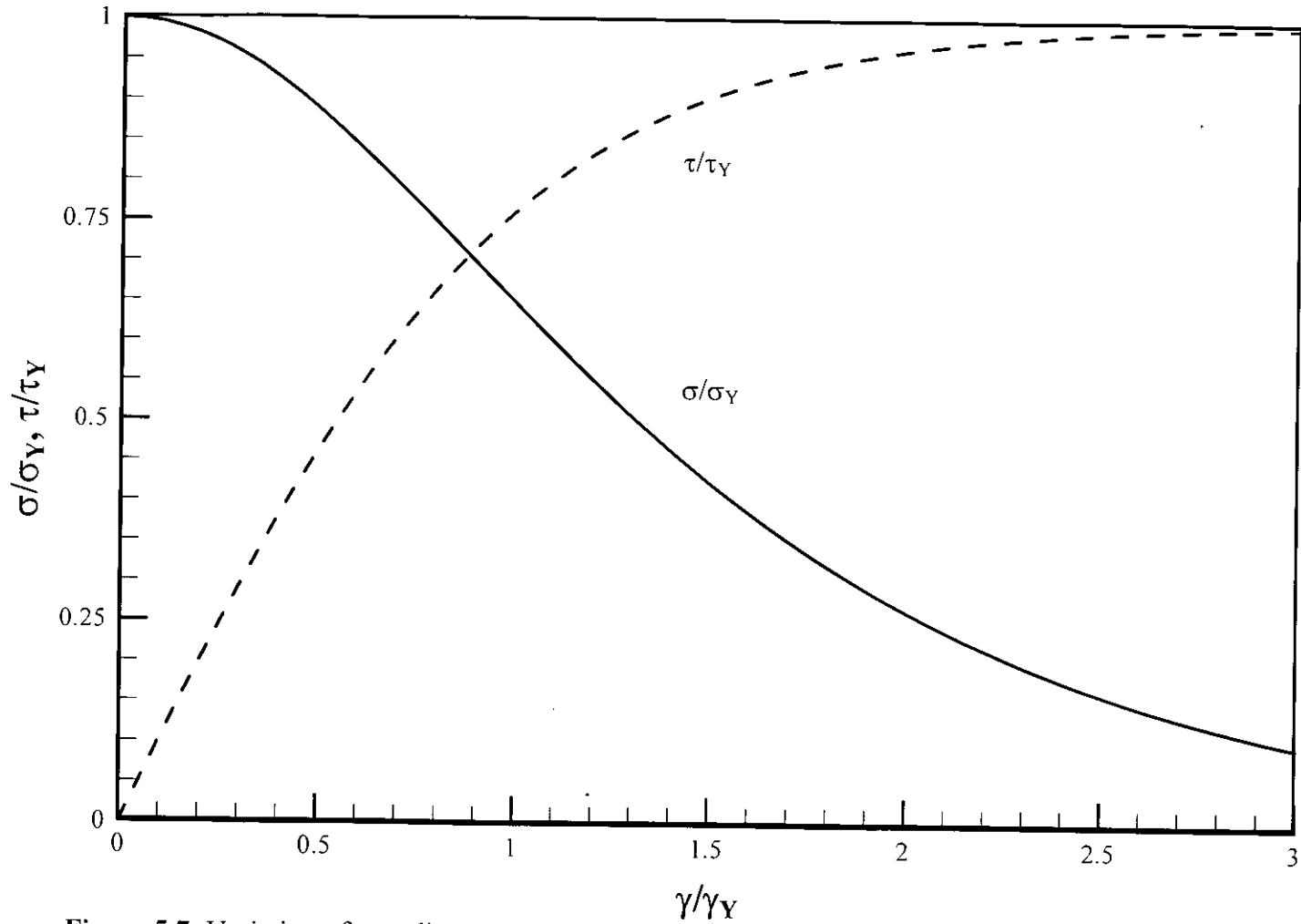


Figure 5.7: Variation of non-dimensional axial and shear stresses at the outer surface of the circular rod for CASE-II
i.e., $\epsilon_0/\epsilon_y=1.0$ & $\xi(=r/a)=1.0$

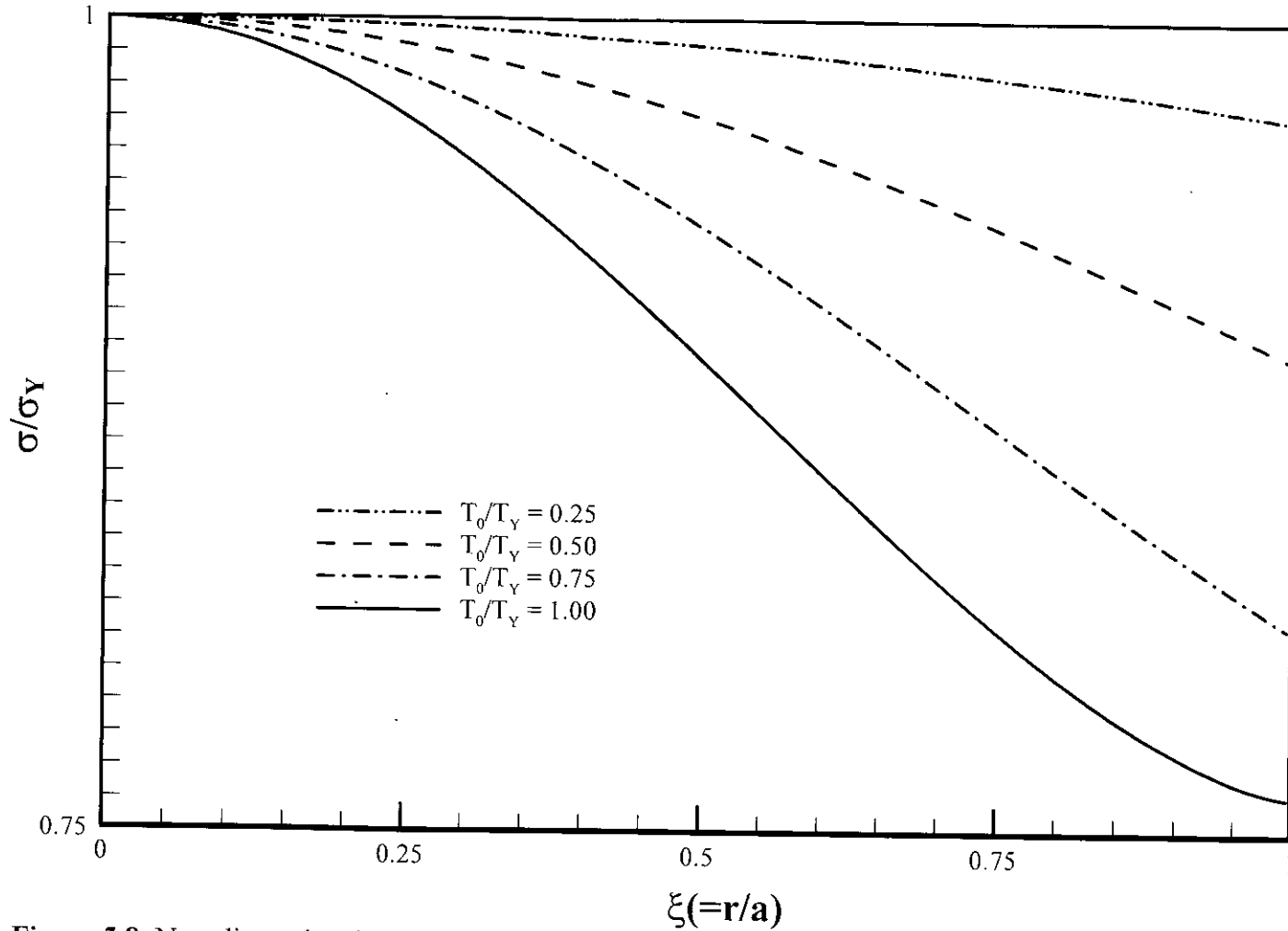


Figure 5.8: Non-dimensional axial stress distribution along the half of the cross-section of a circular rod for the conditions $\varepsilon/\varepsilon_Y=1.0$ & different levels of initially applied torque, i.e., $P (= \gamma_0/\gamma_Y)$

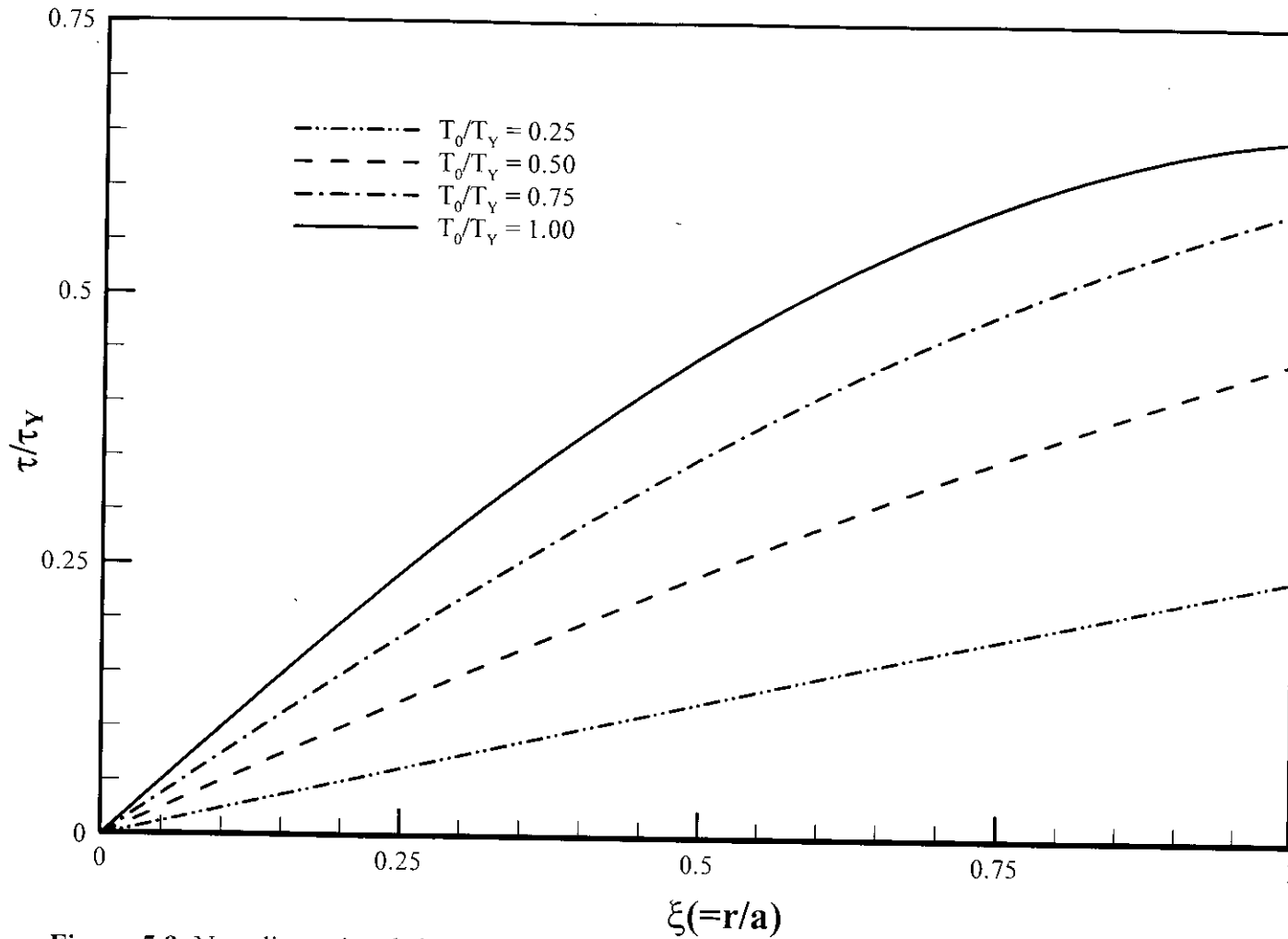


Figure 5.9: Non-dimensional shear stress distribution along the half of the cross-section of a circular rod for the conditions $\varepsilon/\varepsilon_Y=1.0$ & different levels of initially applied torque, i.e., $P (=T_0/T_Y)$

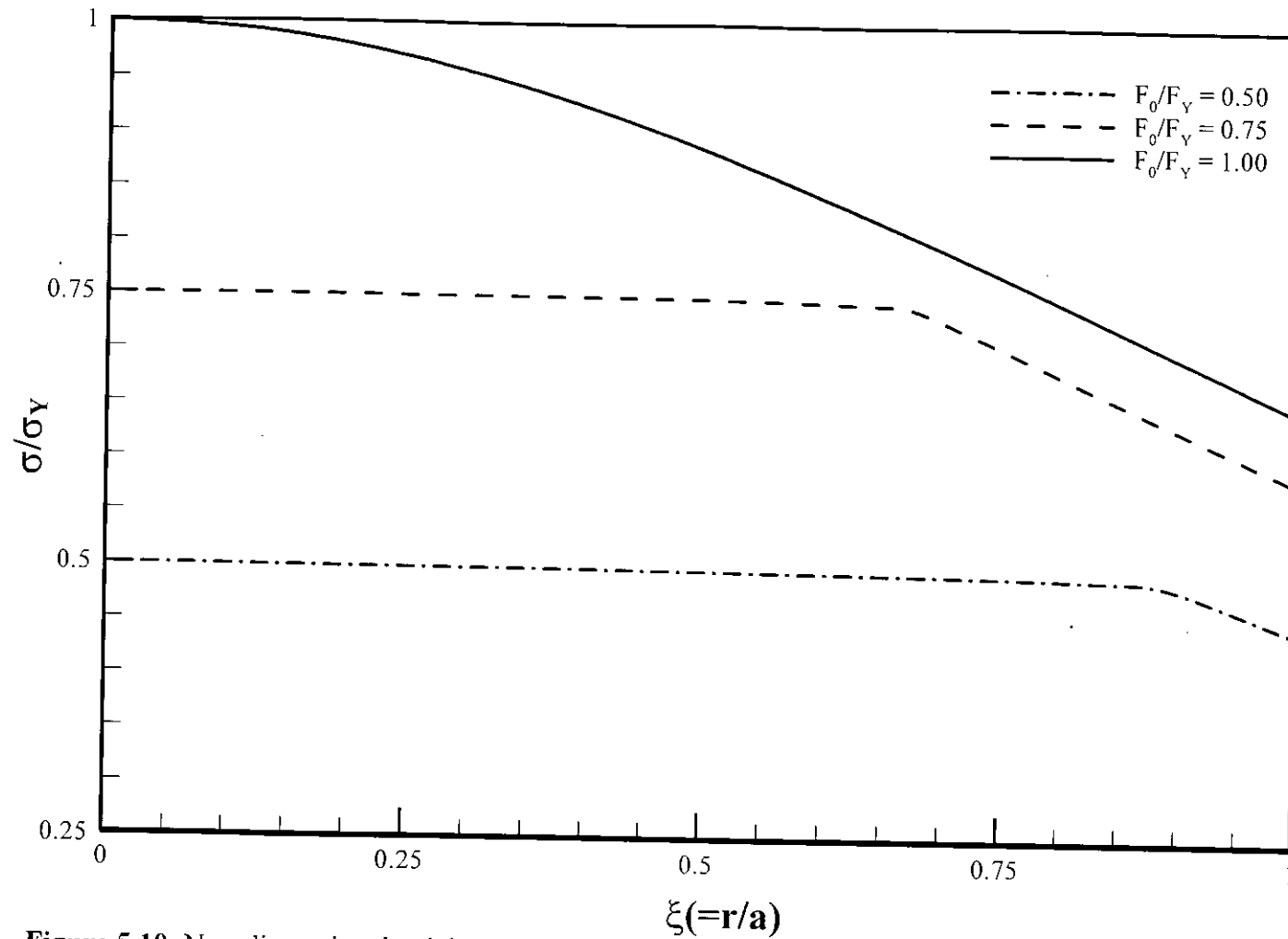


Figure 5.10: Non-dimensional axial stress distribution along the half of the cross-section of a circular rod for the Condition $\gamma/\gamma_y=1.0$ & different levels of initially applied axial load, i.e., $Q (= \epsilon_0/\epsilon_y)$

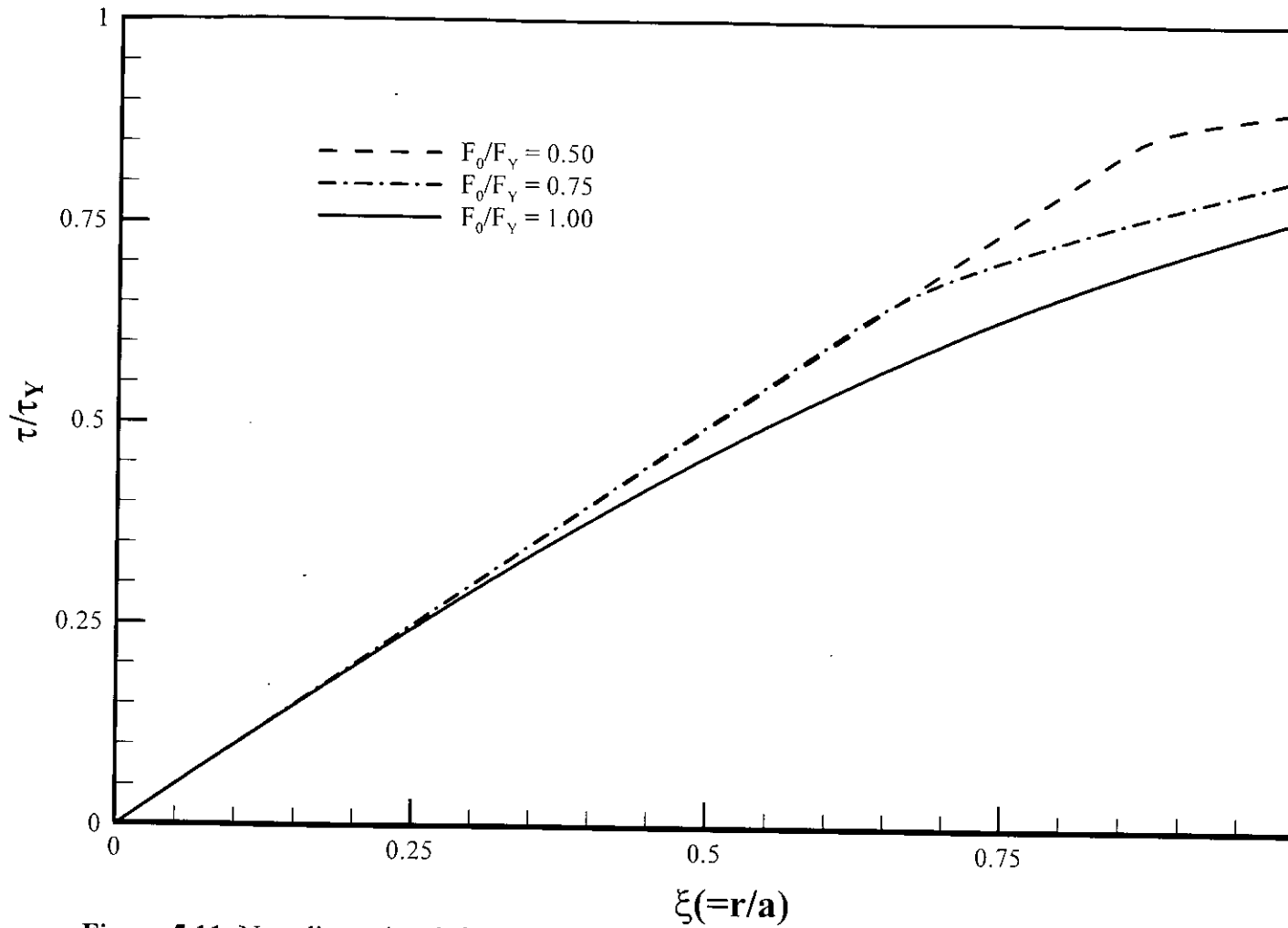


Figure 5.11: Non-dimensional shear stress distribution along the half of the cross-section of a circular rod for the condition $\gamma/\gamma_y = 1.0$ & different levels of initially applied axial load, i.e., $Q (= \epsilon_0/\epsilon_y)$

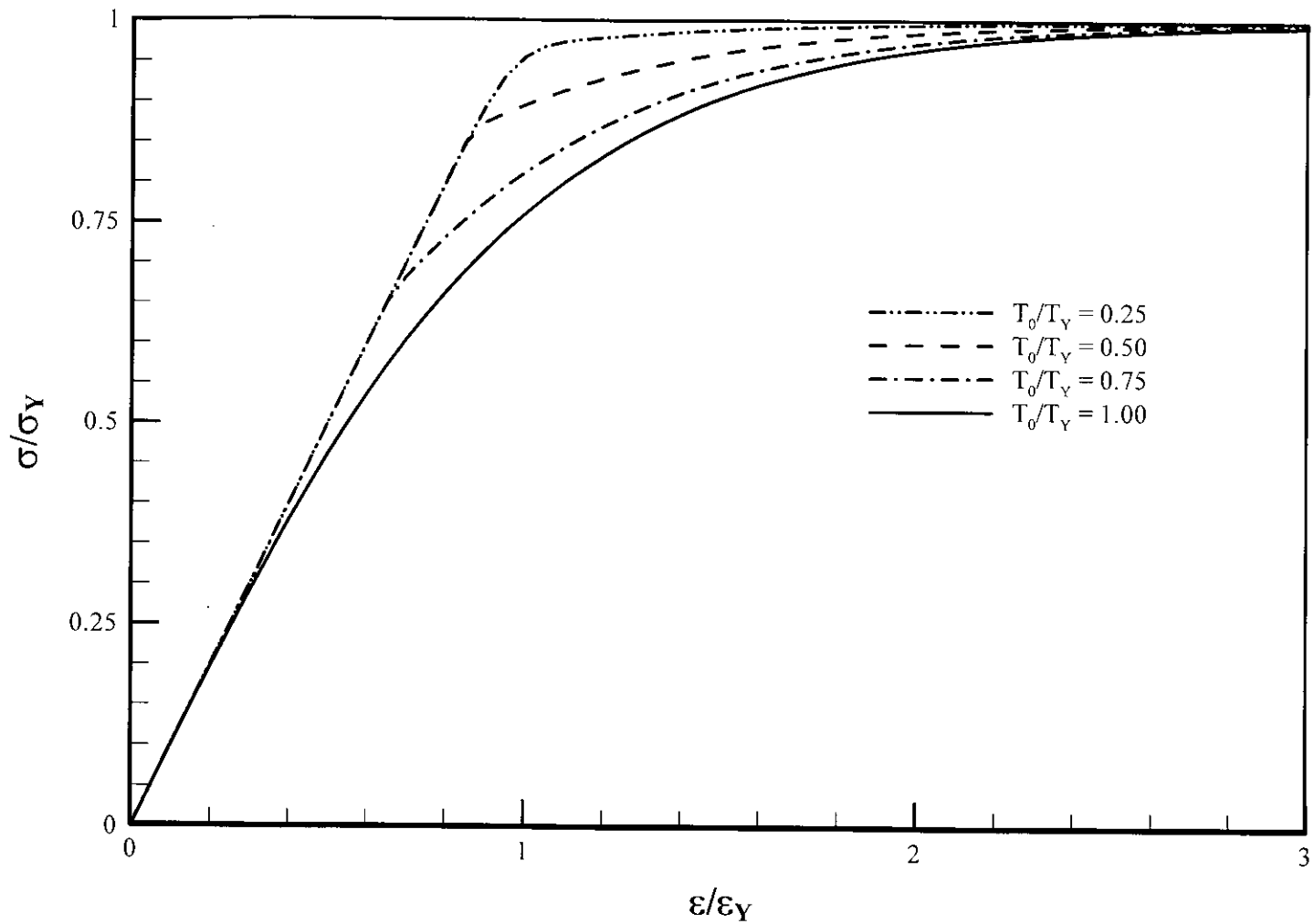


Figure 5.12: Variation of non-dimensional axial stress with subsequently applied axial strain for different levels of initial torque, when the circular bar is twisted first

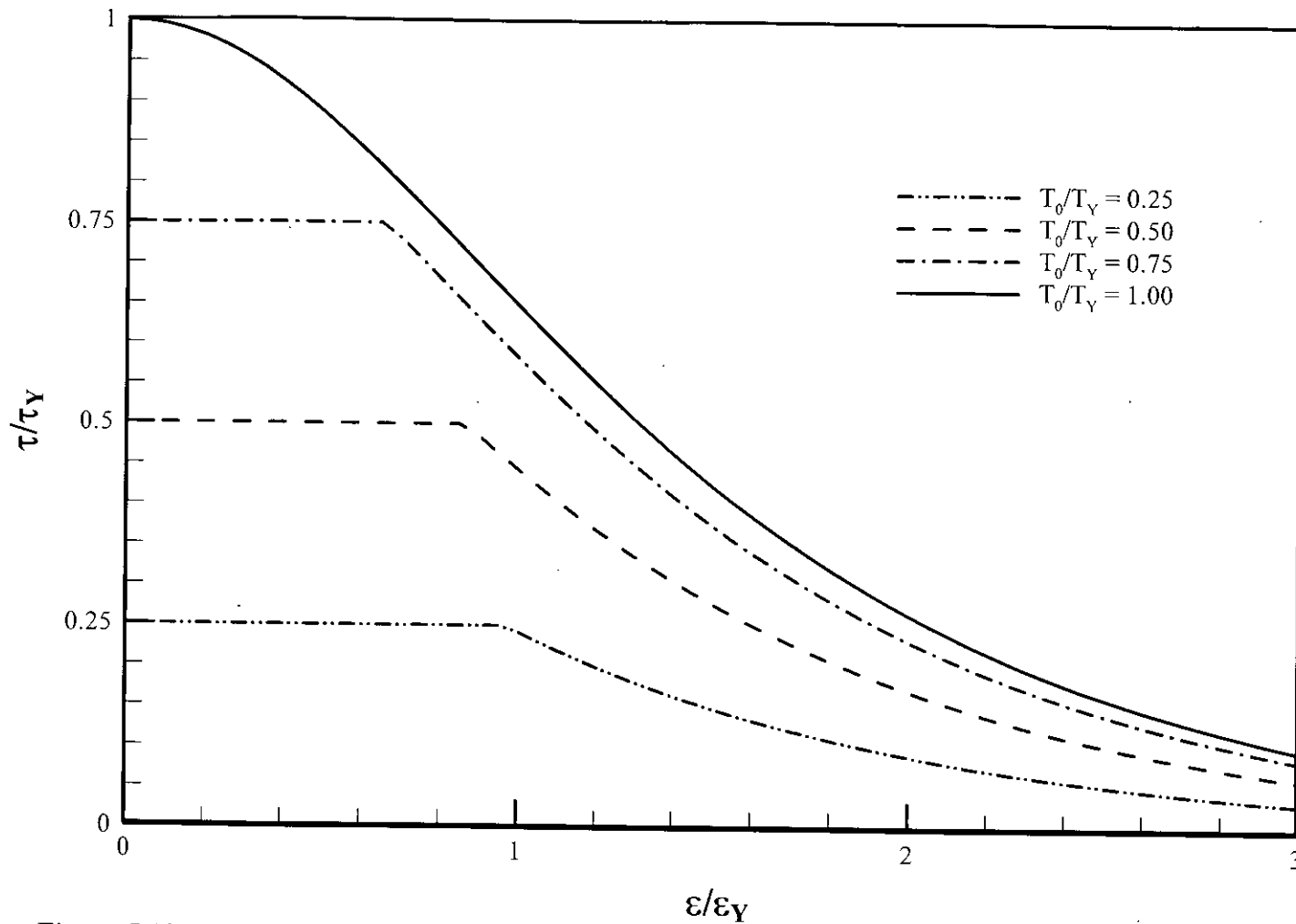


Figure 5.13: Variation of non-dimensional shear stress with subsequently applied axial strain for different values of initial torque, when the circular bar is twisted first

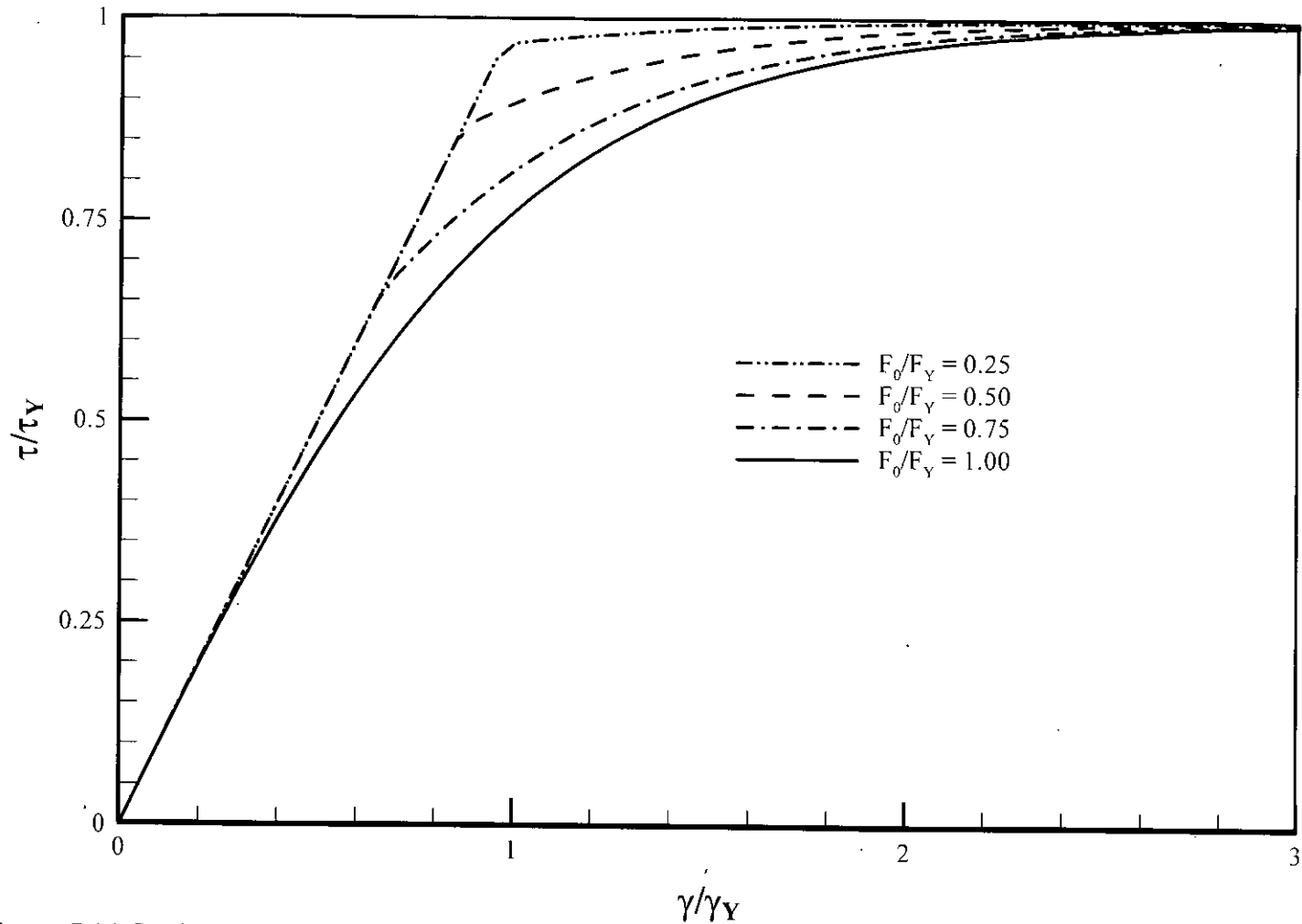


Figure 5.14: Variation of non-dimensional shear stress with subsequently applied shear strain for different levels of initially applied axial load, when the circular bar is axially loaded first

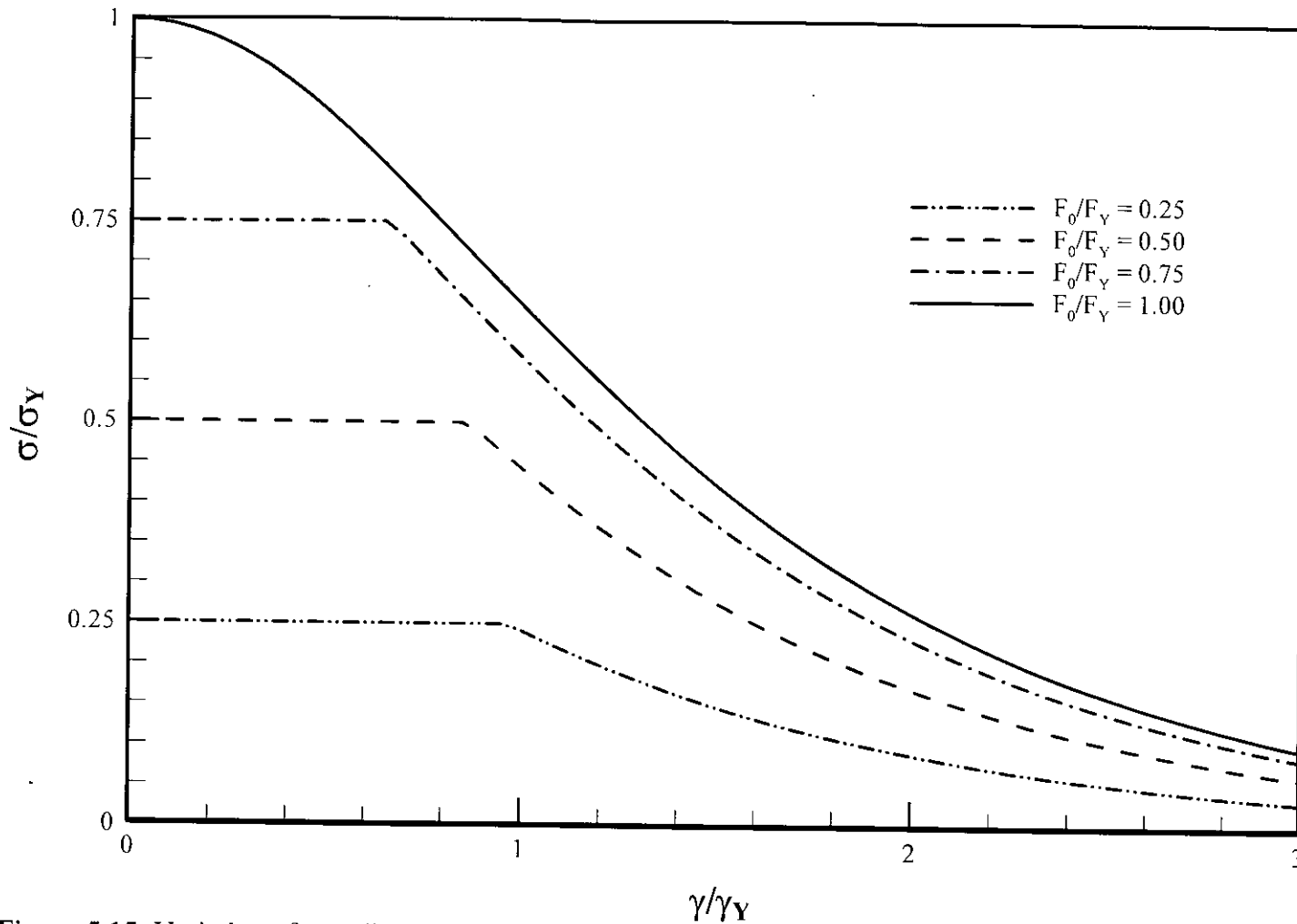


Figure 5.15: Variation of non-dimensional axial stress with subsequently applied axial strain for different levels of initially applied axial load, when the circular bar is axially loaded first

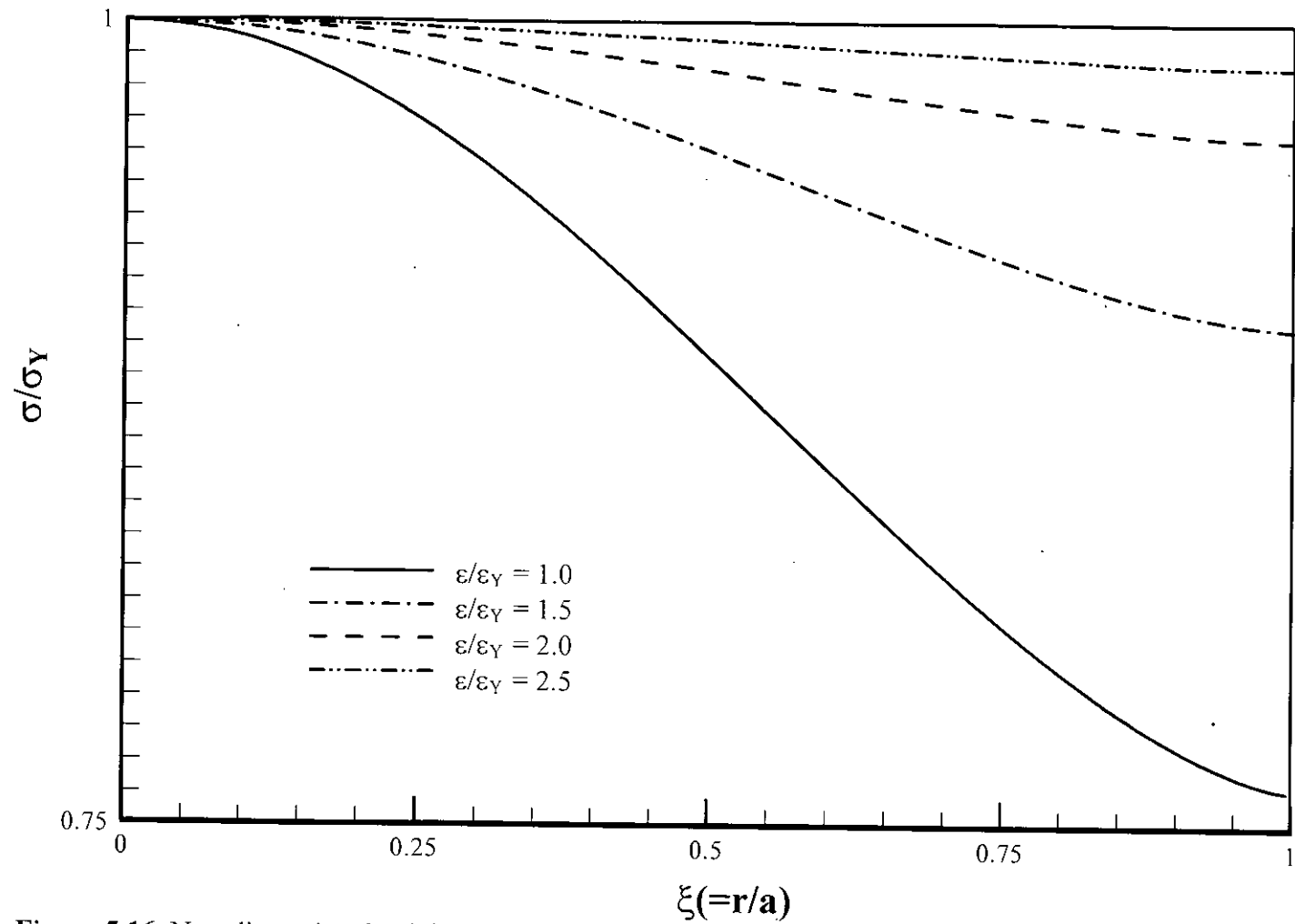


Figure 5.16: Non-dimensional axial stress distribution along the half of the cross-section of a circular rod for different levels of subsequently applied axial strain for the condition P ($=\gamma_0/\gamma_Y$)=1.0

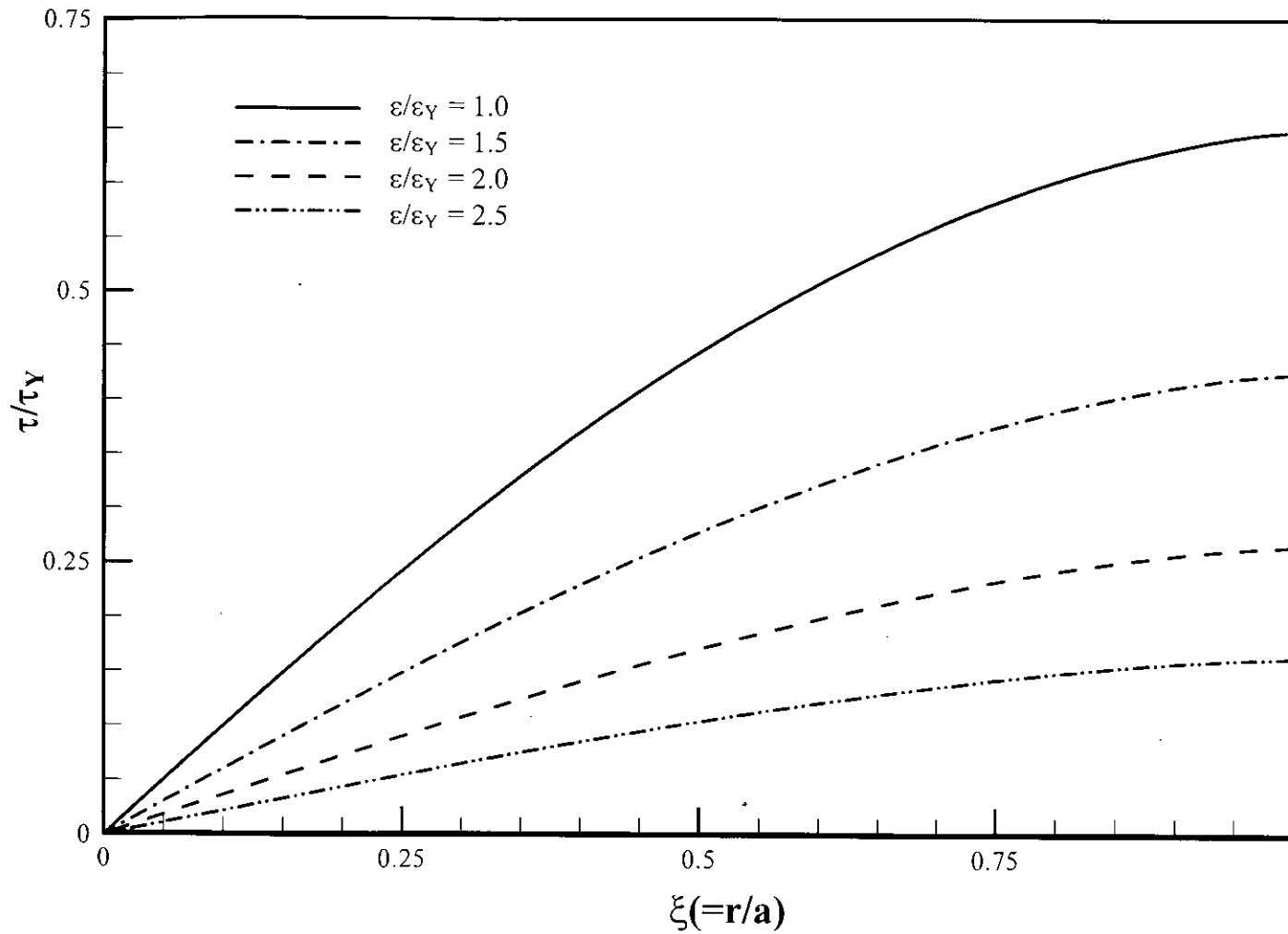


Figure 5.17: Non-dimensional shear stress distribution along the half of the cross-section of a circular rod for different levels of subsequently applied axial strain for the condition $P (= \gamma_0/\gamma_y) = 1.0$

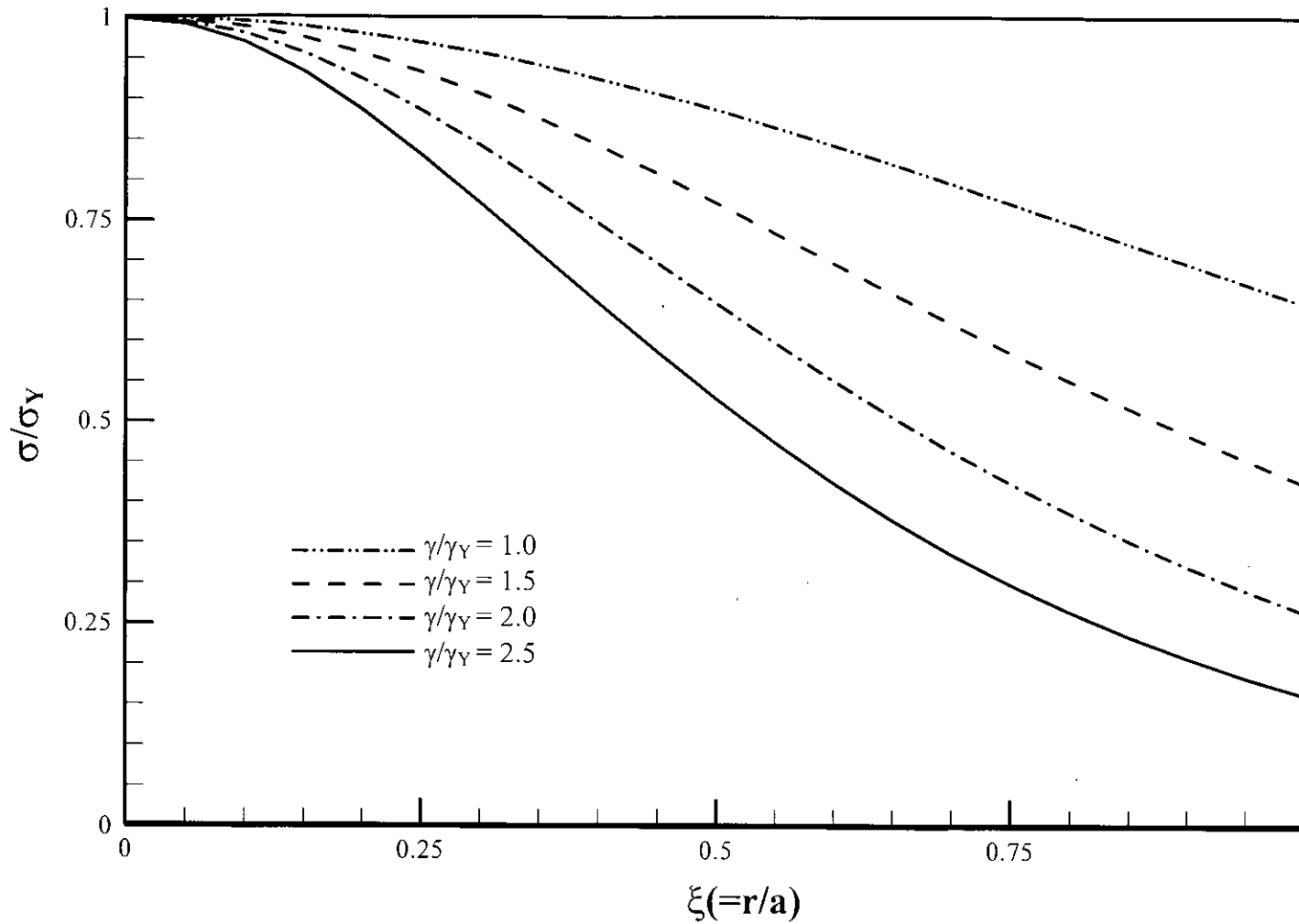


Figure 5.18: Non-dimensional axial stress distribution along the half of the cross-section of a circular rod for different levels of subsequently applied shear strain for the condition $Q (= \epsilon_0/\epsilon_y) = 1.0$

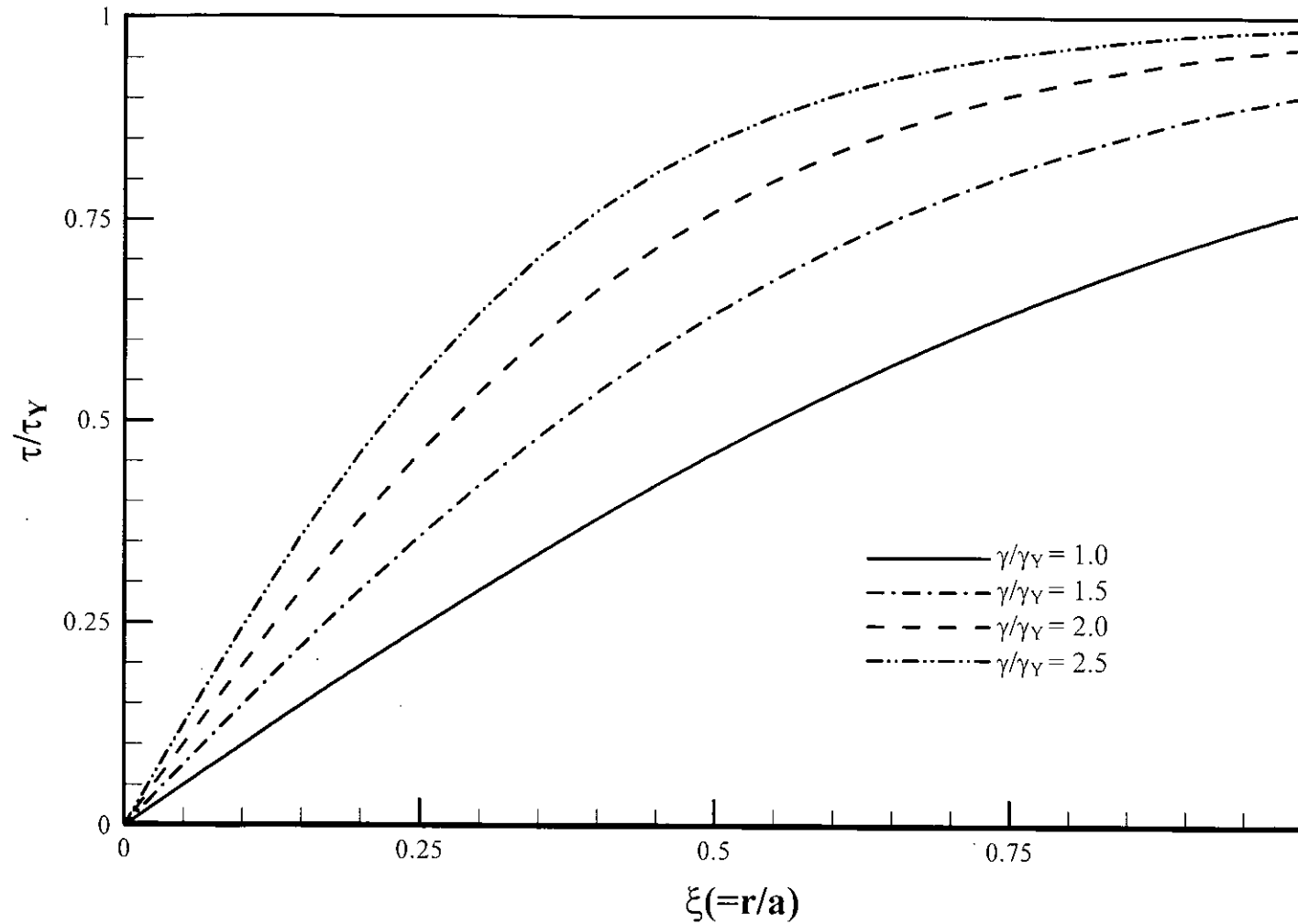


Figure 5.19: Non-dimensional shear stress distribution along the half of the cross-section of a circular rod for different levels of subsequently applied shear strain for the condition $Q (= \epsilon_0/\epsilon_y) = 1.0$

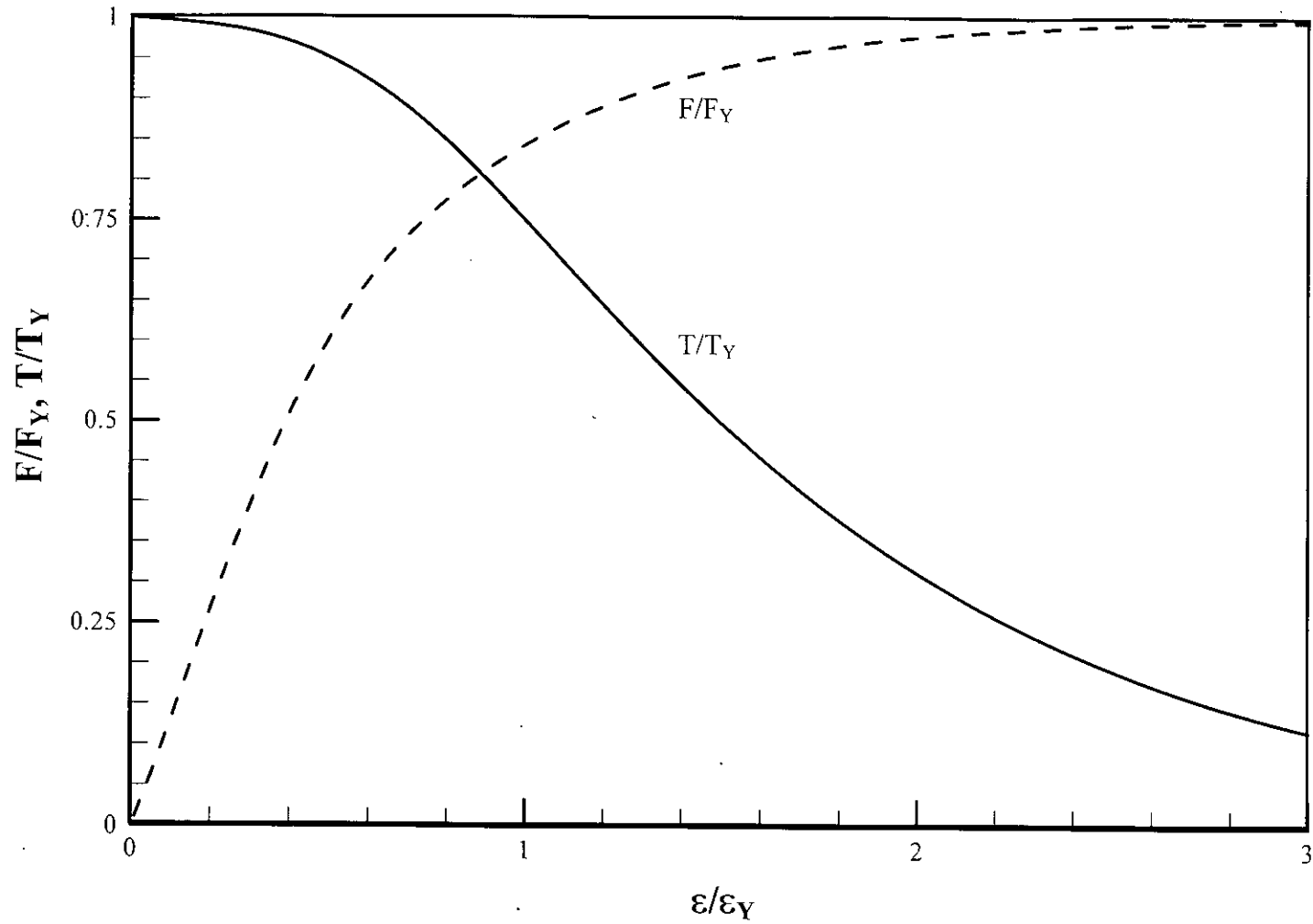


Figure 5.20: Variation of normalized axial load and torque with subsequently applied normalized axial strain in a circular rod for CASE-I, i.e., $T_0/T_Y=1.0$

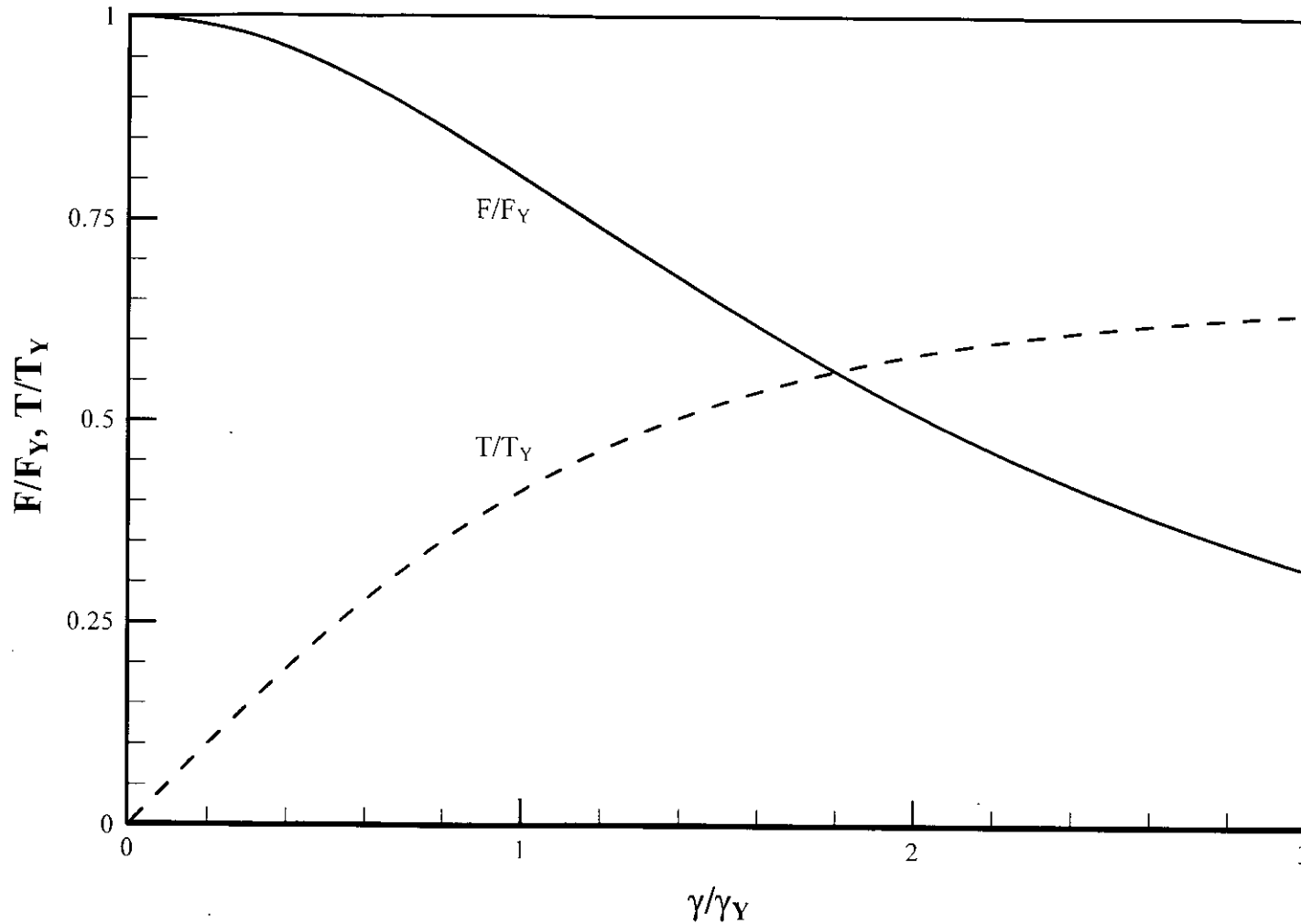


Figure 5.21: Variation of normalized axial load and torque with subsequently applied normalized shear strain in a circular rod for CASE-II, i.e., $F_0/F_Y=1.0$

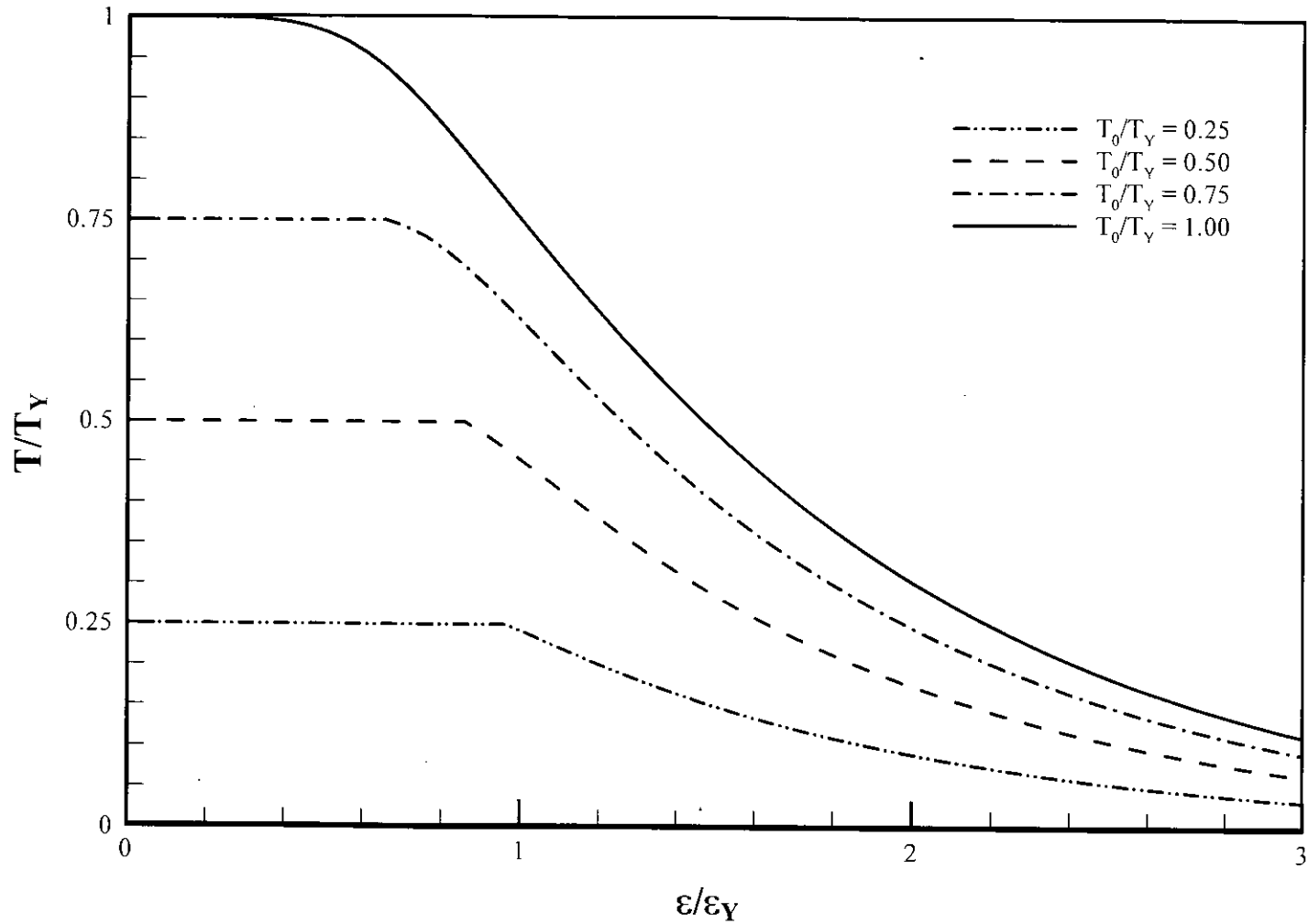


Figure 5.22: Variation of normalized torque with subsequently applied axial strain for different values of initial torque when the circular bar is twisted first

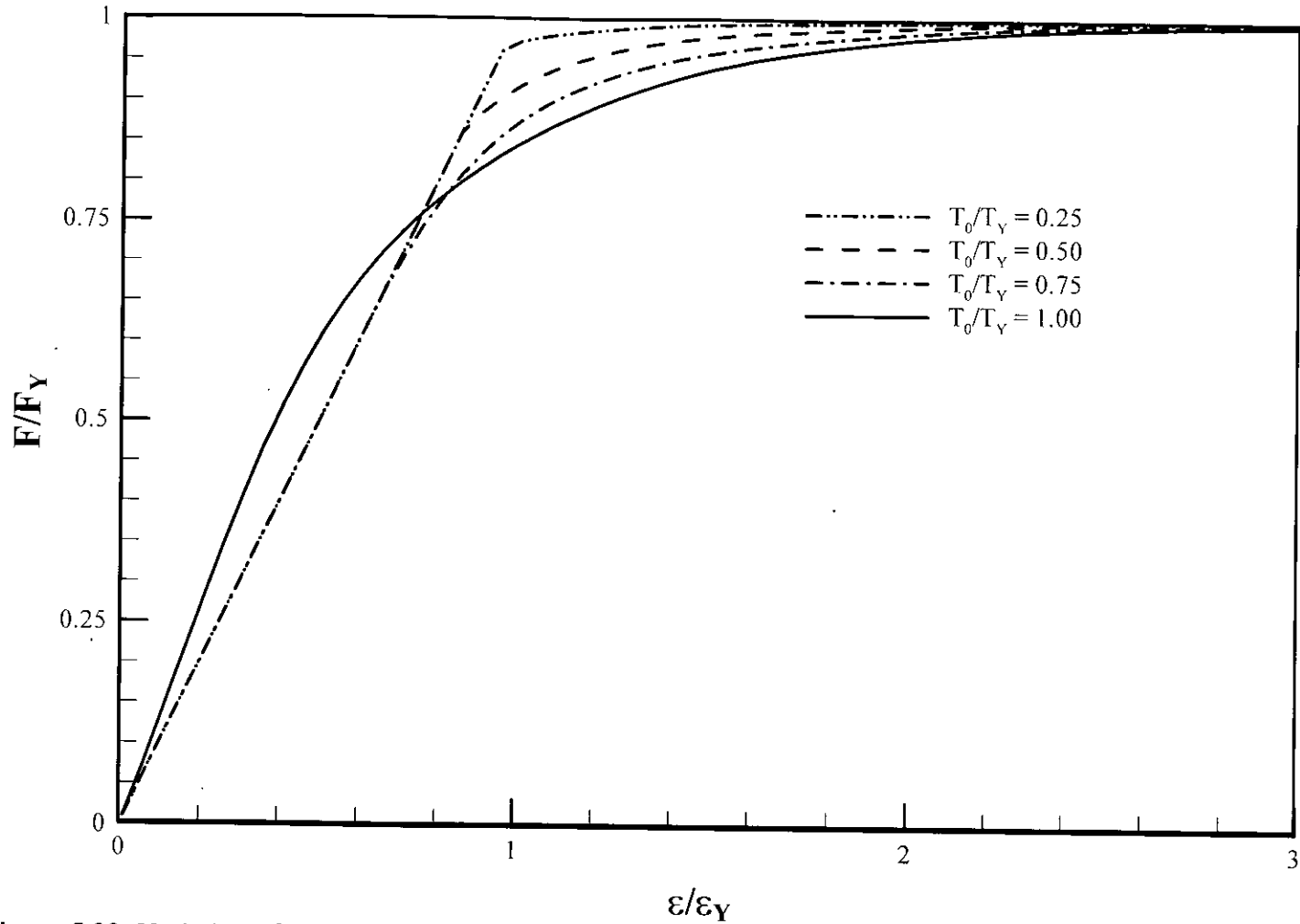


Figure 5.23: Variation of normalized axial load with subsequently applied axial strain for different values of initial torque when the circular bar is twisted first

94974

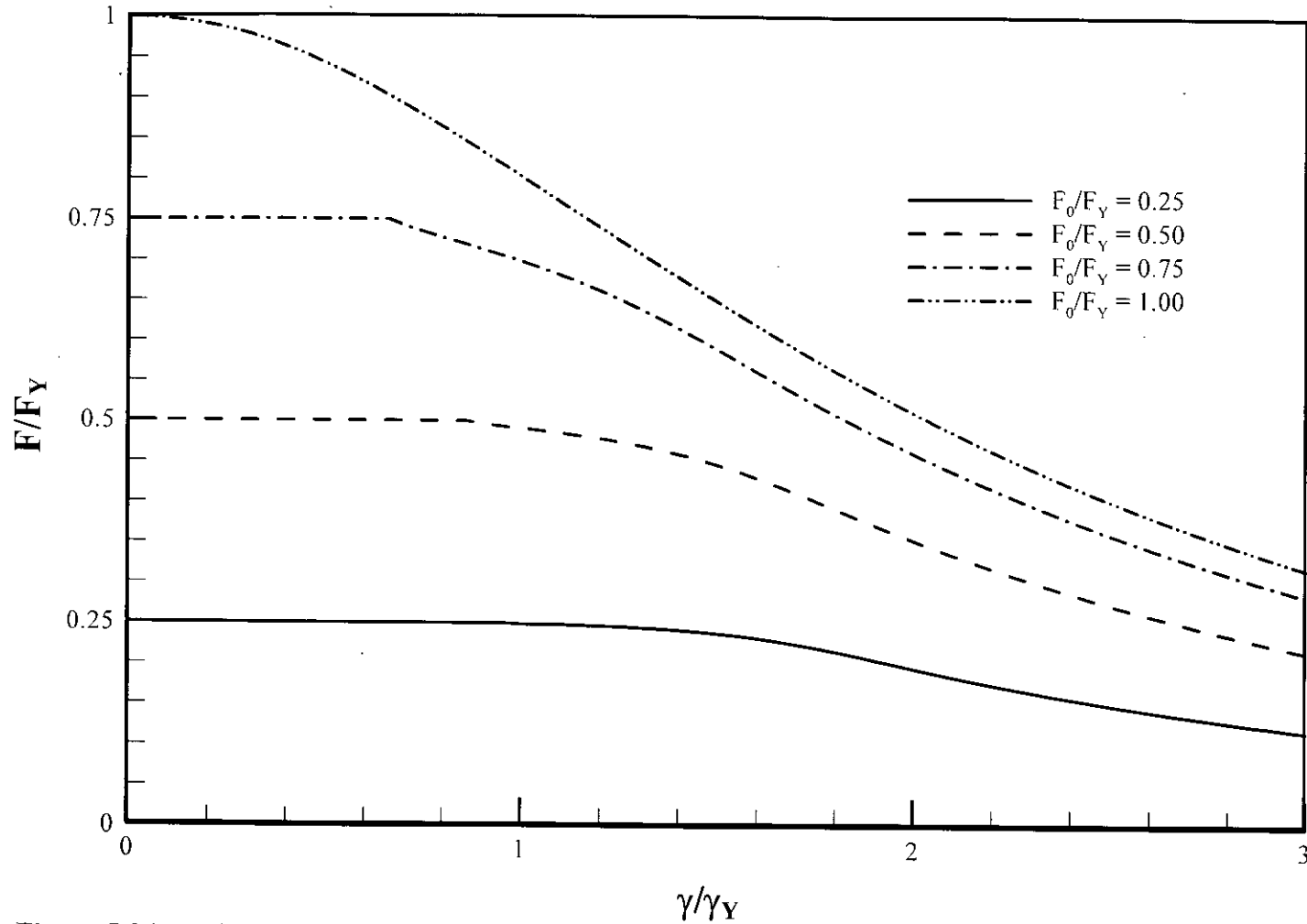


Figure 5.24: Variation of normalized axial load with subsequently applied shear strain for different values of initially applied axial load when the circular bar is extended first

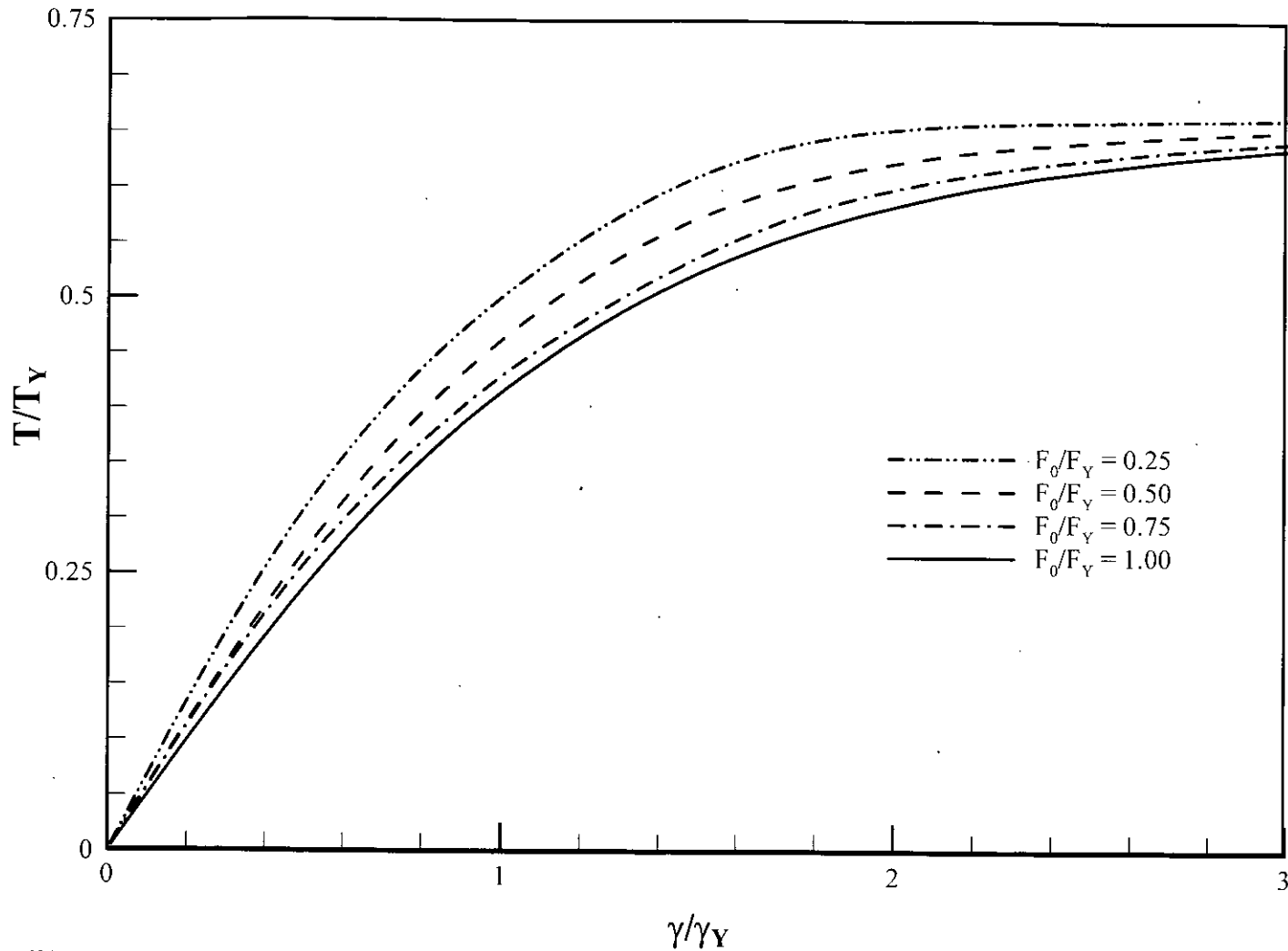


Figure 5.25: Variation of normalized torque with subsequently applied shear strain for different values of initially applied axial load when the circular bar is extended first

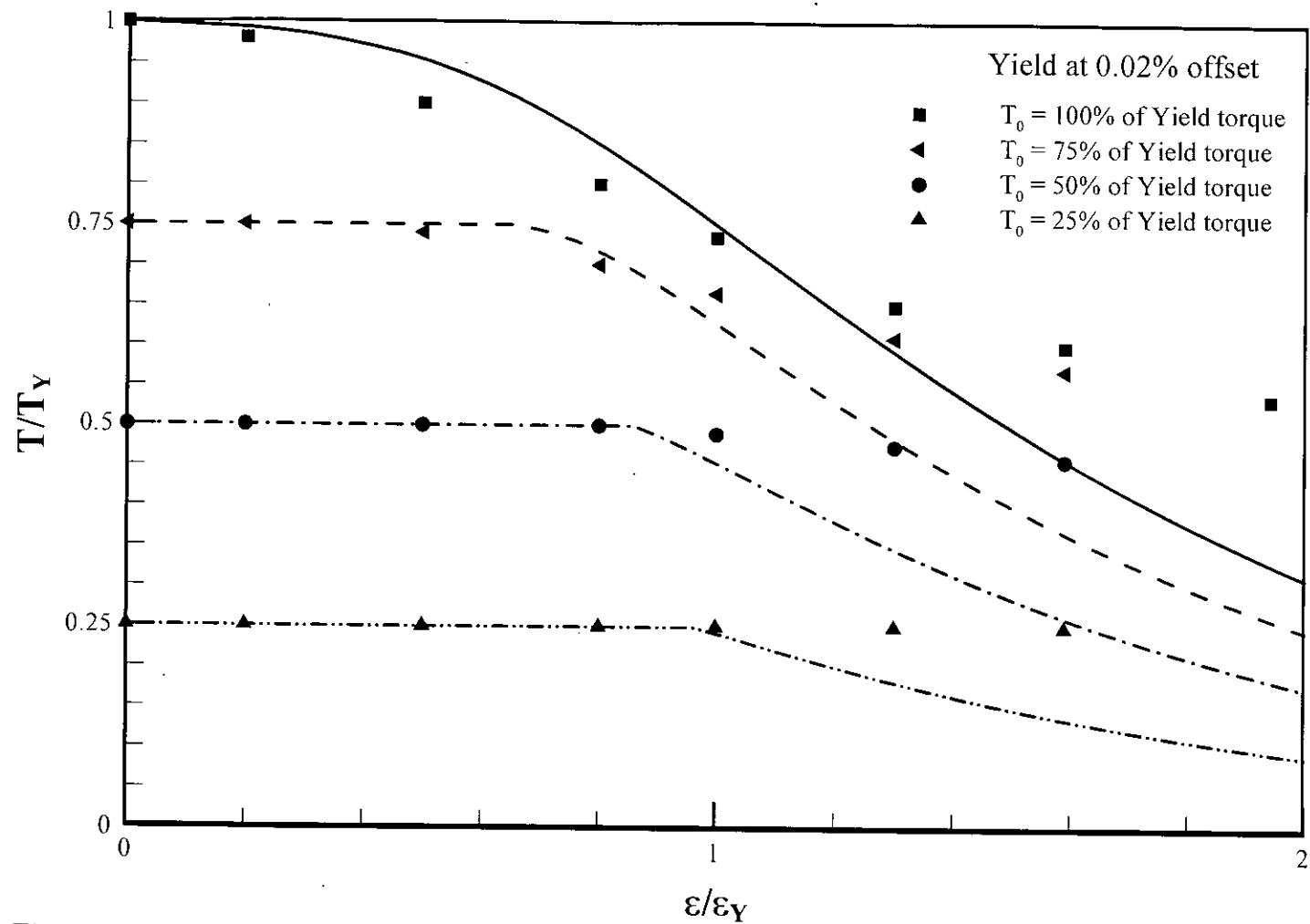


Figure 5.26: Comparison of the theoretical and experimental [18-19] results of steel for CASE-I, when yield at 0.02% offset

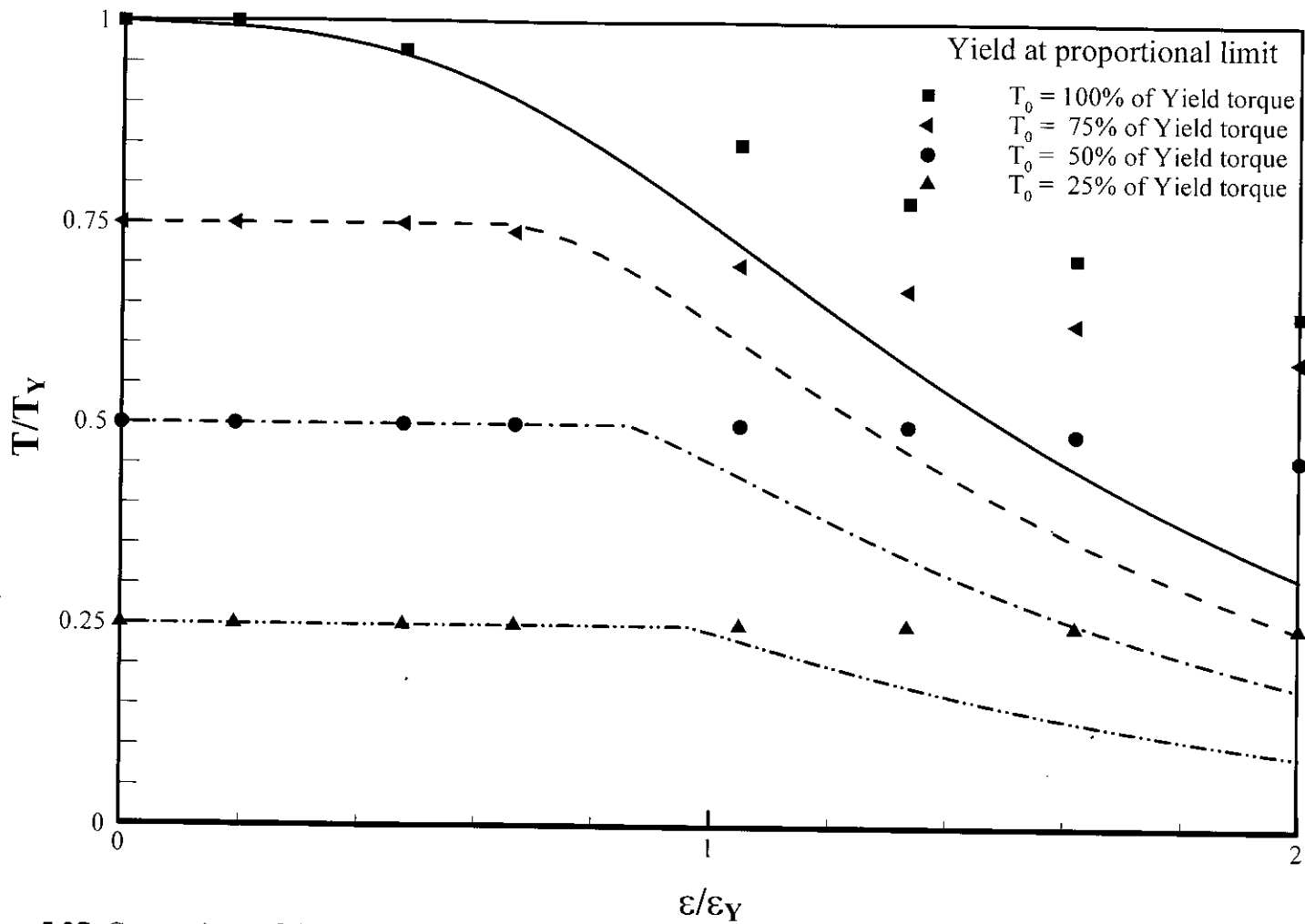


Figure 5.27: Comparison of the theoretical and experimental [18-19] results of steel for CASE-I, when yield at proportional limit

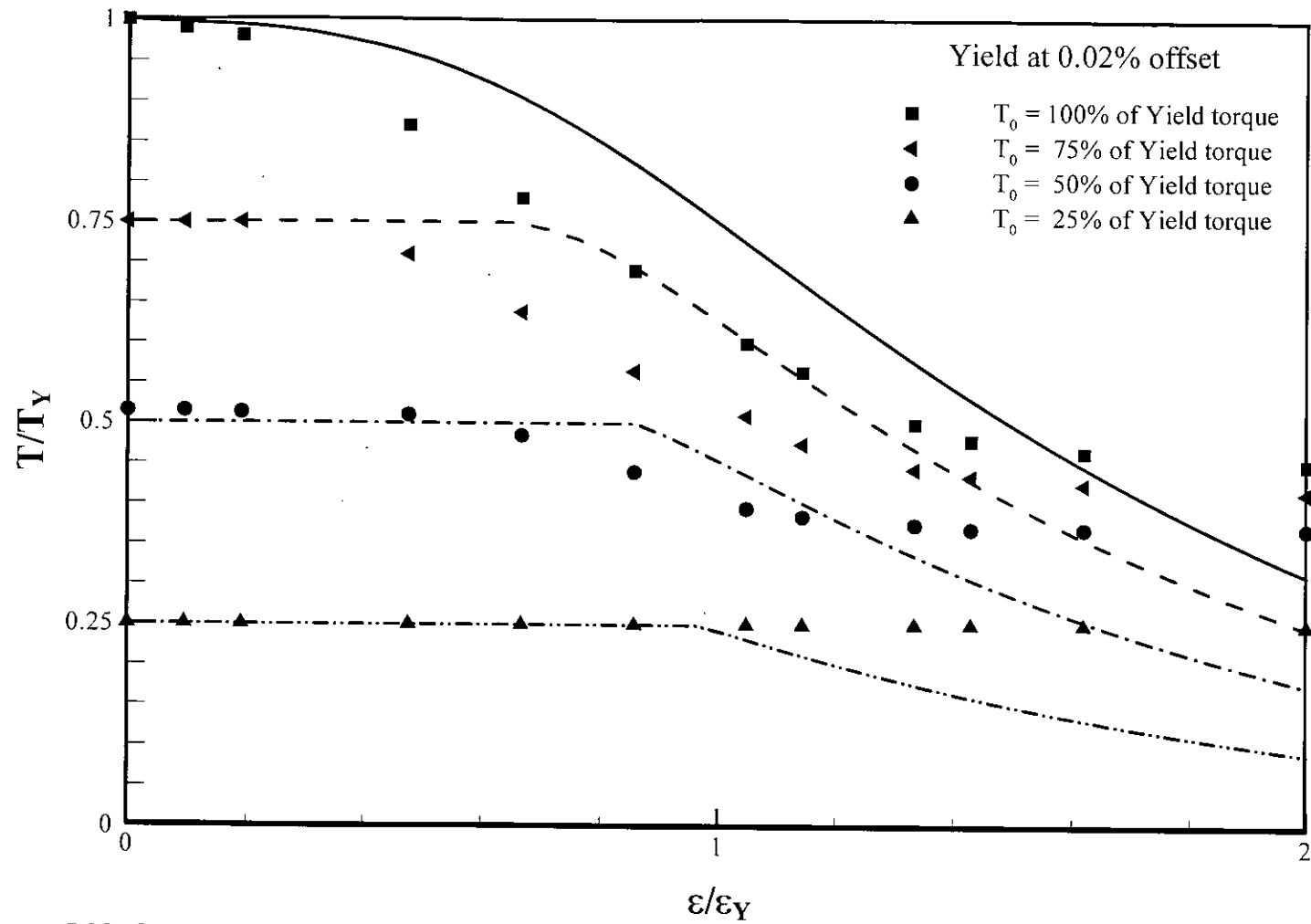


Figure 5.28: Comparison of the theoretical and experimental [18-19] results of copper for CASE-I, when yield at 0.02% offset

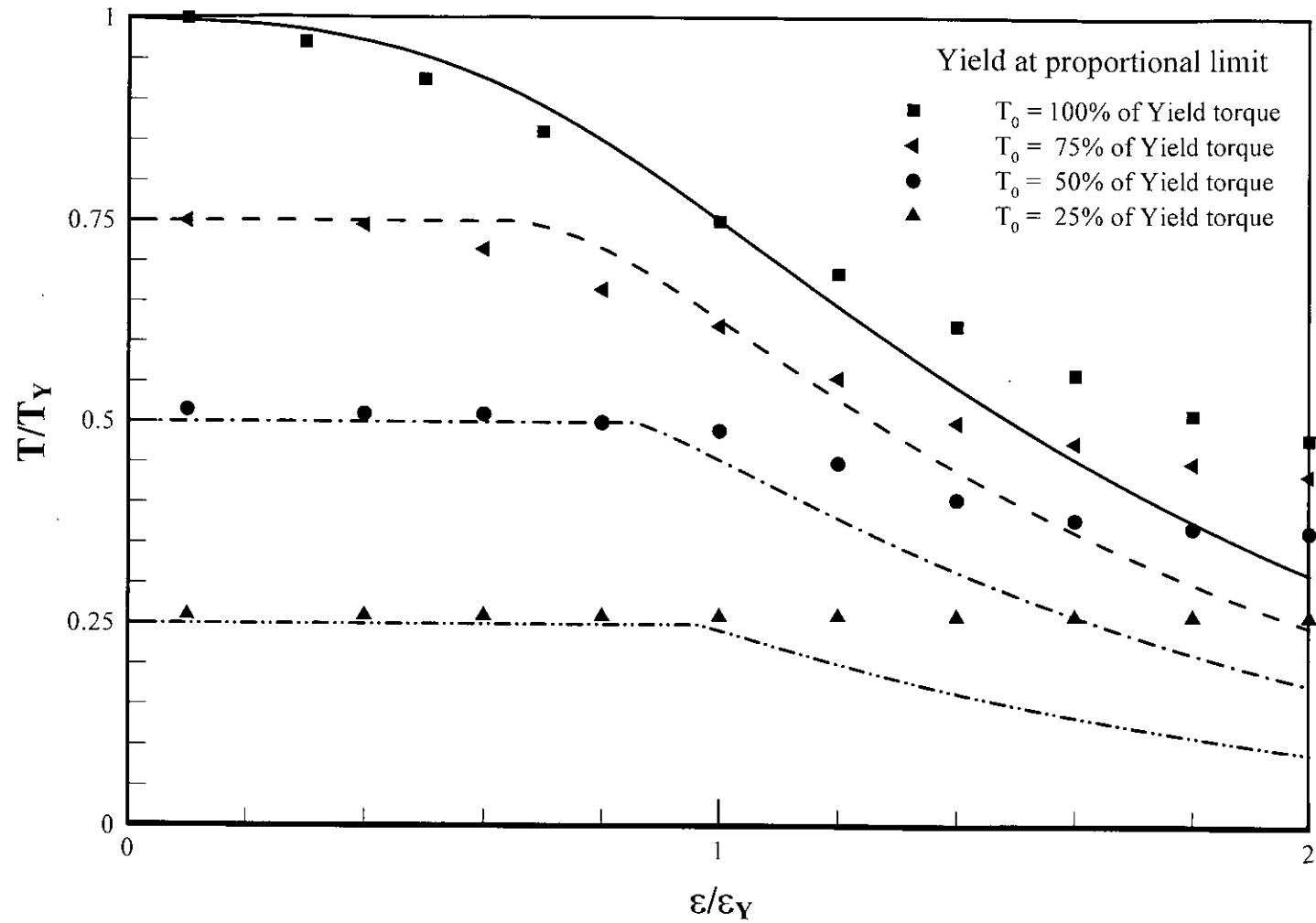


Figure 5.29: Comparison of the theoretical and experimental [18-19] results of copper for CASE-I, when yield at proportional limit

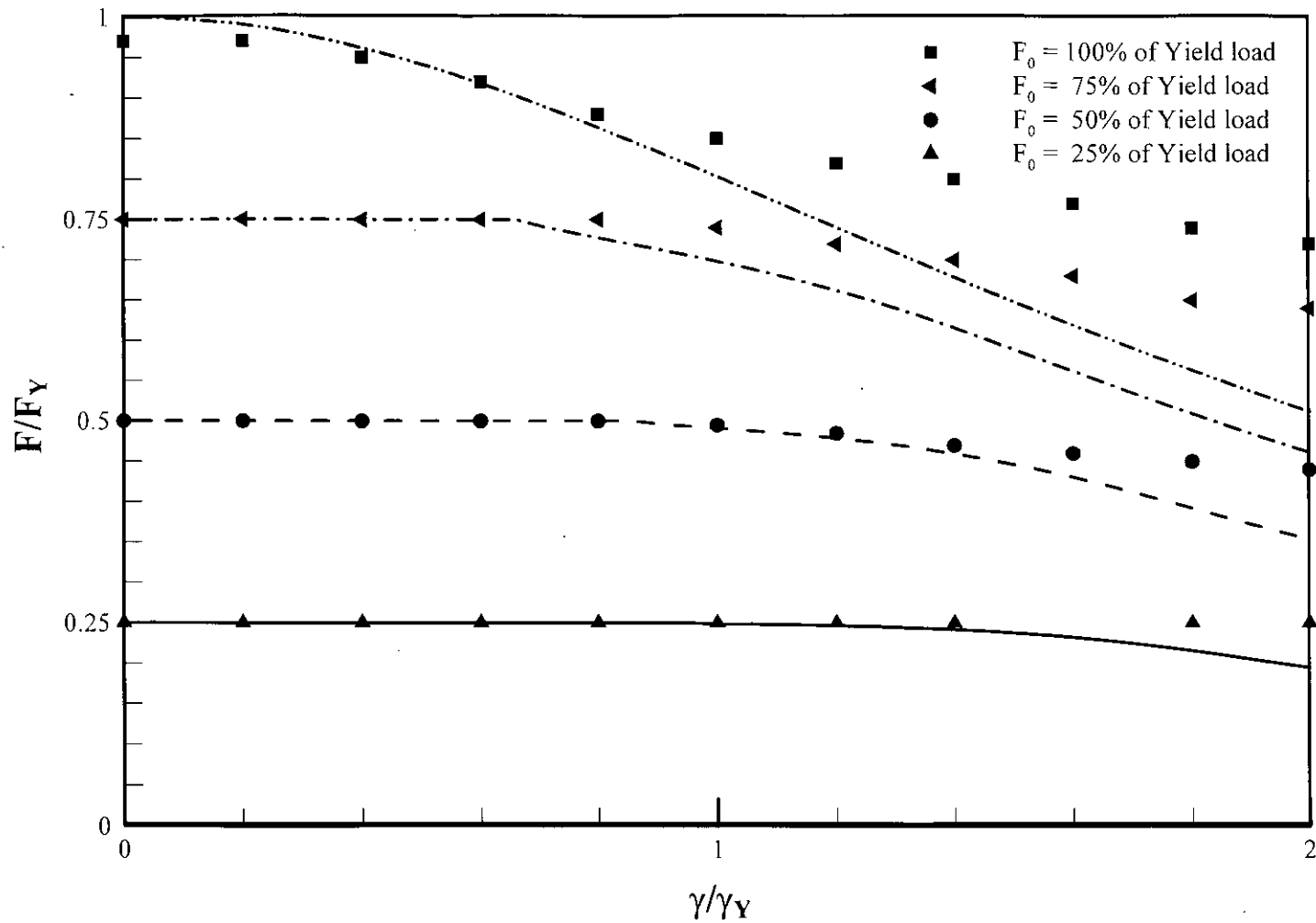


Figure 5.30: Comparison of the theoretical and experimental [18-19] results of steel for CASE-II

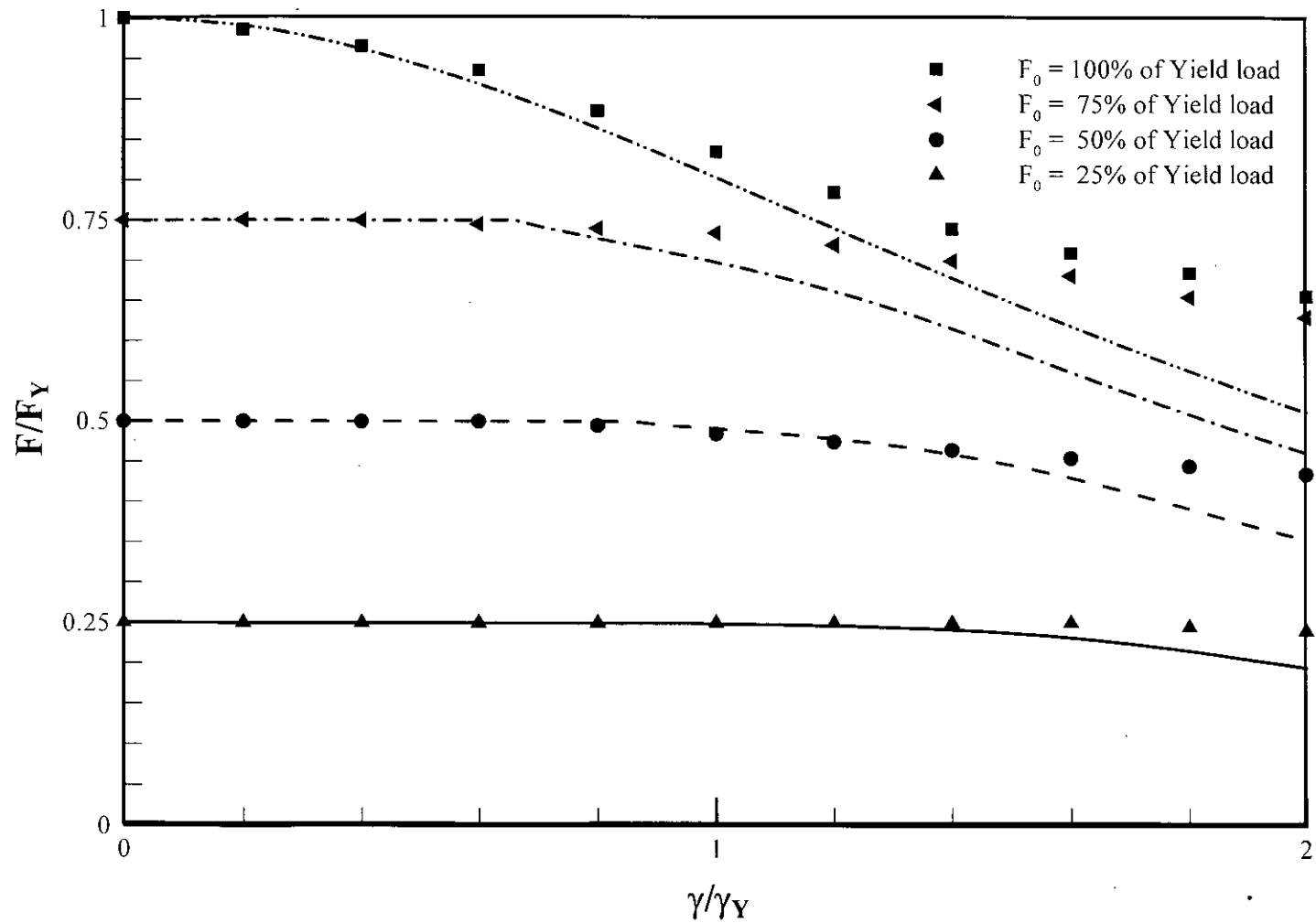


Figure 5.31: Comparison of the theoretical and experimental [18-19] results of COPPER for CASE-II

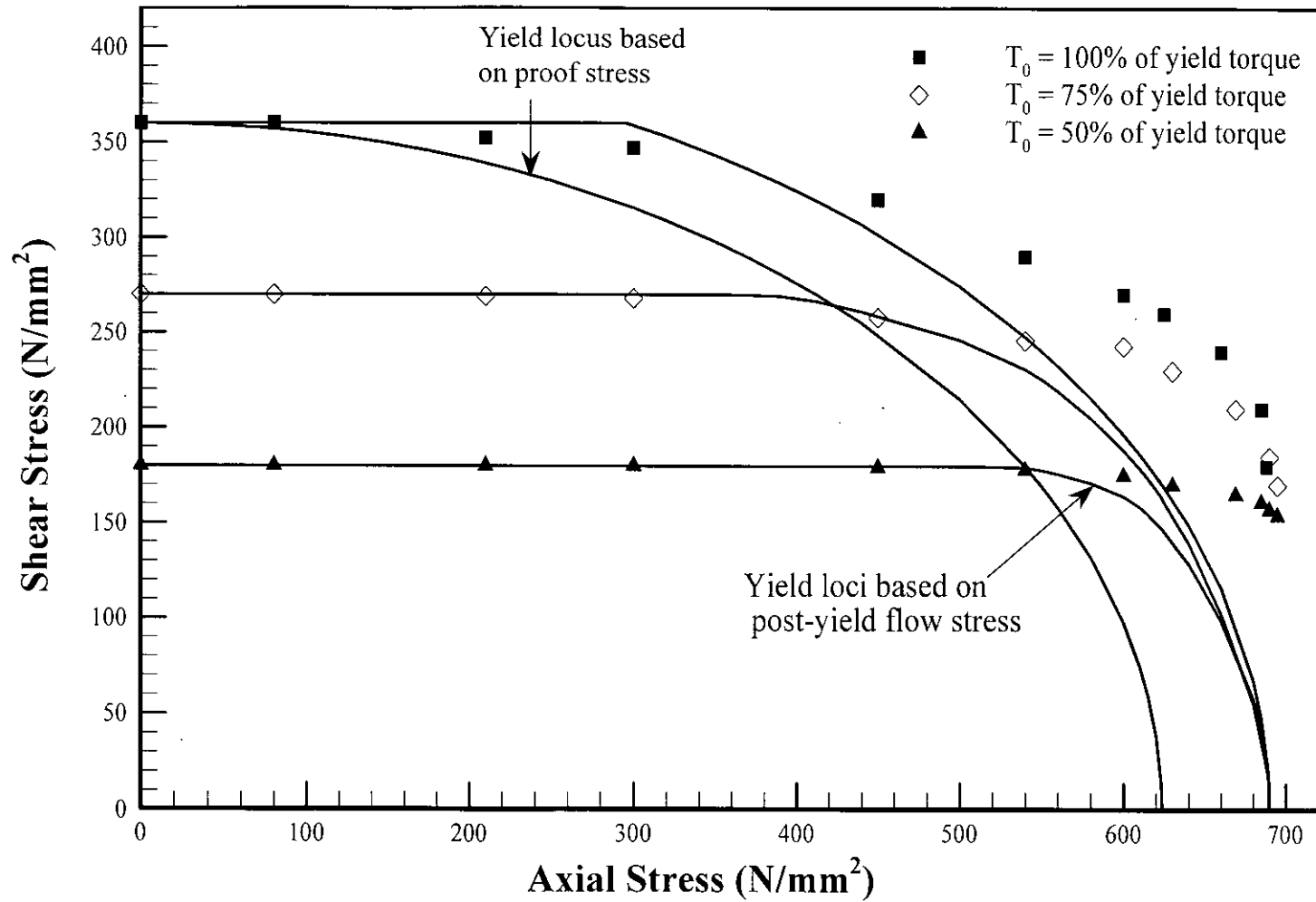


Figure 5.32: Comparison of the theoretical results obtained considering post yield flow stresses with the available experimental [18-19] results of steel for CASE-I

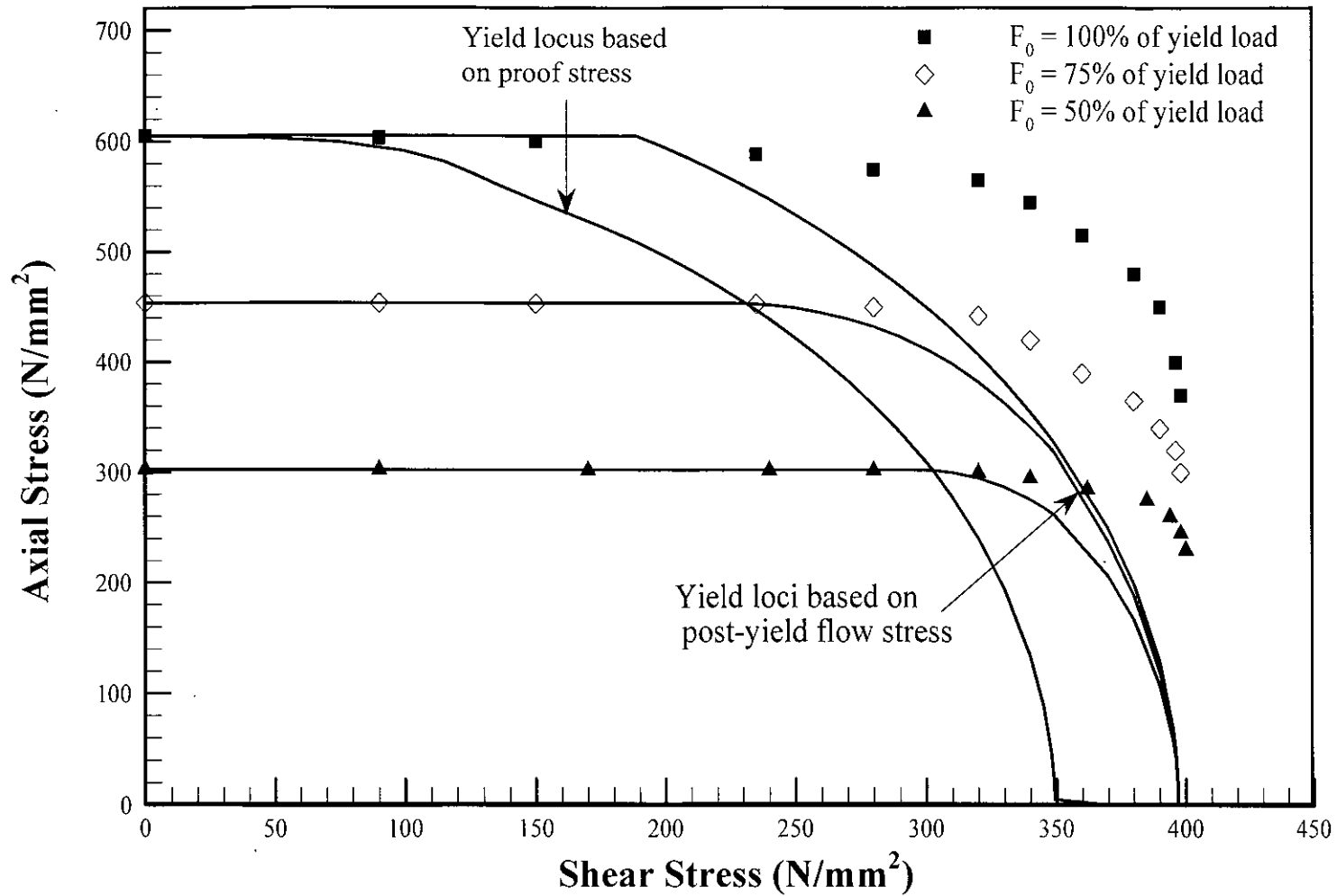


Figure 5.33: Comparison of the theoretical results obtained considering post yield flow stresses with the available experimental [18-19] results of steel for CASE-II.

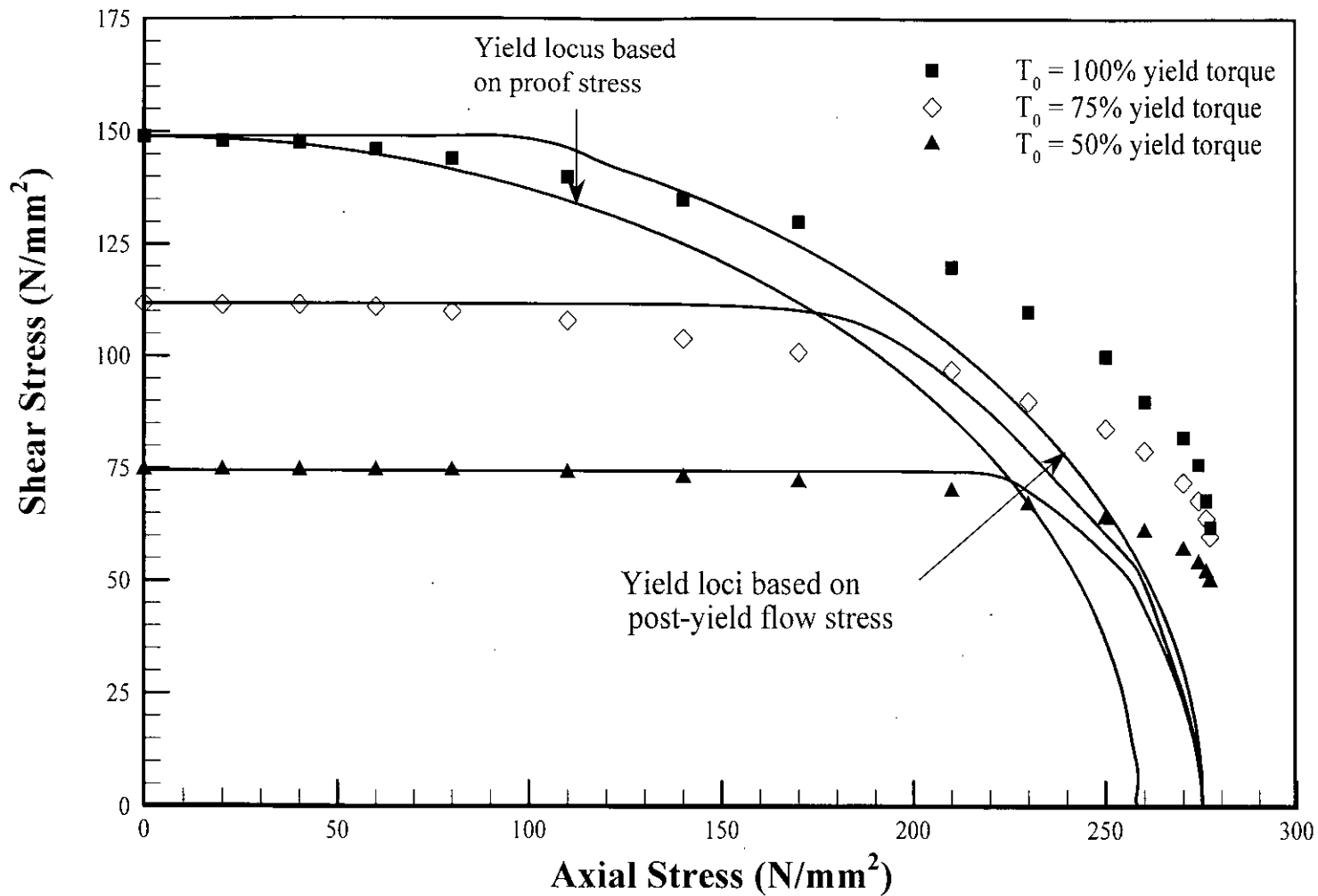


Figure 5.34: Comparison of the theoretical results obtained considering post yield flow stresses with the available experimental [18-19] results of copper for CASE-I

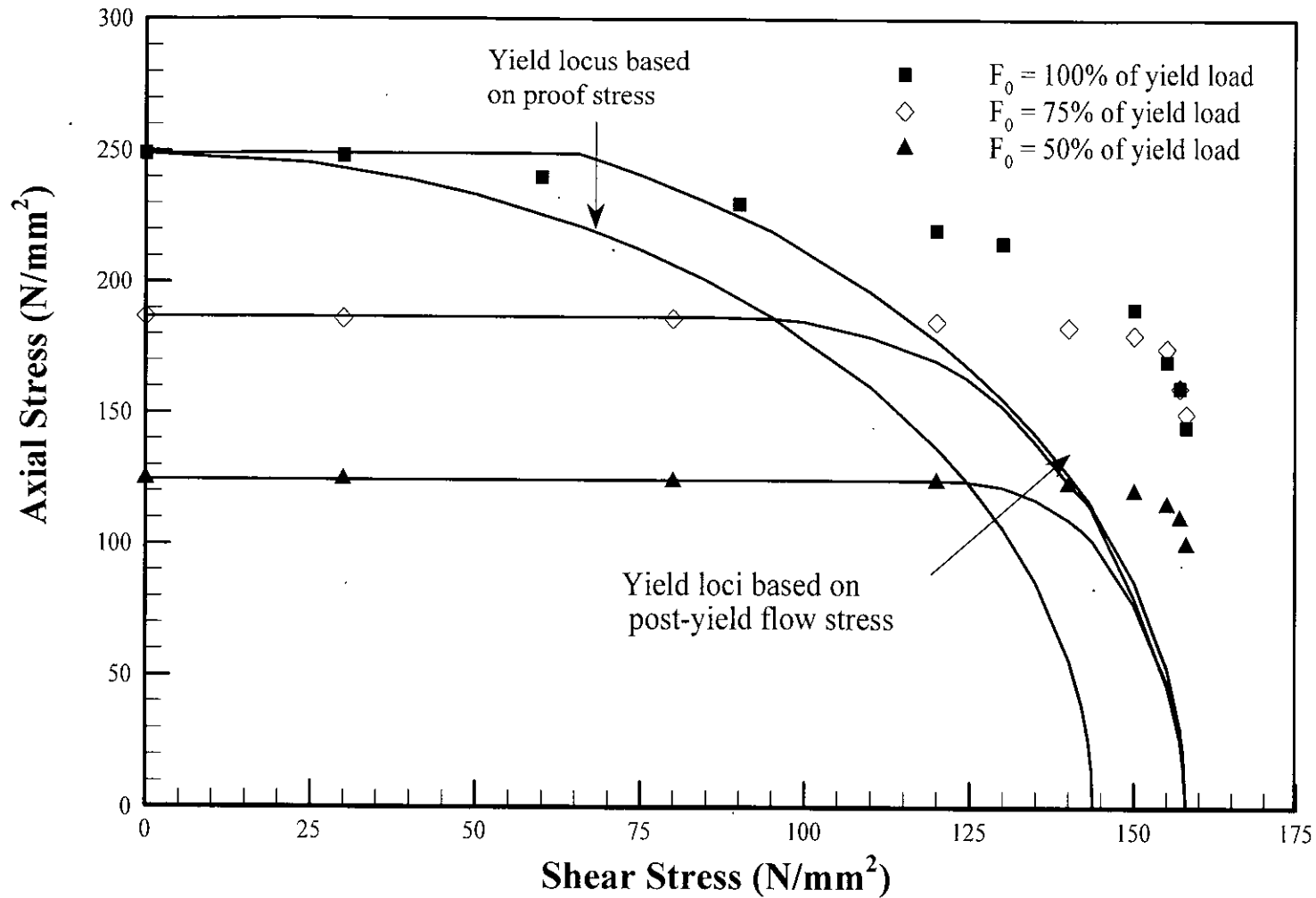


Figure 5.35: Comparison of the theoretical results obtained considering post yield flow stresses with the available experimental [18-19] results of copper for CASE-II

REFERENCES:

- [1] Tresca, H., "Sur, l'écoulement des corps solides soumis a de fortes pression", Compt. Rend. 59, pp. 754, 1864.
- [2] Saint-Venant, B. de., "Memorie sur l'établissement des equations differentielles des mouvements intereurs operes dans less corps solides ductiles au dela des limites ou l'elasticite pourrait less ramener a leur premier etat", Compt. Rend. 70, pp. 473-480, 1870.
- [3] Levy, M., "Memorie sur less equations generales des mouvements interieurs des corps solides ductiles au dela des limites ou Telasticite pourrait less ramener a leur premier etat", Compt. Rend. 70, pp. 1323-1325, 1864.
- [4] R. von Mises, Mechanik der festen Koerper im plastisch deformablen Zustand, Goettinger nachar, Math.-Phys. KI., pp. 582-592, 1913.
- [5] Hencky, H. "Zur Theorie plastischer Deformationen und der hierdurch im Material hervorgerufenen Nebenspannungen", Proceedings of the 1st International Congress on Applied Mechanics, Delft, Technische Boekhandel en Druckerij, J. Waltman, Jr., pp. 312-317, 1925.
- [6] Prandtl, L., "Spannungsverteilung in plastischen Koerpern", Proceedings of the 1st International Congress on Applied Mechanics, Delft, pp. 43-54, 1924.
- [7] Hill, R. "The Mathematical Theory of Plasticity", Oxford University Press, London, 1950.
- [8] Westergaard, B.W., "Theory of Elasticity and Plasticity", Harvard University Press, Cambridge, 1952.
- [9] Drucker, D.C. "Relation of Experiments to Mathematical Theories of Plasticity", ASME Journal of Applied Mechanics, vol.71, pp. 349-357, 1949.
- [10] Drucker, D.C. "The Significance of the Criterion for Additional Plastic Deformation of Metals", Journal of Colloid Science, vol.4, pp. 299-311, 1949.
- [11] Edelman, F. and Drucker, D.C. "Some Extensions of Elementary Plasticity Theory" Journal of the Franklin Institute, vol.251, pp. 581-605, 1951.

- [12] Stockton, F. D. and Drucker, D. C., "Fitting Mathematical Theories of Plasticity to Experimental Results", *Journal of Colloid Science*, vol. 5, pp. 239-250, 1950.
- [13] Monaghan, J. and Duff, B., "The effect of external loading on a yield tightened joint", *International Journal of Machine Tools Manufact.*, vol.27, no.4, pp. 443-455, 1987.
- [14] Newnham, J., Curley, L., and Boos, H.P., "The response to external loads of bolted joint tightened to yield", *VDI BERICHTE NR. 766*, 1989.
- [15] Chapman, I., Newnham, J., and Wallace, "The tightening of bolts to yield and their performance under load", *ASME Journal of Vibration, Acoustics, Stress, and Reliability in Design*, vol.108, pp. 213-221, 1986.
- [16] Hagiwara, M., Ohashi, N., and Yoshimoto, I., "Characteristics of bolted joints in plastic region tightening", *Bull Japan Soc. of Prec. Engg.*, vol.20, no.4, 1986.
- [17] Hariri, B. H., M. Eng. Thesis, Dublin City University, Ireland, 1990.
- [18] Ali, A.R.M. and Hashmi, M.S.J., "Plastic yielding of a solid bar under combined torque and tension", *Proceedings of the twelfth International Conference of the Irish Manufacturing Committee, IMC 12*, pp-483-490, Cork, Ireland, 1995.
- [19] Ali, A.R.M., "Effect of simultaneously applied torque and tension on a solid rod within the plastic region" *IE (India) Journal*, vol.79, pp. 65-69, 1998.
- [20] Prager, W. and Hodge, P. G., "Theory of Perfectly Plastic Solids", John Wiley, New York, 1951.
- [21] Sved, G. and Brooks D. S., "Elasto-plastic behaviour of a round bar subjected to axial force and torque", *Acta. Techn. Hung.*, vol.50, 1965.
- [22] Reuss, E., "Beruecksichtigung der elastischen Formaenderungen in der Plastizitaetstheorie", *Z. Angew. Math. Mech.*, vol. 10, pp.266-274, 1930.
- [23] J. Chakrabarty, "Theory of Plasticity", McGraw-Hill, Inc., 1987.
- [24] Mendelson, A., "Plasticity: Theory and Application", The MacMillan Company, New York, 1968.

APPENDIX – A

COMPUTER PROGRAM

```

*****
* A FORTRAN PROGRAM TO EVALUATE VARIATION OF LOAD BETWEEN *
* LIMITS A & B USING SIMSON 1/3 RULE. *
*****

*****
* THE INTEGRAL IS DEFINED AS A FUNCTION & A DIFFERENT *
* SUBROUTINE IS USED FOR INTEGRATION METHODS SAY *
* F(X)=X*(EXP(-X)),UPPER LIMIT=1.0,LOWER LIMIT=0.0 *
*****

*****
* MAIN PROGRAM FOR THE INTEGRATION *
*****
PRINT*, 'ENTER THE PROBLEM TYPE'
PRINT*, 'PRESS "1" FOR CASE-I (THE BAR IS INITIALY SUBJECTED BY A
1AXIAL LOAD THEN SUBJECTED BY A TORSIONAL LOAD)'

PRINT*, 'PRESS "2" FOR CASE-II (THE BAR IS INITIALY TWISTED THEN
1SUBJECTED TO AN AXIAL LOAD)'
204 PRINT*, 'CASE-'
READ*, CASE

*****
* CALCULATION BLOCK FOR CASE-I *
*****

IF(CASE.EQ.1)THEN

PRINT*, 'ENTER NUMBER OF STEPS'
212 PRINT*, 'PUT ANY EVEN NUMBER SO THAT ALL MULTIPLES ARE "2"'
PRINT*, 'SUCH AS 2,4,8,16,'
PRINT*, 'NO. OF STEPS, N= '
READ*, N

211 PRINT*, 'ACCURACY='
READ*, EPS
A=0.0001
B=0.99999999
PRINT*, 'ENTER THE VALUE FOR "P"'
203 PRINT*, '"P" = INITIAL SHEAR STRAIN/YIELD SHEAR STRAIN'
PRINT*, 'P='
READ*, P
P=ABS(P)

OPEN(UNIT=6,FILE='TORQUE1.ÖUT')
OPEN(UNIT=26,FILE='FORCE1.OUT')

```



```

*****
*   CALCULATION BLOCK FOR VARIATION OF TORQUE WITH AXIAL   *
*   STRAIN IN A ROD INITIALLY TWISTED                     *
*****

IF(P.EQ.1.0)THEN
WRITE(6,*) 'E/EY'      "T/TY"
DO EEY1=0.05,4,0.05

IF(EEY1.LT.1)THEN
A=1.0-EEY1
ANS2=0.0

DO J=2,N,2
H=(B-A)/J
N1=J/2
SUM=0.0
DO I=1,N1
X=A+(2*I-1)*H
SUM=SUM+4*T1(X,EEY1,P)
IF(I.NE.N1)THEN
X1=X+H
SUM=SUM+2*T1(X1,EEY1,P)
ENDIF
ENDDO
SUM=SUM+T1(A,EEY1,P)+T1(B,EEY1,P)
ANS=SUM*(H/3)
ANS1=ANS
IF((ABS(ANS1-ANS2)).LE.EPS)GO TO 100

ANS2=ANS
ENDDO
100 WRITE(*,*)'VALUE OF T/TY=',ANS2,'FOR E/EY=',EEY1
ANS2=ANS2+TAOW1(EEY1,P,A)

ELSE

ANS2=0.0
DO J=2,N,2
H=(B-A)/J
N1=J/2
SUM=0.0
DO I=1,N1
X=A+(2*I-1)*H
SUM=SUM+4*T1(X,EEY1,P)
IF(I.NE.N1)THEN
X1=X+H
SUM=SUM+2*T1(X1,EEY1,P)
ENDIF
ENDDO
SUM=SUM+T1(A,EEY1,P)+T1(B,EEY1,P)
ANS=SUM*(H/3)
ANS1=ANS

IF((ABS(ANS1-ANS2)).LE.EPS)GO TO 201
ANS2=ANS
ENDDO
201 PRINT*, 'VALUE OF THE INTEGRATION FOR T/TY=',ANS2,'FOR E/EY=',EEY1

```

```

WRITE(*,*)EEY1,ANS2
ENDIF

WRITE(6,*)EEY1,ANS2
ENDDO

ELSE IF(P.LT.1.0)THEN

EEY3=SQRT(1.0-P*P)
WRITE(6,*)"EEY3" "E/EY" "T/TY"
DO EEY2=0.05,4,0.05

IF(EEY2.LE.EEY3)THEN
A=1.0
ANS=TAOW1(EEY2,P,A)
WRITE(6,*)EEY3,EEY2,ANS
ELSE
A=B-(EEY2-0.05-EEY3)
ANS2=0.0
DO J=2,N,2
H=(B-A)/J
N1=J/2
SUM=0.0
DO I=1,N1
X=A+(2*I-1)*H
SUM=SUM+4*T1(X,EEY2,P)
IF(I.NE.N1)THEN
X1=X+H
SUM=SUM+2*T1(X1,EEY2,P)
ENDIF
ENDDO
SUM=SUM+T1(A,EEY2,P)+T1(B,EEY2,P)
ANS=SUM*(H/3)
ANS1=ANS
IF((ABS(ANS1-ANS2)).LE.EPS)GO TO 101

ANS2=ANS
ENDDO
101 WRITE(*,*)"VALUE OF T/TY=",ANS2,"FOR E/EY=",EEY2
ANS2=ANS2+TAOW1(EEY2,P,A)
WRITE(6,*)EEY3,EEY2,ANS2

ENDIF

ENDDO

ELSE
PRINT*, 'ENTER THE VALUE FOR "P" BETWEEN "0" & "1"'
GOTO 203
ENDIF

```

```

*****
* CALCULATION BLOCK FOR VARIATION OF AXIAL LOAD WITH AXIAL *
* STRAIN IN A ROD INITIALLY TWISTED.(CASE-I) *
*****

```

```

IF(P.EQ.1.0)THEN
WRITE(26,*) "E/EY" "F/FY"
DO EEY1=0.05,4,0.05

```

Appendix - A: Computer Program

```

IF(EEY1.LT.1.0)THEN
  A=B-EEY1
  ANS2=0.0

  DO J=2,N,2
  H=(B-A)/J
  N1=J/2
  SUM=0.0
  DO I=1,N1
    X=A+(2*I-1)*H
    SUM=SUM+4*F1(X,EEY1,P)
  IF(I.NE.N1)THEN
    X1=X+H
    SUM=SUM+2*F1(X1,EEY1,P)
  ENDIF
  ENDDO
  SUM=SUM+F1(A,EEY1,P)+F1(B,EEY1,P)
  ANS=SUM*(H/3)
  ANS1=ANS
  IF((ABS(ANS1-ANS2)).LE.EPS)GO TO 300

  ANS2=ANS
  ENDDO
300  WRITE(*,*)'VALUE OF F/FY=',ANS2,'FOR E/EY=',EEY1
  ANS2=ANS2+SIGMA1(EEY1,P,A)

ELSE

  ANS2=0.0
  DO J=2,N,2
  H=(B-A)/J
  N1=J/2
  SUM=0.0
  DO I=1,N1
    X=A+(2*I-1)*H
    SUM=SUM+4*F1(X,EEY1,P)
  IF(I.NE.N1)THEN
    X1=X+H
    SUM=SUM+2*F1(X1,EEY1,P)
  ENDIF
  ENDDO
  SUM=SUM+F1(A,EEY1,P)+F1(B,EEY1,P)
  ANS=SUM*(H/3)
  ANS1=ANS
  IF((ABS(ANS1-ANS2)).LE.EPS)GO TO 301
  ANS2=ANS
  ENDDO
301  PRINT*, 'VALUE OF THE INTEGRATION FOR F/FY=',ANS2,'FOR E/EY=',EEY1
  WRITE(*,*)EEY1,ANS2
  ENDIF

  WRITE(26,*)EEY1,ANS2
  ENDDO

ELSE IF(P.LT.1.0)THEN

  EEY3=SQRT(1.0-P*P)

```

```

WRITE(26,*)"EEY3"    "E/EY"    "F/FY"
DO EEY2=0.05,4,0.05

  IF(EEY2.LE.EEY3)THEN
    A=1.0
    ANS=TAOW1(EEY2,P,A)
    WRITE(26,*)EEY2,ANS
  ELSE
    A=B-(EEY2-0.05-EEY3)
    ANS2=0.0
    DO J=2,N,2
      H=(B-A)/J
      N1=J/2
      SUM=0.0
      DO I=1,N1
        X=A+(2*I-1)*H
        SUM=SUM+4*F1(X,EEY2,P)
      IF(I.NE.N1)THEN
        X1=X+H
        SUM=SUM+2*F1(X1,EEY2,P)
      ENDIF
    ENDDO
    SUM=SUM+F1(A,EEY2,P)+F1(B,EEY2,P)
    ANS=SUM*(H/3)
    ANS1=ANS
    IF((ABS(ANS1-ANS2)).LE.EPS)GO TO 331

    ANS2=ANS
    ENDDO
331  WRITE(*,*)"VALUE OF F/FY=",ANS2,"FOR E/EY=",EEY2
    ANS2=ANS2+SIGMA1(EEY2,P,A)
    WRITE(26,*)EEY3,EEY2,ANS2

  ENDIF

ENDDO

ELSE
  PRINT*,'ENTER THE VALUE FOR "P" BETWEEN "0" & "1"'
  GOTO 203

ENDIF

*****
*   CALCULATION BLOCK FOR CASE-II   *
*****

  ELSE IF(CASE.EQ.2)THEN
    PRINT*,'ENTER NUMBER OF STEPS'
232  PRINT*,'PUT ANY EVEN NUMBER SO THAT ALL MULTIPLES ARE "2"'
    PRINT*,'SUCH AS 2,4,8,16,'
    PRINT*,'NO. OF STEPS, N= '
    READ*,N

231  PRINT*,'ACCURACY='
    READ*,EPS
    A=0.001
    B=0.999999

```

```

PRINT*, 'ENTER THE VALUE FOR "Q"'
223 PRINT*, "Q" = INITIAL AXIAL STRAIN/YIELD STRAIN'
PRINT*, 'Q='
READ*, Q
Q=ABS(Q)

```

```

OPEN(UNIT=16, FILE='TORQUE2.OUT')
OPEN(UNIT=36, FILE='FORCE2.OUT')

```

```

*****
*  CALCULATION BLOCK FOR VARIATION OF TORQUE WITH SHEAR STRAIN *
*  IN A BAR INITIALLY EXTENDED (CASE-II) *
*****

```

```

IF(Q.EQ.1.0)THEN

DO GGY1=0.1,4,0.1

IF(GGY1.LT.B)THEN
  A=B-EEY1
  ANS2=0.0

  DO J=2,N,2
    H=(B-A)/J
    N1=J/2
    SUM=0.0
    DO I=1,N1
      X=A+(2*I-1)*H
      SUM=SUM+4*T2(X,GGY1,Q)
    IF(I.NE.N1)THEN
      X1=X+H
      SUM=SUM+2*T2(X1,GGY1,Q)
    ENDIF
  ENDDO
  SUM=SUM+T2(A,GGY1,Q)+T2(B,GGY1,Q)
  ANS=SUM*(H/3)
  ANS1=ANS
  IF((ABS(ANS1-ANS2)).LE.EPS)GO TO 120

  ANS2=ANS
  ENDDO
120 WRITE(*,*)'VALUE OF T/TY=',ANS2,'FOR G/GY=',GGY1
  ANS3=ANS2+TAOW2(GGY1,Q,A)
  WRITE(*,*)GGY1,ANS3

ELSE

  ANS2=0.0
  DO J=2,N,2
    H=(B-A)/J
    N1=J/2
    SUM=0.0
    DO I=1,N1
      X=A+(2*I-1)*H
      SUM=SUM+4*T2(X,GGY1,Q)
    IF(I.NE.N1)THEN
      X1=X+H
      SUM=SUM+2*T2(X1,GGY1,Q)

```

```

ENDIF
ENDDO
SUM=SUM+T2(A,GGY1,Q)+T2(B,GGY1,Q)
ANS=SUM*(H/3)
ANS1=ANS
IF((ABS(ANS1-ANS2)).LE.EPS)GO TO 221
ANS2=ANS
ENDDO
221 PRINT*, 'VALUE OF THE INTEGRATION FOR T/TY=',ANS2, 'FOR G/GY=',GGY1
WRITE(*,*)GGY1,ANS2
ENDIF

WRITE(16,*)GGY1,ANS2
ENDDO

ELSE IF(Q.LT.1.0)THEN

GGY3=SQRT(1.0-Q*Q)
WRITE(16,*)GGY3, G/GY, T/TY'
DO GGY2=0.1,4,0.1

IF(GGY2.LE.GGY3)THEN
A=1.0
ANS=TAOW2(GGY2,Q,A)
WRITE(16,*)GGY2,ANS
ELSE
A=B-(GGY2-GGY3)
ANS2=0.0
DO J=2,N,2
H=(B-A)/J
N1=J/2
SUM=0.0
DO I=1,N1
X=A+(2*I-1)*H
SUM=SUM+4*T2(X,GGY2,Q)
IF(I.NE.N1)THEN
X1=X+H
SUM=SUM+2*T2(X1,GGY2,Q)
ENDIF
ENDDO
SUM=SUM+T2(A,GGY2,Q)+T2(B,GGY2,Q)
ANS=SUM*(H/3)
ANS1=ANS
IF((ABS(ANS1-ANS2)).LE.EPS)GO TO 121

ANS2=ANS
ENDDO
121 WRITE(*,*)'VALUE OF T/TY=',ANS2, 'FOR G/GY=',GGY2
ANS2=ANS2+TAOW1(GGY2,Q,A)
WRITE(16,*)GGY3,GGY2,ANS2

ENDIF
ENDDO

ELSE
PRINT*, 'ENTER THE VALUE FOR "Q" BETWEEN "0" & "1"'
GOTO 223
ENDIF

```

```

*****
*   CALCULATION BLOCK FOR VARIATION OF AXIAL LOAD WITH SHEAR *
*   STRAIN IN A BAR INITIALLY EXTENDED (CASE-II)           *
*****

IF(Q.EQ.1.0)THEN

DO GGY1=0.1,4,0.1

IF(GGY1.LT.B)THEN
  A=B-EEY1
  ANS2=0.0

DO J=2,N,2
  H=(B-A)/J
  N1=J/2
  SUM=0.0
  DO I=1,N1
    X=A+(2*I-1)*H
    SUM=SUM+4*F2(X,GGY1,Q)
  IF(I.NE.N1)THEN
    X1=X+H
    SUM=SUM+2*F2(X1,GGY1,Q)
  ENDIF
  ENDDO
  SUM=SUM+F2(A,GGY1,Q)+F2(B,GGY1,Q)
  ANS=SUM*(H/3)
  ANS1=ANS
  IF((ABS(ANS1-ANS2)).LE.EPS)GO TO 520

  ANS2=ANS
  ENDDO
520  WRITE(*,*)'VALUE OF F/FY=',ANS2,'FOR G/GY=',GGY1
  ANS2=ANS2+SIGMA2(GGY1,Q,A)
  WRITE(*,*)GGY1,ANS2

ELSE

  ANS2=0.0
  DO J=2,N,2
    H=(B-A)/J
    N1=J/2
    SUM=0.0
    DO I=1,N1
      X=A+(2*I-1)*H
      SUM=SUM+4*F2(X,GGY1,Q)
    IF(I.NE.N1)THEN
      X1=X+H
      SUM=SUM+2*T2(X1,GGY1,Q)
    ENDIF
    ENDDO
    SUM=SUM+F2(A,GGY1,Q)+F2(B,GGY1,Q)
    ANS=SUM*(H/3)
    ANS1=ANS
    IF((ABS(ANS1-ANS2)).LE.EPS)GO TO 521
    ANS2=ANS
    ENDDO
521  PRINT*, 'VALUE OF THE INTEGRATION FOR F/FY=',ANS2,'FOR E/EY=',GGY1

```

```

WRITE(*,*)GGY1,ANS2
ENDIF

WRITE(36,*)GGY1,ANS2
ENDDO

ELSE IF(Q.LT.1.0)THEN

GGY3=SQRT(1.0-Q*Q)
WRITE(36,*)'GGY3,  G/GY,  F/FY'
DO GGY2=0.1,4,0.1

  IF(GGY2.LE.GGY3)THEN
    A=1.0
    ANS=SIGMA2(GGY2,Q,A)
    WRITE(36,*)GGY2,ANS
  ELSE
    A=B-(GGY2-GGY3)
    ANS2=0.0
    DO J=2,N,2
      H=(B-A)/J
      N1=J/2
      SUM=0.0
      DO I=1,N1
        X=A+(2*I-1)*H
        SUM=SUM+4*F2(X,GGY2,Q)
      IF(I.NE.N1)THEN
        X1=X+H
        SUM=SUM+2*F2(X1,GGY2,Q)
      ENDIF
    ENDDO
    SUM=SUM+F2(A,GGY2,Q)+F2(B,GGY2,Q)
    ANS=SUM*(H/3)
    ANS1=ANS
    IF((ABS(ANS1-ANS2)).LE.EPS)GO TO 523

    ANS2=ANS
    ENDDO
523  WRITE(*,*)'VALUE OF F/FY=',ANS2,'FOR G/GY=',GGY2
    ANS3=ANS2+SIGMA2(GGY2,Q,A)
    WRITE(36,*)GGY3,GGY2,ANS3

  ENDIF
ENDDO

ELSE
  PRINT*,'ENTER THE VALUE FOR "Q" BETWEEN "0" & "1"'
  GOTO 223
ENDIF

ELSE

PRINT*,'ENTER THE VALUES OF "1" OR "2" FOR CASE-I OR CASE-II'
GOTO 204

ENDIF

```


STOP
END

```

*****
*   SUBROUTINE FOR DEFINING THE FUNCTION FOR TORQUE FOR CASE-I *
*****
      FUNCTION T1(X,EEY,P)
      T1=4.0*(X**2)*SQRT(1.0-(TANH(EEY-SQRT(1-P*P*X*X)+
      1 0.5*ALOG((1+SQRT(1-P*P*X*X))/(1-SQRT(1-P*P*X*X))))**2)
C   F=1/(EXP(X**2))
      RETURN
      END
*****
*   SUBROUTINE FOR DEFINING THE FUNCTION FOR AXIAL LOAD FOR CASE-I *
*****
      FUNCTION F1(X,EEY,P)
      F1=2*X*TANH(EEY-SQRT(1-P*P*X*X)+0.5*ALOG
      1((1+SQRT(1-P*P*X*X))/(1-SQRT(1-P*P*X*X))))
      RETURN
      END
*****
*   SUBROUTINE FOR DEFINING THE FUNCTION FOR SHEAR STRESS *
*   FOR ELASTIC CORE FOR CASE-I *
*****
      FUNCTION TAOW1(EEY,P,A)
      AT=SQRT(1-P*P*A*A)
      ATH1=0.5*ALOG((1+AT)/(1-AT))
      SIGMA=TANH(EEY-AT+ATH1)
      TAOW1=SQRT(1-SIGMA**2)*(A**3)
      RETURN
      END
*****
*   SUBROUTINE FOR DEFINING THE FUNCTION FOR AXIAL STRESS *
*   FOR ELASTIC CORE FOR CASE-I *
*****
      FUNCTION SIGMA1(EEY,P,A)
      AT=SQRT(1-P*P*A*A)
      ATH1=0.5*ALOG((1+AT)/(1-AT))
      SIGMA1=TANH(EEY-AT+ATH1)*(A*A)
      RETURN
      END
*****
*   SUBROUTINE FOR DEFINING THE FUNCTION FOR AXIAL LOAD CASE-II *
*****
      FUNCTION F2(X,GGY,Q)
      F2=2.0*X*SQRT(1.0-(TANH(GGY*X-SQRT(1-Q*Q)+
      10.5*ALOG((1+SQRT(1-Q*Q))/(1-SQRT(1-Q*Q))))**2)
      RETURN
      END
*****
*   SUBROUTINE FOR DEFINING THE FUNCTION FOR TORQUE CASE-II *
*****
      FUNCTION T2(X,GGY,Q)
      T2=2.0*(X**2)*TANH(GGY*X-SQRT(1-Q*Q)+
      10.5*ALOG((1+SQRT(1-Q*Q))/(1-SQRT(1-Q*Q))))
      RETURN
      END
*****

```

```

* SUBROUTINE FOR DEFINING THE FUNCTION FOR SHEAR STRESS *
* FOR ELASTIC CORE FOR CASE-II *
*****
FUNCTION TAOW2(GGY,Q,A)
AT=SQRT(1-Q*Q)
ATH1=0.5*A*LOG((1+AT)/(1-AT))
TAOW2=TANH(GGY*A-AT+ATH1)*(A**3)
RETURN
END
*****
* SUBROUTINE FOR DEFINING THE FUNCTION FOR AXIAL STRESS *
* FOR ELASTIC CORE FOR CASE-II *
*****
FUNCTION SIGMA2(GGY,Q,A)
AT=SQRT(1-Q*Q)
ATH1=0.5*A*LOG((1+AT)/(1-AT))
TAOW=TANH(GGY*A-AT+ATH1)
SIGMA2=(SQRT(1-TAOW**2))*(A*A)
RETURN
END
*****

```

```

*****
* CALCULATION BLOCK FOR CASE-I ( TORSION FOLLOWED BY AXIAL LOAD) *
*****

```

```

OPEN(UNIT=6,FILE='SIGMA.PLT')
OPEN(UNIT=7,FILE='TAOW.PLT')
C E=E/EY
C P=G0/GY
C Z=R/A
C SIGMA=S/SY
C E=1.0
P=1.0
Z=1.0
C DO 10 Z=1.0,0,-0.05
DO 100 E=0,3.01,0.05
AT=SQRT(1-P*P*Z*Z)
ATH1=0.5*A*LOG((1+AT)/(1-AT))
SIGMA=TANH(E-AT+ATH1)
TAOW=SQRT(1-SIGMA**2)
WRITE(6,20)E,SIGMA
WRITE(7,20)E,TAOW
PRINT*,E,SIGMA,TAOW
20 FORMAT(1X,F10.4,4X,F10.4)
100 CONTINUE
C 10 CONTINUE
STOP
END

```

```

*****
* CALCULATION BLOCK FOR CASE-II ( TENSION FOLLOWED BY TORQUE) *
*****

```

```

OPEN(UNIT=6,FILE='SIGMA.PLT')
OPEN(UNIT=7,FILE='TAOW.PLT')
C Q=E0/EY
C G=G/GY

```

```
C  Z=R/A
C  SIGMA=S/SY
Q=1.0
*  Z=1.0
G=1.0
DO 10 Z=0.0001,1.0,0.005
*  DO 100 G=0.0,3.01,0.05
    AT=SQRT(1-Q*Q)
    ATH1=0.5*ALOG((1+AT)/(1-AT))
    TAOW=TANH(G*Z-AT+ATH1)
    SIGMA=SQRT(1-TAOW**2)
    WRITE(6,20)G,SIGMA
    WRITE(7,20)G,TAOW
    PRINT*,G,SIGMA,TAOW
20  FORMAT(1X,F10.4,4X,F10.4)
* 100  CONTINUE
C 10  CONTINUE
STOP
END
```

APPENDIX – B

MECHANICAL PROPERTIES OF STEEL AND COPPER

It contains the uni-axial stress-strain curves of the steel and copper rods, which were used by Ali *et al* [18-19] for conducting experimental investigation under similar type of bi-axial torque-tension loading, as has been considered theoretically in the present investigation. Figure B1 shows the uni-axial stress-strain curve of the steel & figure B2 that of copper. The steel used was En8 (BS970) whose typical composition were: 0.36% C, 0.10% Si, 0.60% Mn, 0.05% P and 0.05% S and copper used was pure copper with 1% impurities. The table given below shows the mechanical properties of the above mentioned two materials.

Materials	Modulus of Elasticity (GPa)	Modulus Of Rigidity (GPa)	Tensile Yield Load (kN)	Yield Torque (Nm)	Tensile Yield Stress (MPa)	Shear Yield Stress (MPa)
STEEL	212	73	30.4	36.2	605	360
COPPER	115	49	12.5	15.1	249	150

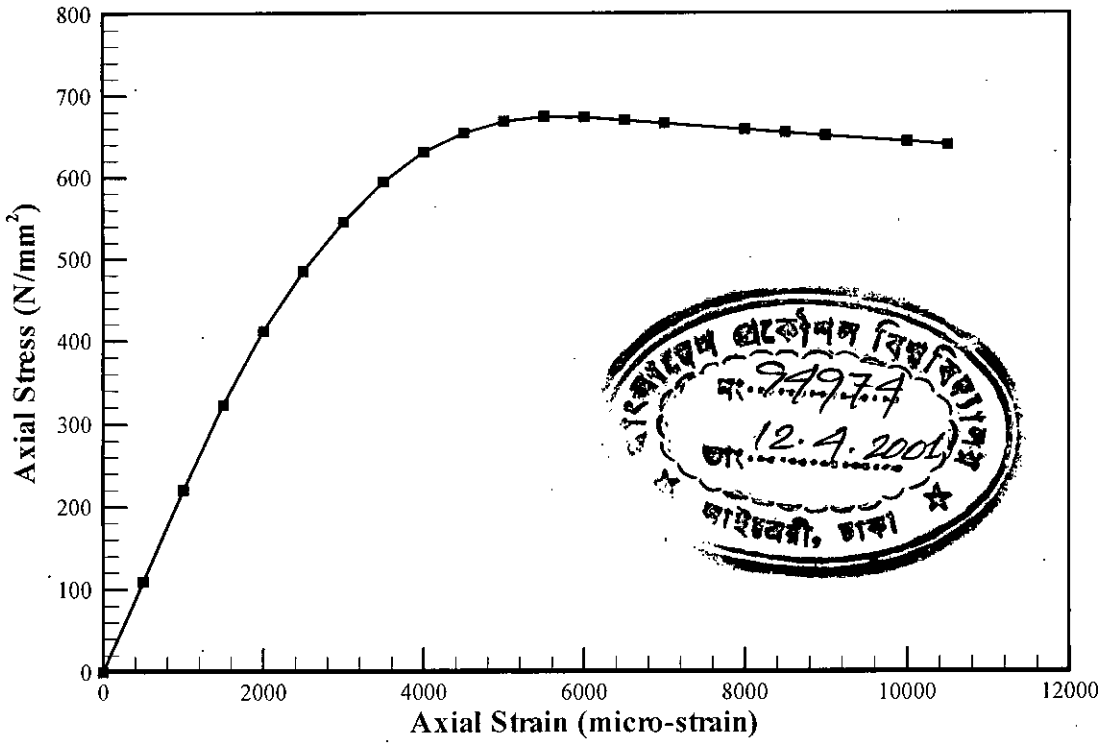


Figure B.1: Axial stress versus axial strain curve for STEEL

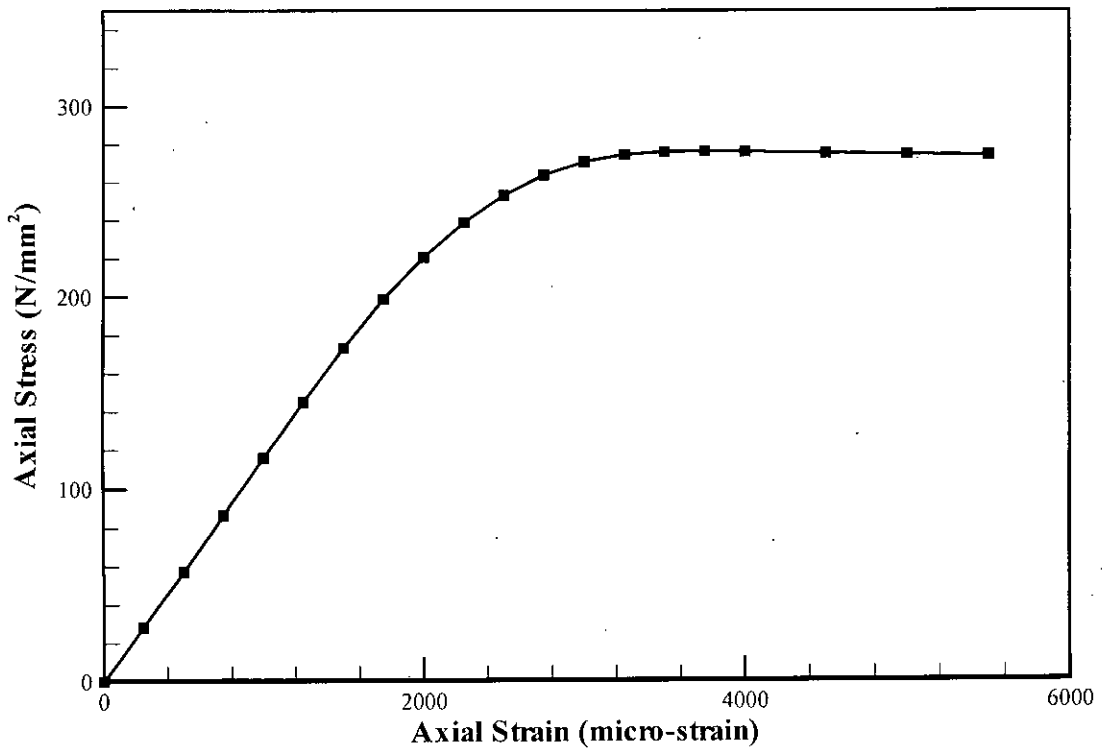


Figure B.2: Axial stress versus axial strain curve for COPPER